

Stand-off Detection of Alpha-Induced Air-Radioluminescence Even Under Daylight Conditions



Anita Jane Crompton, MEng, BA(Hon), PGDip

Department of Engineering

Lancaster University

A thesis submitted for the degree of

Doctor of Philosophy

July 2019

For my Dad, the best engineer I've ever known.

Acknowledgments

I would like to thank my academic supervisor, Kelum Gamage, for giving me the opportunity to undertake this PhD. Though it has been difficult and frustrating at times, it has always been interesting ... and I am sure that Kelum can say the same is true of supervising me. I thank him for his patience and support. I would also like to thank James Taylor, my other academic supervisor, for stepping in to the role part way through my work, and for his sage advice, support and help. I am grateful to my industrial supervisors, Divyesh Trivedi and Alex Jenkins, not only for their industrial understanding and technical expertise, but also their support and personal guidance. To all my supervisors, every supervisory meeting I faced with trepidation, but came out of with a renewed enthusiasm and sense of purpose. Your help was invaluable.

I gratefully acknowledge the funding provided by the Nuclear Decommissioning Authority (NDA) and Sellafield Ltd which allowed me to undertake the PhD, and to the Nuclear Security Science Network (NuSec) which supported some of the research activities.

I would also like to thank the people who provided resources, time and technical knowhow, including Steven Bell (NPL) for use of his lab space and for his assistance, Dan Whittaker (NNL) for his help in carrying out experiments at Central Labs, Jackie Pates (LEC) for the use of her lab space and sources, Russell Harvey (Physics) for the loan of his alpha source, and Richard Wilbraham for the use of the lab space and the friendly advice. I would also like to thank Peter Jones for his help, his friendship and lots of cups of tea. And to James Walkerdine who gave me invaluable advice on getting through a PhD, and who talked me round every time it got too much.

To my partner Andy, without whom this would not have been possible, thank you for getting me where I needed to be and keeping me safe; my partner, chauffeur, bodyguard, roadie and fellow engineer.

And to my Mum, thank you for being there for me every day from day one.

Stand-off Detection of Alpha-Induced Air-Radioluminescence Even Under Daylight Conditions

Anita Jane Crompton. MEng, BA(Hon), PGDip - Department of Engineering-
Lancaster University

A thesis submitted for the degree of Doctor of Philosophy, July 2019

Abstract

Alpha radiation detector technology lags behind gamma and beta due to difficulties presented by the short travel of alpha particles in environments complicated by mixed radiation fields, complex geometries, areas of high dose, and limited operator access. Yet, it is vital in nuclear decommissioning, safety and security operations. Recent developments focus on alpha-induced radioluminescence as a mechanism for long-range alpha detection. Detection in the 300–400 nm wavelength range has been achieved in special lighting conditions, but interference from background light hampers detection in daylight.

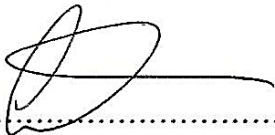
This thesis looks at the viability of detecting ultraviolet C (UVC, 180 – 280 nm) radioluminescence photons, focusing on characterising a flame sensor (UVTRON, Hamamatsu) sensitive to photons only in this wavelength range. UVC is already used in the detection of fires and corona discharge as Earth's atmosphere absorbs UVC from the sun and artificial lighting does not produce UVC. UVC radioluminescence from a 6.95 MBq ^{210}Po sample was detected in normal lighting conditions using the UVTRON, with very low background counts found in all environments. As the UVC radioluminescence signal is small, gas flows of Ar, Xe, Ne, N₂, Kr and P10 were

directed over the ^{210}Po sample to enhance radioluminescence with positive effect. In one instance Xe doubled the count in relation to an air atmosphere. Tests showed that the UVTRON reacts to the presence of gamma and beta radiation. However, it may be possible to identify alpha radioluminescence by separating the gamma and UVC parts of the signal.

Research presented herein shows it is possible to use a UVC flame sensor to detect alpha radiation through radioluminescence, and therefore an approach which uses the UVC portion of the radioluminescence spectrum may be successful in the development of a stand-off alpha detector, which would overcome many of the difficulties affecting traditional alpha detection methods.

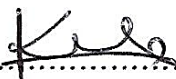
Declaration

I, Anita Jane Crompton, hereby certify that this thesis has been written by me and has not been submitted in any previous application for a higher degree. The work presented here was carried out at the University of Lancaster between October 2015 and July 2019

Signed 

Date 15/11/2019

I, Doctor Kelum Asanga Akurugoda Gamage, hereby certify that the candidate has fulfilled the conditions of the resolution and regulations appropriate for the degree of Doctor of Philosophy in the University of Lancaster and that the candidate is qualified to submit this thesis in application for that degree

Signed 

Date 15/11/2019

Contents

Acknowledgements	iii
Abstract	iv
Declaration	vi
Contents	vii
List of Figures	xii
List of Tables	xvi
Abbreviations	xvii
1 Introduction	1
1.1 Introduction to the project.....	1
1.2 Aim and scope of the work	4
1.3 Achievements of the project	5
1.3.1 Journal papers	5
1.3.2 Conference papers.....	6
1.3.3 Awards	7
1.4 Novelty of the project	7
1.5 Outline of each chapter	7
1.6 Background	10
1.6.1 UK nuclear industry and decommissioning	10
1.6.2 Nuclear Security.....	11
1.7 Traditional alpha detection.....	12
1.7.1 Traditional alpha detection methods	12
1.7.2 Advantages and disadvantages of traditional methods	12
1.7.3 Overcoming the limitations of traditional alpha detection methods	14
1.8 Underpinning science.....	14
1.8.1 Alpha radiation.....	14

1.8.2	Beta and gamma radiation.....	16
1.8.3	Radioluminescence	17
1.8.4	Sunlight and artificial light.....	19
1.8.5	Transmittance of UV light through translucent materials	21
1.8.6	Reflectance of UV light	22
2	Alpha Particle Detection Using Alpha-Induced Air Radioluminescence: A Review and Future Prospects for Preliminary Radiological Characterisation for Nuclear Facilities Decommissioning .	24
2.1	Abstract.....	24
2.2	Introduction.....	25
2.3	Alpha Radiation	27
2.4	Alpha-Induced Air-Radioluminescence.....	29
2.5	Advantages and Drawbacks of Using Radioluminescence	37
2.6	Alpha Particle Detectors	42
2.6.1	Traditional Detectors.....	42
2.6.2	Alpha-Induced Air Radioluminescence Detectors	44
2.6.3	Solar-Blind Detectors.....	46
2.6.4	UVA and UVB Cameras.....	49
2.6.5	UVA and UVB PMT Based Detector	53
2.6.6	Other Detector Types	60
2.7	Future Prospects for Alpha Induced Radioluminescence Detection	63
3	Experimental approach and set up.....	66
3.1	Approach.....	66
3.2	Equipment selection.....	67
3.2.1	UVTRON sensor.....	67
3.2.2	UVTRON – model R9533	70
3.2.3	Driving circuit	72
3.2.4	Counting device – the Arduino Uno	75
3.3	Experimental set up.....	76
3.4	Preliminary testing	79
3.4.1	Distance test	79

3.4.2	Pulse characteristics	80
3.4.3	Background test.....	82
3.4.4	Source location testing	82
3.5	Conclusions of initial testing.....	85
4	First Results of Using a UVTRON Flame Sensor to Detect Alpha-Induced Air Fluorescence in the UVC Wavelength Range.....	87
4.1	Abstract.....	87
4.2	Introduction.....	88
4.3	Materials and Methods.....	91
4.3.1	Detector.....	93
4.3.2	Source	94
4.3.3	Gas Flow Box and Gas Flow Set-Up	94
4.3.4	Measurement.....	95
4.3.5	Gases	96
4.3.6	Verification of Signal Source.....	97
4.4	Results.....	98
4.4.1	Background Count	98
4.4.2	Air Atmosphere Results	99
4.4.3	Gas Flow Results	100
4.4.4	Pulse Shape	102
4.5	Conclusions.....	103
5	Gas Flow to Enhance the Detection of Alpha-Induced Air Radioluminescence Based on a UVTRON Flame Sensor.....	106
5.1	Abstract.....	106
5.2	Introduction.....	107
5.3	Gas Atmosphere Influence on Radioluminescence Spectrum and Yield.....	108
5.4	Materials and Methods.....	112
5.5	Results.....	116
5.5.1	Background	116
5.5.2	Air Atmosphere Results	116
5.5.3	Gas Flow Results	117

5.6	Discussion and Conclusions.....	119
6	The Effect of Gamma and Beta Radiation on a UVTRON Flame Sensor: Assessment of the Impact on Implementation in a Mixed Radiation Field	123
6.1	Abstract.....	123
6.2	Introduction.....	124
6.3	Materials and Methods.....	126
6.4	Results.....	133
6.5	Conclusions and Discussion.....	138
7	Performance characteristics of a Tungsten collimator and UVTRON flame sensor for the detection of alpha-induced radioluminescence; Impact of UVC reflecting mirror and the effect of beta and gamma radiation sources.	141
7.1	Abstract.....	141
7.2	Background.....	142
7.3	Experimental set up.....	143
7.3.1	UVTRON.....	143
7.3.2	Collimator	144
7.3.3	Sources.....	146
7.3.4	Set up	147
7.4	Results.....	148
7.4.1	Background	148
7.4.2	UVC / alpha response	148
7.4.3	Beta response	153
7.4.4	Gamma response	155
7.4.5	Mixed radiation response	157
7.5	Conclusions and discussion	158
8	Discussion and conclusion	161
8.1	Summary	161
8.2	Outlook	165

8.3	Future work.....	166
8.3.1	Changes to the instrument design	167
8.3.2	UVC sensor technology	168
8.3.3	Beta detection.....	169
8.3.4	Electronics.....	169
8.3.5	Research.....	170
8.3.6	Optics	171
8.3.7	Arrays and scanning platforms.....	172
Appendix A.....		173
	UVC Detection as a Potential for Alpha Particle Induced Air Fluorescence Localisation	173
Appendix B		179
	Detecting Alpha-induced Radioluminescence in the UVC Wavelength Range Using a UVTRON Flame Sensor, and the Effect of a Gas Flow on Detection Rates as Compared to an Air Atmosphere.....	179
Appendix C		183
	NuSec Summary Project Report – November 2017	183
Appendix D.....		192
	Outdoor experiments data	192
References.....		195

List of Figures

Figure 1-1: Decay chain of ^{238}U [8]	15
Figure 1-2: Braggs curve for 5.49 MeV alpha particles [9]	18
Figure 1-3: Extra-terrestrial light spectrum and daylight spectrum at sea level [11]	19
Figure 1-4: Light transmittance by wavelength through different materials [20]	21
Figure 1-5: Reflectance curve of mirrors with specialist VUV (vacuum UV) and DUV (deep UV) coating [22]	23
Figure 2-1: The different delineated areas show nominal waste classification according to activity level and half-life. Half-lives range from seconds to millions of years, with ‘short lived’ considered to be less than approximately 30 years. Reproduction of the conceptual illustration of the waste classification scheme diagram, from: International Atomic Energy Agency, Classification of Radioactive Waste, IAEA Safety Standards Series, No. GSG-1, IAEA, Vienna, 2009 [23]. Reproduced with permission from IAEA.	26
Figure 2-2: Average decay energies of U-238 and U-235 series. Source: WISE Uranium Project [25].	28
Figure 2-3: Model of: (a) Radioluminescence photons induced by alpha particles showing the hemisphere in which they are initially created by the alpha particles; (b) Showing the random directions in which the photons are emitted from the hemisphere in (a) and their longer path length—Using FRED Optical Engineering Software (Photon Engineering LLC) [17]. Reprinted with permission from the author.	30
Figure 2-4: (a) Scheme of energy states of the 2P and 1N electronic-vibration band system of N_2 and N_2^+ ; (b) Nitrogen radioluminescence spectrum between 300 nm and 400 nm in dry air. The same colours are used in (a,b) for the corresponding spectral bands. Reprinted from [29] with permission from Elsevier.	31
Figure 2-5: Comparison of the spectrum of alpha-induced photon wavelength in comparison with the spectrum of sunlight at the surface of the earth [18, 31]. Image (a) produced using data with the permission of the author [18]; Image (b) reprinted from [31] by permission from Springer Customer Service Centre GmbH.	32
Figure 2-6: Increase in radioluminescence in the 200–400 nm wavelength range using an N_2 purge. Reprinted from [32] with permission from IEEE.	33

Figure 2-7: Number of photons emitted per mm ² attributed to the 337 nm emission in a 200 × 200 mm area as observed from above a ²⁴¹ Am source dispersed over a 2 cm radius circle on an Aluminium surface. The ticks give the x and y positions in mm. Reprinted from [35].....	36
Figure 2-8: Number of photons emitted per mm ² attributed to the 337 nm emission in a 500 × 500 mm area as observed from above a ⁶⁰ Co source dispersed over a 2 cm radius circle on an Aluminium surface. The ticks give the x and y positions in mm. Reprinted from [35].....	36
Figure 2-9: Number of photons emitted per mm ² attributed to the 337 nm emission in a 500 × 500 mm area as observed from above a P-32 source dispersed over a 2 cm radius circle on an Aluminium surface. The ticks give the x and y positions in mm. Reprinted from [35].....	37
Figure 2-10: Deployment of photon v. excited state absorption detector systems.....	62
Figure 3-1: UVTRON R9533 – courtesy of Hamamatsu Photonics K.K.	70
Figure 3-2: Comparison of UVTRON spectral response to sunlight, gas flame and Tungsten light - courtesy of Hamamatsu Photonics K.K. [53].....	71
Figure 3-3: UVTRON R9533 size specification - courtesy of Hamamatsu Photonics K.K. [54]	71
Figure 3-4: UVTRON R9533 field of view - courtesy of Hamamatsu Photonics K.K. [54].	72
Figure 3-5: Photograph of UVTRON driving circuit (Hamamatsu, C10807) – with factory pre-set background rejection jumper.	73
Figure 3-6: Circuit configuration diagram (Hamamatsu C10807) - courtesy of Hamamatsu Photonics K.K. [55]	73
Figure 3-7: Operation time chart for Drive circuit and UVTRON - courtesy of Hamamatsu Photonics K.K. [55]	74
Figure 3-8: Photograph of Arduino Uno.....	75
Figure 3-9: Driving circuit power and output connections - courtesy of Hamamatsu Photonics K.K. [55].....	76
Figure 3-10: Examples of typical pulse shapes from the UVTRON before processing – with an enhanced view of the 200 – 210 μs time period	77
Figure 3-11: Full equipment set up connections schematic – with oscilloscope	77
Figure 3-12: Photograph of project box housing electronics a) box closed b) box open to show the driving circuit, pull-up resistor and Arduino Uno.....	78
Figure 3-13: Equipment on trolley carrying out distance testing using a UVC light source ...	79
Figure 3-14: Graph showing signal frequency of UVTRONs v distance between UVTRON and UVC light source	80
Figure 3-15: Photograph showing conditioned pulse in green and direct pulse in yellow from the UVTRON.....	81
Figure 3-16: UVTRON scanning platform – showing collimator and driving circuit.....	83

Figure 3-17: Plots of scan data showing location of UVC source.	84
Figure 4-1: Schematic of equipment set-up.	91
Figure 4-2: Photographs (a, b) showing the ^{210}Po source inside the gas flow box (silver disk with mesh surface and yellow edge) and the UVTRON (small glass bulb), attached to the grey box housing the detector electronics. In photograph (b) the tube through which the gas was flowed over the source can be seen above and to the left of the source.....	92
Figure 4-3: Spectral response of UVTRON in comparison to sunlight, Tungsten light, and gas flame [53]......	93
Figure 4-4: Transmission spectrum of fused silica window material [58]......	95
Figure 4-5: Average counts per second (CPS) per hour - ^{210}Po source in air.	99
Figure 4-6: Comparison of average CPS in different gas atmospheres.	100
Figure 4-7: Pulse shape comparison of different gas atmospheres.	102
Figure 4-8: Limits of detectability showing the drop off in signal due to increased distance between sensor and source. The recorded background count \pm the calculated error is shown.	104
Figure 5-1: Radioluminescence spectrum of 100% Argon. Figure reproduced from [62]. ...	110
Figure 5-2: Schematic of equipment set up.....	113
Figure 5-3: Photograph showing the ^{210}Po source inside the gas flow box (silver disk with mesh surface and yellow edge), with the gas flow pipe above and to the left. The UVTRON (small glass bulb) is external to the box and is attached to the grey box in the foreground which houses the detector electronics.....	114
Figure 5-4: Showing the CPS for each of the gas flows in each of the three experiment groups (note: not all gases were tested in the second group due to time constraints) comparing the results of those in the first group reported by Crompton et al. [33] with two following groups.	117
Figure 5-5: Showing the increase in CPS for the different gas flows as a percentage of the air atmosphere results.....	118
Figure 6-1: Spectral response of the R9533 UVTRON. Derived from data from Hamamatsu [54] and OSRAM [75].	127
Figure 6-2: Comparison of the pulse recorded directly from the UVTRON and the processed pulse generated by the driver circuit (C10807, Hamamatsu) during normal UVC detection operation. The two pulses generated for three separate photon events (1, 2, 3) are shown. ..	128
Figure 6-3: Block diagram of the set up used in these experiments.	128
Figure 6-4: Showing the set up at the National Nuclear Laboratory (a) view from the side showing the vertical alignment of the UVTRON and source, and (b) showing the horizontal alignment of the UVTRON to the source.	130

Figure 6-5: The set up at Lancaster University. (a) UVTRON connected to the (closed) electronics housing containing the driver circuit and Arduino microprocessor, and the clamp used to support the source. (b) The UVTRON is exposed to the source with Lead shielding of the electronic driver circuit and Arduino microprocessor, which can just be seen in the lid of the electronics housing. (c) Top view of the shielded electronics and exposed UVTRON, showing the driver circuit (green), which can be seen in the base of the electronics housing. 132

Figure 6-6: Results of the experiments carried out at Lancaster University. The error bars shown are the confidence interval as included in Table 3. Where no error bar is shown, this is due to the count being below the threshold to calculate the confidence interval, i.e., less than the limit of detection as laid out by Hurtgen et al [71]..... 134

Figure 7-1: Tungsten collimator: a) & b) internal electronics showing placement of UVC reflecting mirror, c) external geometry (front view), d) external geometry (top view) 145

Figure 7-2: Modelling of different mirror angles (45° , 60° and 70°) using FRED32 raytracing software [80]; a), b) and c) show the rays passing through the collimator hole and reflecting from the mirror onto the UVTRON cathode; d), e) and f), show the rays incident on the UVTRON cathode. Using a limited number of rays, it is possible to see the decrease in incident rays with increase in angle, from 55 at 45° , to 48 at 60° , to 32 at 70° . At 70° not all rays impact on the mirror. 146

Figure 7-3: set up of the collimator, uncollimated UVTRON and source - showing the separation distances..... 147

Figure 7-4: Response of UVTRON within collimator and with collimator body removed, at a separation between the bulb and collimator of 2 m and 15 cm..... 150

Figure 8-1: COMSOL lens simulations - showing the effect of a single or dual lens system on the focus and collimation of light from a point source 171

List of Tables

Table 2-1: Summary of alpha particle detection research to date.....	44
Table 4-1: Table of gases.....	96
Table 4-2: Variation in average counts per second (CPS) by gas in comparison to air.....	101
Table 5-1: Table of gases showing flow rates and experiment groups.....	115
Table 5-2: Table of gas flow results.....	118
Table 6-1: List and properties of radionuclides used.....	129
Table 6-2: Background reading comparisons.....	134
Table 6-3: Results of experiments carried out at Lancaster University.....	135
Table 7-1: Sources.....	147
Table 7-2: Comparison between the signal between the collimated and uncollimated UVTRON when exposed to ^{210}Po , and the recorded background.....	149
Table 7-3: Showing the expected and actual results of exposure to ^{210}Po	152
Table 7-4: Results of exposure of collimated and uncollimated UVTRONs to ^{90}Sr source ..	153
Table 7-5: Results of exposure of collimated UVTRON to gamma sources.....	156
Table 7-6: Results of mixed radiation field.....	157

Abbreviations

AGR – advance gas-cooled reactor

CCD – charge coupled device

COTS – commercial off the shelf

CPS – counts per second

DUV – deep ultraviolet (light of wavelengths between 120- 280 nm)

EMCCD – electron multiplying charge coupled device

FWHM – full width half maximum

HAUVA – Handheld Alpha UV Application

ICCD – intensified charge coupled device

LEC – Lancaster Environment Centre, Lancaster University, Lancaster, UK.

LRAD – Long-Range Alpha Detector

MFP – mean free path

NDA - Nuclear Decommissioning Authority

NNL – National Nuclear Laboratory

NPL – National Physical Laboratory, Teddington, UK

PMT – photomultiplier tube

POCO – post operational clean out

PPE – personal protective equipment

SNM – special nuclear material

THORP – Thermal Oxide Reprocessing Plant

UV – ultraviolet (light of wavelengths between 10 nm and 400 nm)

UVA – ultraviolet A (light of wavelengths between 315 nm and 400 nm)

UVB – ultraviolet B (light of wavelengths between 280 nm and 315 nm)

UVC – ultraviolet C (light of wavelengths between 180 nm - 280 nm)

VUV – vacuum ultraviolet (light of wavelength between 10 – 200 nm)

Chapter 1

Introduction

1.1 Introduction to the project

With a large legacy of nuclear facilities requiring decommissioning over the next century or so, any efficiencies can generate great cost, time and safety benefits. One necessary element of the process is the accurate and timely characterisation of sites prior to planning and carrying out decommissioning tasks. This requires the location and characterisation of all sources of contamination of a site, including the location and type of gamma, beta and alpha emitting radioisotopes, often in large areas with complex geometries and access restrictions. Although alpha radiation poses the greatest biological hazard of the three radiation types mentioned, due to the difficulties in detecting alpha particles, it is the area with the least development in detector technology, although the importance of this has been realised and work towards better alpha detectors is being supported.

As alpha particles are positively charged, they interact strongly with atoms and molecules, travelling only a few centimetres in air, up to about 5 cm depending on their energy. They transfer all their energy in a short distance, which is why they are biologically so hazardous. However, they are easily stopped by matter, unable to penetrate a sheet of paper or skin.

It is this short travel that makes alpha particles so problematic to detect. Methods which require direct interaction between the sensor and alpha particles, must be used within the mean free path of the alpha particle, in practice around 1 cm from the surface being scanned [5]. This can be time consuming, especially for large areas or those with a complex geometry. It also means the sensor is in danger of becoming contaminated should the probe touch the contaminated surface. It also places the operator in close proximity to the radiation source, which can be hazardous. Alpha could be ingested, for example by disturbing contaminated dust, or there could be a mixed radiation field in which the operator would be required to work, requiring PPE (personal protective equipment) and exposure to a dose of radiation. Hence, a method for stand-off alpha detection has long been sought.

As alpha particles travel they transfer their energy to the surrounding air, causing ionisation, which leads to the emission of ultraviolet photons. These are primarily in the 300 – 400 nm wavelength range, ultraviolet A and ultraviolet B (UVA and UVB), with approximately 95% in this range [1]. These photons travel in the order of kilometres and hence provide a potential avenue for stand-off alpha detection. Various attempts have been made to detect this UV light (see Chapter 2; *Alpha Particle Detection Using Alpha-Induced Air Radioluminescence: A Review and Future Prospects for Preliminary Radiological Characterisation for Nuclear Facilities Decommissioning*). However, the interference from sunlight has proven a major stumbling block to success. To date,

despite the use of filters or other methods to reduce the impact of background daylight, special lighting conditions are required to detect the radioluminescence from alpha radiation.

However, a small proportion of the radioluminescence is in the ultraviolet C (UVC) wavelength range (180-280 nm). As UVC from the sun is blocked by the ozone layer, and normal artificial lighting does not produce UVC, there is no background to interfere with detection. This could provide the avenue for radioluminescence detection in normal field conditions. The solution then becomes finding a suitable sensor which is solar-blind, that is to say unresponsive to light outside of the UVC wavelength range, which is sensitive enough to detect the UVC radioluminescence.

In this thesis a solar-blind flame detector, the UVTRON, was characterised in terms of suitability for inclusion in a stand-off alpha-induced radioluminescence detector. It was found that the UVTRON was capable of detecting the radioluminescence emitted by a ^{210}Po source at further than the mean free path (MFP) of the alpha particles. The UVTRON has a very low background count which is generated by its operation, not natural or artificial light. This work also established that a flow of certain gases over the alpha source increased the signal strength, with up to double the signal detected from a Xenon flow as opposed to an air atmosphere.

It was found that the UVTRON is susceptible to gamma and beta radiation, of sufficient magnitude to mask the alpha detection. However, as the addition of individually tested alpha and gamma sources is approximately equal to the signal from the two tested in combination, it may be possible to subtract the signal caused by the UVC from that caused by the gamma to determine the presence of an alpha source. A Tungsten alloy collimator was tested with the UVTRON and found to be able to detect UVC radioluminescence whilst attenuating beta and some gamma radiation.

1.2 Aim and scope of the work

Alpha radiation is arguably the most challenging of the radiation types to detect, mainly due to the short travel of alpha particles in air, around 50 mm depending on energy. Yet many of the materials used for and produced through nuclear energy generation are primarily alpha emitters: including Pu, U and Am. As gamma is highly penetrating, it may be only through the detection of alpha that surface contamination be identified. Indeed, some isotopes, for example ^{210}Po , only emit alpha radiation and hence are undetectable to other types of radiation monitors. Therefore, the detection of alpha radiation is essential to the full characterisation of decommissioning sites, monitoring for health physics, and contamination control. However, due to the difficulties posed by detection of alpha particles, developments in new detector technology in this area has lagged behind that of other types of radiation.

This project seeks to identify a new approach to alpha particle detection, which will overcome the difficulties with traditional detectors. It will focus on the hitherto untapped potential of the UVC wavelength range to overcome the issues with background light from the sun and artificial lighting encountered by other radioluminescence detectors trialled to date. The use of an existing flame detection sensor which can be used for this entirely new purpose, locating alpha radiation, brings the benefits of readily available, tried and tested technology to a new application. This will result in a faster and easier method of alpha detection, with the benefits of cost and time reductions, a reduced hazard to operators, and the potential for deployment in areas where a traditional detector may not have access. Although the nuclear industry is necessarily cautious in terms of accepting new technologies, the unique challenges that are presented, especially in terms of decommissioning, also makes it open to the introduction of new ways to do things, if shown to be robust and safe. Therefore, the

development of a new way to detect alpha radiation is both necessary to and desired by the nuclear industry.

This project seeks to address the need of the nuclear industry for a robust, stand-off alpha detector, through the phenomenon of alpha-induced radioluminescence by carrying out the following activities:

- Research into the radioluminescence phenomenon and how this can be applied in a detector system, with special reference to any unexploited potential
- Assessment of progress to date in the design and development of a stand-off alpha detector, identifying strengths and weaknesses on which to build
- Determination of a new potential method for stand-off alpha detection which will meet the requirement for use in the field – including use in daylight conditions which has not as yet been fully achieved
- Determining detector elements, with a focus on the sensor, ideally identifying an existing sensor which can be utilised in this new application
- Testing and characterising a potential sensor – including laboratory and field tests to determine its use in this new application
- Using all collected data to inform the design of a prototype detector which can be used in the field under normal lighting conditions

1.3 Achievements of the project

1.3.1 Journal papers

1. *Crompton, A.; Gamage, K.; Bell, S.; Wilson, A.; Jenkins, A.; Trivedi, D. First Results of Using a UVTRON Flame Sensor to Detect Alpha-Induced Air Fluorescence in the UVC Wavelength Range. Sensors 2017, 17(12), 2756; <https://doi.org/10.3390/s17122756>. <http://www.mdpi.com/1424-8220/17/12/2756>*

2. *Crompton, A.; Gamage, K.; Jenkins, A.; Taylor, C. Alpha Particle Detection Using Alpha-Induced Air Radioluminescence: A Review and Future Prospects for Preliminary Radiological Characterisation for Nuclear Facilities Decommissioning.* Sensors 2018, 18(4), 1015; <https://doi.org/10.3390/s18041015>.
<http://www.mdpi.com/1424-8220/18/4/1015>
3. *Crompton, A.; Gamage, K.; Bell, S.; Wilson, A.; Jenkins, A.; Trivedi, D. Gas Flow to Enhance the Detection of Alpha-Induced Air Radioluminescence Based on a UVTRON Flame Sensor.* Sensors 2018, 18(6), 1842; <https://doi.org/10.3390/s18061842>. <http://www.mdpi.com/1424-8220/18/6/1842>
4. *Crompton, A.; Gamage, K.; Trivedi, D.; Jenkins, A. The Effect of Gamma and Beta Radiation on a UVTRON Flame Sensor: Assessment of the Impact on Implementation in a Mixed Radiation Field.* Sensors 2018, 18(12), 4394; <https://doi.org/10.3390/s18124394>. <http://www.mdpi.com/1424-8220/18/12/4394>
5. *Crompton, A.; Gamage, K.; Jenkins, A.; Bell, S.; Trivedi, D. Performance characteristics of a Tungsten collimator and UVTRON flame sensor for the detection of alpha-induced radioluminescence; Impact of UVC reflecting mirror and the effect of beta and gamma radiation sources.* In submission.

1.3.2 Conference papers

1. *Crompton, A.J., Gamage, K.A.A. UVC Detection as a Potential for Alpha Induced Air Fluorescence Localisation,* 15th International Conference on Environmental Science and Technology, Rhodes, Greece, 31 August to 2 September 2017

2. *Anita J. Crompton, Kelum A. A. Gamage, Alex Jenkins and Divyesh Trivedi. Detecting Alpha-induced Radioluminescence in the UVC Wavelength Range Using a UVTRON Flame Sensor, and the Effect of a Gas Flow on Detection Rates as Compared to an Air Atmosphere. 2018 IEEE Nuclear Science Symposium and Medical Imaging Conference, 10 – 17 November 2018, International Conference Centre, Sydney, Australia.*

1.3.3 Awards

Award for the Best Presentation at the 7th NDA PhD Seminar - awarded by the Nuclear Decommissioning Authority, January 2019

1.4 Novelty of the project

This project seeks to utilise the hitherto untapped potential of alpha-induced radioluminescence in the UVC wavelength range to overcome difficulties with traditional alpha detectors, and more recent stand-off alpha detectors. The UVTRON flame sensor used in this work has the potential to also be employed to detect alpha-induced radioluminescence at a distance and operates in normal lighting conditions. By using an established sensor in a completely new application, the benefits of a tried and tested device, which is easily obtainable and low in cost, can be exploited.

1.5 Outline of each chapter

This thesis presents the results and findings of research towards a new stand-off alpha detection system, using the UVC portion of the alpha-induced radioluminescence spectrum, focusing on a potential sensor for use in such a system, the UVTRON by Hamamatsu (Japan).

- **Chapter 1.** This chapter looks at the motivation and background to the work and the intention of this research. It includes an overview of the underpinning science, with reference to where further information is included in the remainder of the thesis, including: the nature of alpha, beta and gamma radiation; the radioluminescence phenomenon; natural and artificial light and its effect on detecting radioluminescence; UV light transmittance and reflection.
- **Chapter 2.** A literature review was carried out to ascertain the work done to date in this area of research and is presented in this chapter. The underpinning science along with the advantages and disadvantages of the radioluminescence approach is followed by a critical analysis of existing prototypes able to detect radioluminescence in any UV wavelength range and other alternative stand-off alpha detectors.
- **Chapter 3.** This chapter details the approach taken in this research, building on the literature review, including: reasons behind the selection of the UVC wavelength range; the sensor selection process; experimental set up; and preliminary testing.
- **Chapter 4.** This chapter documents experiments carried out at the National Physical Laboratory (NPL) in Teddington, London to determine if the UVTRON R9533 can detect radioluminescence in the UVC wavelength range. The setup of the experiment along with the results are presented. The sensor was able to detect the UVC radioluminescence from a ^{210}Po source, with a clear signal compared to background. The estimated limit of detection for this source and sensor configuration is 240 mm, well beyond the range of alpha particles in air. The low background count of the UVTRON in normal commercial/laboratory lighting was also established.

- **Chapter 5.** This chapter documents experiments carried out at NPL, Teddington, London, to determine the effect on detection of flowing gas over an alpha source. It showed that a flow of gas of around 65 mL/min was sufficient to increase the signal detected in all gases tried: Ar, Xe, Ne, N₂, Kr and P-10. In one instance a flow of Xe increased the count by 105% compared to an air atmosphere. As the UVC signal is much smaller than that in the UVA and UVB range, an increase in the number of UVC photons may be crucial in determining the sensitivity of the detector for lower activity implementations.
- **Chapter 6.** As the detector may be required to work in a mixed radiation field, the effect of gamma and beta radiation was tested on both the UVTRON sensor and its associated electronics, with the results presented in this chapter. Experiments were carried out in the Lancaster Environment Centre (LEC) at Lancaster University. The experiments showed that the UVTRON R9533 responds to both gamma and beta radiation, and at a level which would mask the UVC signal. This has implications for implementation of this sensor for nuclear applications.
- **Chapter 7.** This chapter looks at experiments carried out at NPL, Teddington, London, on the effect of using a Tungsten alloy collimator with the UVTRON. A UVC mirror proved successful in reflecting alpha-induced radioluminescence onto the UVTRON, allowing an internal collimator geometry which prevents a direct shine path for any beta and gamma radiation. The collimator reduced the signal generated by both beta and gamma radiation and the alpha-induced radioluminescence count as well. Using a fused silica window, it was possible to further reduce the signal generated by the beta source. The combined count from individual alpha, beta and gamma sources was very similar to a single

count from the three sources together. This provides a potential avenue for the identification of the UVC part of the signal.

- **Chapter 8.** A summary of the research done and results, with suggestions for future work relating to the findings is presented in this chapter.

1.6 Background

1.6.1 UK nuclear industry and decommissioning

The birth of the nuclear industry in the UK occurred in the 1940s on the site now known as Sellafield. Its initial purpose was to produce Pu for weapons. But realising the potential use of the heat which was generated as a consequence of Pu production, in 1956 the site moved into energy generation, with Calder Hall the first nuclear power station of industrial-size in the world, and later the Windscale advanced gas-cooled reactor (AGR) which was the template for other reactors around the country. Fuel reprocessing began in 1964 with the Magnox Reprocessing Plant, and later THORP (Thermal Oxide Reprocessing Plant) which is the largest building on the Sellafield site. Commercial power generation at the site is no longer carried out and reprocessing is planned to end in 2020, at which point Sellafield will become focused on Pu management, waste treatment and decommissioning of the site. Over the 70⁺ years of its operation it has grown to cover an area of two square miles with more than 200 nuclear facilities which vary in size, layout and use. It is the most complex nuclear site in the world and houses four of the biggest nuclear risks and hazards in the world.

Sellafield and the other 16 nuclear sites in the UK which are at the end of their operational lives present a significant legacy of nuclear facilities requiring decommissioning. It is estimated that approximately 4.77 million m³ of contaminated waste will be generated as these facilities are dismantled and disposed of, and the land

which they now occupy is returned to a state where other activities can take place [2]. Decommissioning is expected to be carried out over the next 120⁺ years at a cost of £121 bn [3]. Therefore, any means to speed up and reduce the cost of decommissioning activities, to reduce waste and improve safety is of great importance to the industry, with very large potential savings in time and money. This is also true for ongoing operations, where monitoring of contamination and remedial action is required.

To effectively deal with contaminated materials, either from operational activities, post operational clean out (POCO) or decommissioning, it is important that waste is classified correctly. This ensures that the disposal method is appropriate, and costs can be kept to a minimum. As the cost in general increases depending on the level of hazard of the waste, characterising the radioactive environment to plan waste disposal is very important. The cost differences between different categories of waste is in the order of tens of thousands of pounds, and therefore savings can be very great indeed.

1.6.2 Nuclear Security

Although this research is primarily focused on decommissioning, there are also security implications for the detection of alpha radiation, in terms of the detection of illicit nuclear materials. For example monitoring to prevent the unsanctioned removal of nuclear materials from secure sites, the illegal import, export or movement of nuclear materials, even to activities like the assassination of Alexander Litvinenko in 2006 using ²¹⁰Po, and the possible use in dirty bombs. The resulting distribution from a radiological dispersal device can be complex and difficult for gamma detectors to measure, and a stand-off alpha detector may be better suited to this task [4]. Once a working technique for alpha detection is determined, it is a matter of different implementation as to what purpose it is put to. Therefore, security needs could also be addressed with the same technique as developed for nuclear industry needs.

1.7 Traditional alpha detection

1.7.1 Traditional alpha detection methods

Alpha radiation is a form of ionising radiation where the emitted particles transfer their energy to the surrounding atmosphere as they travel, slowing the particles and limiting their distance of travel. Having a relatively large mass, atomically speaking, and being positively charged, alpha particles travel only a short distance in air, approximately 50 mm, compared to a few metres for beta electrons and many metres for gamma photons, depending on energy (See section 1.8 *Underpinning Science* for the nature of alpha radiation).

Traditional detectors require direct interaction with the alpha particle, which means they must be operated within approximately 10 mm from the surface being scanned for alpha contamination [5]. Proportional counters and scintillators can differentiate between radiation types, though many detectors are sensitive to both alpha and beta radiation. It is usual in alpha detection to take swabs, have the isotopes chemically separated and then spectroscopy is carried out to determine the nature of the contamination, which can take a matter of weeks to complete and for results to be known.

1.7.2 Advantages and disadvantages of traditional methods

Although alpha detection has somewhat lagged behind that of the developments in gamma and beta detection, traditional detectors do present mature technologies with a great deal of understanding and experience behind them. See Chapter 2, section 2.6.1 *Traditional detectors* for more information.

Alpha detectors are easily available as commercial off the shelf (COTS) products from established suppliers. They offer reliability and have been designed to be robust for field use. And they are available in a number of configurations as may suit

their implementation, including for example a probe small enough to check inside wounds for the presence of contamination [6].

However, there are significant drawbacks. The close proximity required to the surface being scanned makes the process time consuming, especially for large areas and surfaces with complex geometries. A simple scan over a work surface to check for contamination in the lab takes only a few minutes to complete. However, if one imagines a glovebox containing tools and stands, a room with pipework, or a long corridor, as may be found on a nuclear site, with all surfaces requiring scanning from approximately 10 mm away, then the time-consuming nature of direct alpha detection becomes easier to comprehend. There are also areas with limited access in terms of size and location, geometries which are difficult to negotiate, or areas of high dose which makes human access impossible. This limits the ability to complete alpha detection activities in these areas, posing difficulties for decommissioning activities. It is also possible that surfaces with an uneven topography emit alpha particles in unexpected directions, which can affect count efficiencies [7].

The detector probes are also quite delicate and contact with a sharp corner or edge can damage them, and they are at risk of contamination themselves should they come in contact with a contaminated surface.

The surface to be scanned may be in an area where the detector operator may be exposed to a mixed radiation field, where contamination may be emitting beta and gamma radiation as well as alpha, requiring the use of PPE and exposing staff to potential radiation doses. Alpha emitting materials are extremely hazardous if ingested, such as by inhalation in the event of accidental liberation of contaminated material, which makes removing personnel from contaminated areas highly desirable for safety reasons.

1.7.3 Overcoming the limitations of traditional alpha detection methods

Due to the issues with traditional alpha detection methods, a stand-off alpha detector has long been sought which will remove the operator from close proximity to the contamination and allow faster scanning of larger areas or complex surfaces. The process could be automated by the use of a scanning platform, freeing operators to work elsewhere. This should provide faster overall characterisation times, reduced operator hours, increase workplace safety, and reduce the costs of decommissioning. The phenomenon of alpha-induced radioluminescence has provided an avenue of possibility for the development of a stand-off detector. The negatives and positives of using radioluminescence for a stand-off detector are explored further in Chapter 2 section 2.5 *Advantages and Drawbacks of Using Radioluminescence*.

1.8 Underpinning science

1.8.1 Alpha radiation

Proton-rich nuclides with a high atomic number may decay through the emission of an alpha particle into a more stable daughter nuclide. An alpha particle comprises two protons and two neutrons and is therefore positively charged, and its emission leaves the daughter nuclide with two extra electrons which are soon lost. The decay process can be described by the following;



In heavy nuclides the electrostatic repulsive forces are greater than the cohesive nuclear force, making the nuclide unstable and more likely to decay by alpha emission. If also unstable, the daughter nuclide may itself decay in a process which continues until the material reaches a stable state, known as a decay chain. As an example, the decay

chain of ^{238}U is shown in Figure 1-1 which includes the type of decay, energy and half-lives of all parent / daughter nuclides in the chain.

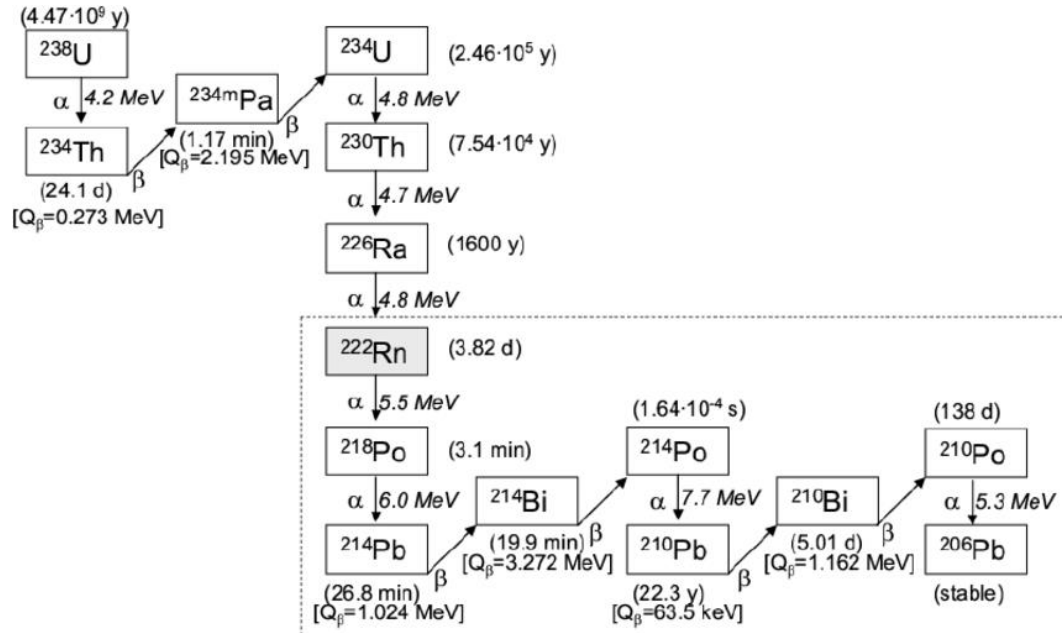


Figure 1-1: Decay chain of ^{238}U [8]

The alpha particle is emitted with such energy as is required to escape the nuclide, which is achieved through quantum tunnelling as the energy of the potential repulsion barrier has been seen to be greater than an emitted alpha particle. As it travels the kinetic energy is transferred to the surrounding atoms and molecules and the alpha particle slows. At a sufficiently low energy it becomes a helium atom through the acquisition of two electrons. Alpha particles are positively charged and atomically relatively large (7000 times more massive than a beta particle), and are therefore easily stopped by solids, liquids and air, travelling at most around 50 mm in air depending on energy. They primarily interact with the electron cloud of atoms, but may in some instances, directly impact on the nucleus. Both these interactions leave the atom in an excited state.

Due to the very short stopping distance within solids, alpha particles are unable to penetrate human skin. However, should they be ingested by inhalation or consumption, or enter the body through injection or breaks in the skin, they release a great deal of energy in a short distance in human tissue, which kills or damages cells, making them extremely toxic to humans.

Chapter 2 section 2.2 *Introduction* includes further information about alpha radiation, with specific reference to the nuclear industry.

1.8.2 Beta and gamma radiation

An unstable radioactive nucleus with an excess of neutrons, as may be produced following neutron bombardment of stable materials in a reactor, may convert one of these neutrons to a proton with the creation of a beta particle and an anti-neutrino. This can be shown by;



where $\bar{\nu}$ is the anti-neutrino. The beta particle is a fast electron and is denoted as β^{-} to show that it differs from a standard electron, e^{-} . The daughter nucleus is left in a positively charged state, but quickly absorbs an electron to return to a neutral charge.

Beta particles are emitted with a range of energies, from zero to a maximum, which is in the range of approximately 10 keV to 4 MeV. Although also interacting due to coulomb forces, they lose their energy at a slower rate than alpha particles due to their smaller mass and lower charge, meaning a longer travel path in the same medium. Still, the thickness of materials such as metal and glass required to stop beta particles is small, with beta particles of less than about 200 keV limited in their penetration of human tissue. In air, a beta particle may travel up to a few metres.

Pure beta emissions, such as ^{90}Sr , achieve ground state after the emission of the beta particle. Other beta emitters remain in an excited state and emit a gamma photon to return to ground state.

The emission of gamma-ray photons mostly occurs when the decay of a parent nuclide by alpha or beta emission leaves the daughter nucleus in an excited state. The daughter nucleus rapidly ($<10^{-9}$ s) emits a gamma photon to return to the ground state. Due to the limited excitation energies of any particular nucleus, gamma photons are monoenergetic from any individual transition and typically of energy of less than approximately 2.8 MeV. The energy of the gamma photons is determined by the energy levels of the daughter nucleus, but they have the half-life characteristics of the parent nucleus, giving the gamma photon characteristics of both parent and daughter nuclide.

Gamma radiation is highly penetrating and requires a significant thickness of absorbing material to attenuate gamma photons, making it difficult to shield against. In air, gamma photons will travel many metres.

1.8.3 Radioluminescence

As alpha particles travel through air, they lose their kinetic energy, transferring it through mainly elastic and infrequent inelastic interactions with the surrounding atoms and molecules. This leaves the air atoms in an excited state from which they may emit a photon to return to ground state. The emitted photons are known as radioluminescence.

The alpha particle's energy is transferred over a range of around 50 mm in air, depending on the initial energy. The amount of energy transferred increases as the particle slows, with a $1/v^2$ relationship (see Figure 1-2) as the stopping power increases with path length. Just before the particle comes to rest, the likelihood it will interact

with the surrounding atoms increases. The peak on the Bragg curve shows the cross section increase as the particle reaches its maximum path length (see Figure 1-2).

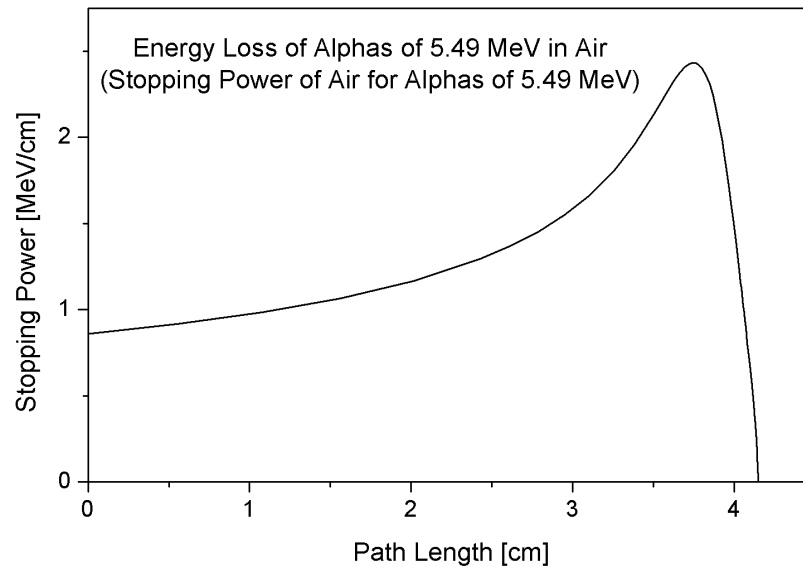


Figure 1-2: Bragg curve for 5.49 MeV alpha particles [9]

The wavelength of the emitted photon is dependent on the gas composition of the surrounding atmosphere. Normal air is 77% Nitrogen, which causes radioluminescence in the 300 – 400 nm wavelength range. Other gases emit photons of other wavelengths, and those relevant to this research are presented in Chapter 5, section 5.3 *Gas Atmosphere Influence on Radioluminescence Spectrum and Yield*. This radioluminescence travels much further than the initial alpha particle and may provide an avenue to stand-off alpha detection. Chapter 2 section 2.4 *Alpha-Induced Air-Radioluminescence* looks in more depth at ionisation and radioluminescence.

There is a small amount of radioluminescence in the UVC wavelength range, though this is still to be quantified and the mechanism determined. Using data from Grum [10], Roberts [4] has calculated that the yield in the UVC wavelength range is approximately 200 times less than that emitted in the 300-420 nm range, with 0.08 photons per MeV of deposited ionising energy. They calculate that for a 10 GBq source

with 1 MeV of deposited energy, the resulting UVC radioluminescence would be 50 photons $\text{cm}^{-2} \text{s}^{-1}$ at a distance of 10 m from the source. However, as the original work was done at a pressure of 3 atm and pressure affects UVC absorption, this figure may not be wholly accurate. However, it does provide an indication of the difference between the yield in the different wavelength ranges. Difficulties in determining the exact yield arises from: the small count being hard to determine against detector dark count; the attenuation of UVC through ordinary glass meaning special optics are required; and the difficulties in finding a solar blind detector set up which will fully block background light.

1.8.4 Sunlight and artificial light

1.8.4.1 Sunlight

Our sun fuses 600 million tonnes of hydrogen into helium every second and as a result emits electromagnetic radiation in the infrared, visible and ultraviolet spectrum. As it passes through the atmosphere, 70 % of the UV light is filtered out by atmospheric gases, with ozone absorbing all light of less than approximately 290 nm, see Figure 1-3.

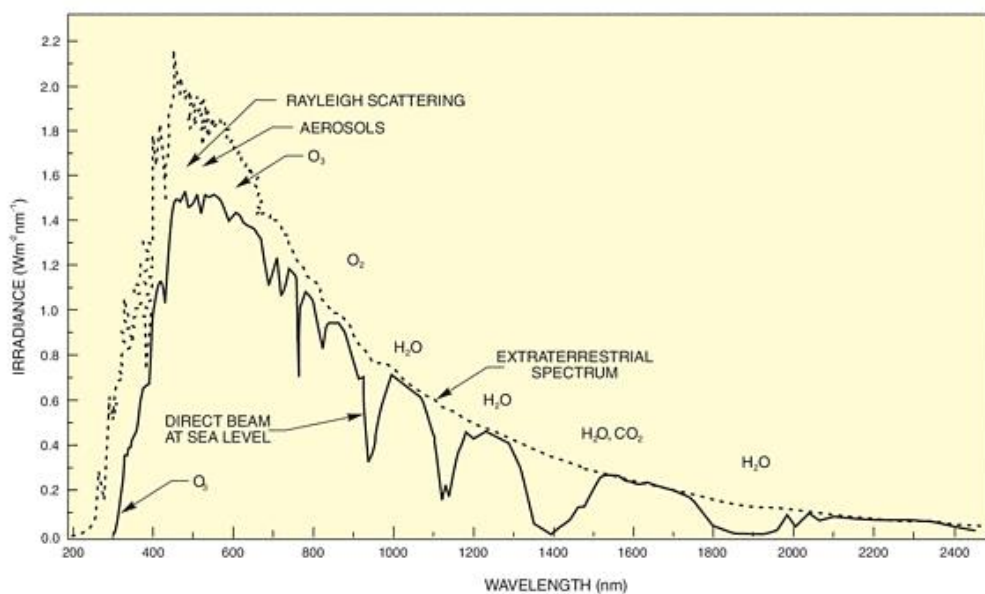


Figure 1-3: Extra-terrestrial light spectrum and daylight spectrum at sea level [11]

10% of the light from the sun which arrives at the edge of our atmosphere is UV, and despite the filtering effect of the atmosphere, a significant amount of UV light in the UVA and UVB wavelength ranges reach the surface of the earth, around $(2-8) \times 10^{-2} \text{ W cm}^{-2} \text{ nm}^{-1}$ [1]. The wavelengths of sunlight and radioluminescence overlap in the UVA and UVB range, which causes issues in detecting the radioluminescence from alpha particle emissions.

1.8.4.2 Artificial light

Humans can see light in the range of approximately 400 – 700 nm, with reflected and absorbed wavelengths of light determining the colour of objects around us. Light outside of this range is not useful for human vision and so lighting is designed to only emit the required wavelengths where possible. Early means of lighting, for example candles, did give off wavelengths down to the UVC range. Incandescent lamps emit most of their light towards the red end of the spectrum, with 80% in the infrared, and gas discharge lamps use phosphors to control the output spectrum. In the main, indoor lighting is focused on the 400 – 700 nm wavelength range. UVC is especially absent in contemporary lighting systems as prolonged exposure to UVC can cause eye damage. Due to the focus on the visible light wavelength range, data on the emission spectrum from different lighting is difficult to find for below 400 nm. However, testing of prototypes for alpha-induced radioluminescence detection had to be carried out in darkness or in special lighting conditions, indicating that UV lighting is found in indoor lighting systems [1, 5, 12 - 18].

1.8.5 Transmittance of UV light through translucent materials

Transmittance of light through translucent materials depends on the exact composition of the material and the wavelength of light. As it travels through a translucent material a constant fraction of the light is absorbed per unit travelled, which results in an exponential drop off in transmittance with absorber thickness. This can be calculated using Lambert's Law;

$$I/I_0 = e^{-\alpha t} \quad (1.3)$$

where I is the intensity of light after passing through the thickness t of the material, I_0 is the intensity of light entering the medium and α is the absorption coefficient of the material. The absorption coefficient is a property of the material and is a function of wavelength, which in some instances makes it harder for UV light to pass than other light wavelengths. Building window glass, unless specifically designed to block UV light, is opaque to UVB, but transmits around 72% of UVA light [19]. Perspex is transparent to UVA and UVB, as is quartz glass. Fused silica and quartz glass are also transparent to UVC light. Figure 1-4 shows the transmittance of different materials used in manufacturing cuvettes.

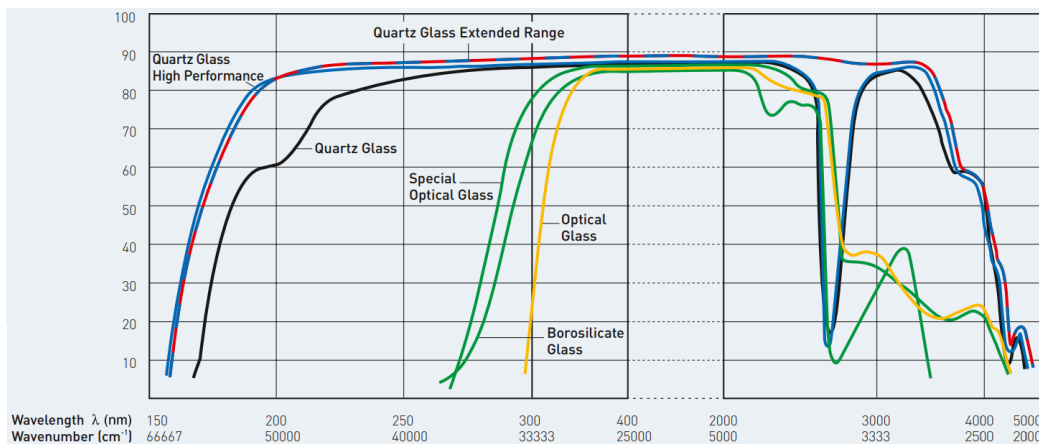


Figure 1-4: Light transmittance by wavelength through different materials [20]

Hence, when detecting UV light the selection of materials for any optics is important. Issues with UV light transmittance also impacts on the detection of radioluminescence through translucent materials already present in the field, for example, plexiglass, Perspex and glass.

Chapter 2 section 2.5 *Advantages and Drawbacks of Using Radioluminescence* reviews research done on the transmittance through materials commonly found in the nuclear industry.

1.8.6 Reflectance of UV light

Commonly found mirrors consist of a reflective surface protected by a layer of ordinary glass. Due to the issues of transmittance of UV light through glass, this makes standard mirrors unsuitable for radioluminescence detection. A front surface mirror or polished metal surface are required for reflecting UV light. Polished metal can reflect light into the UV wavelength range, but with limited reflectance and there are the dangers of damaging the surface or surface reactions with certain environments (such as humidity and heat) which would reduce the reflectance [21].

Coatings of different substrates can produce mirrors which offer peak reflectance at specific wavelengths, and offer differing levels of reflectance, for example, enhanced Aluminium (where multi-layered films of dielectrics are used to increase reflectance in the required wavelength range) and MgF₂ coatings. These produce mirrors capable of reflecting light from 120 nm to 11000 nm wavelengths. An example of the wavelength transmittance of two types of enhanced Aluminium is shown in Figure 1-5.

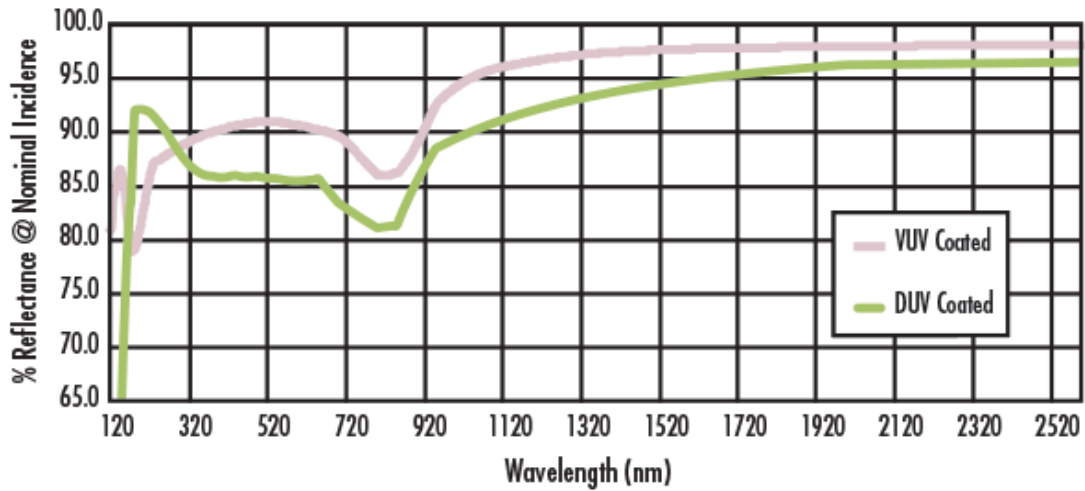


Figure 1-5: Reflectance curve of mirrors with specialist VUV (vacuum UV) and DUV (deep UV) coating [22]

The reflectance of UV light is important in the field for two reasons. First, any unwanted reflection from surfaces may make locating the source of radioluminescence problematic. Secondly, as it may be necessary to shield the detector system against other radiation in the field, mirrors could be used to reflect the UV whilst allowing gamma radiation to pass through, thus removing the sensor and any electronics from the shine path.

Chapter 2

Alpha Particle Detection Using Alpha-Induced Air Radioluminescence: A Review and Future Prospects for Preliminary Radiological Characterisation for Nuclear Facilities Decommissioning

Anita J. Crompton, Kelum A. A. Gamage, Alex Jenkins and Charles James Taylor

Reprinted from Sensors, 18(4), 1015; March 2018, with permission from Sensors.

2.1 Abstract

The United Kingdom (UK) has a significant legacy of nuclear installations to be decommissioned over the next 100 years and a thorough characterisation is required prior to the development of a detailed decommissioning plan. Alpha radiation detection is notoriously time consuming and difficult to carry out due to the short range of alpha particles in air. Long-range detection of alpha particles is therefore highly desirable and this has been attempted through the detection of secondary effects from alpha radiation,

most notably the air-radioluminescence caused by ionisation. This chapter evaluates alpha induced air radioluminescence detectors developed to date and looks at their potential to develop a stand-off, alpha radiation detector which can be used in the nuclear decommissioning field in daylight conditions to detect alpha contaminated materials.

2.2 Introduction

Since its inception in the 1940s firstly as a means to produce Pu for weapons and later for energy generation, the UK nuclear industry has as a consequence of operations seen radioactive contamination of its facilities across the UK. This is an unavoidable consequence of nuclear processes and an anticipated phenomenon. At the end of their useful life, these facilities require decommissioning and clean up to remove hazardous substances in order that the site can be repurposed or reused. This produces significant quantities of waste, which is forecast to reach a total of 4.7 million tonnes over the next 100 years [2]. This waste falls into several categories depending on the type, levels, activity, half-life, etc. of radioactivity of the waste including: very short lived waste (VSLW); very low level waste (VLLW), low level waste (LLW), intermediate level waste (ILW) or high level waste (HLW); and waste which does not exhibit any radioactive contamination (EW—Exempt Waste) (see Figure 2-1).

How the different types of waste are collected and treated differs, from the PPE required by personnel, to the process of collection and processing, and the storage of the waste, all of which have associated cost implications. In general HLW is much more costly to deal with than LLW, which is in turn more costly than uncontaminated waste. This is due to the increasing safety precautions required with increased activity: for example lower safe exposure times for staff meaning shorter working times, increased

amounts of PPE required, pre-storage decontamination and other treatment, greater shielding required of storage receptacles and facilities, specialist equipment, e.g. robots in areas too active for human intervention.

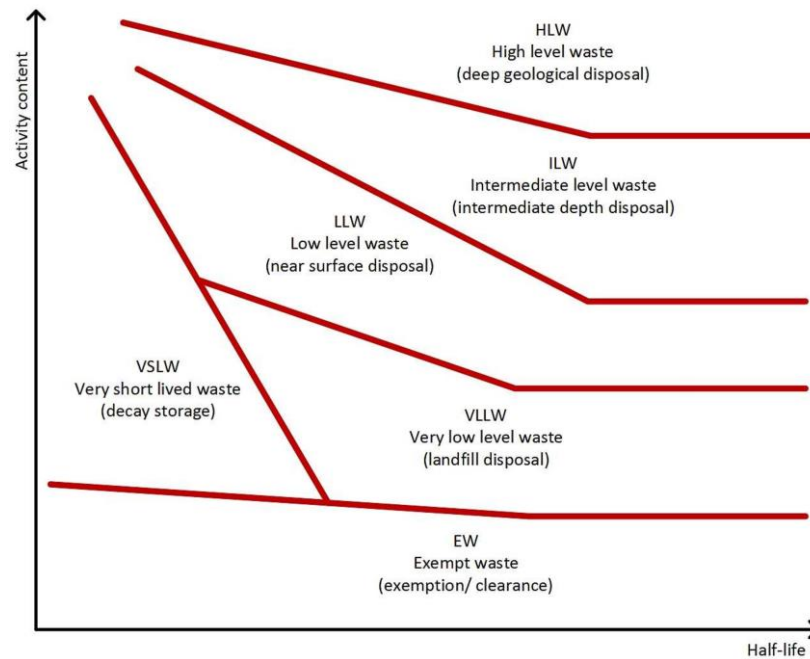


Figure 2-1: The different delineated areas show nominal waste classification according to activity level and half-life. Half-lives range from seconds to millions of years, with 'short lived' considered to be less than approximately 30 years. Reproduction of the conceptual illustration of the waste classification scheme diagram, from: International Atomic Energy Agency, Classification of Radioactive Waste, IAEA Safety Standards Series, No. GSG-1, IAEA, Vienna, 2009 [23]. Reproduced with permission from IAEA.

It is therefore important for financial and safety reasons that plant and equipment is correctly characterised prior to decommissioning taking place in order that a suitable, efficient and safe plan for the removal and storage of waste can be drawn up and implemented. As part of this characterisation process, the identification and location of alpha radiation emitting sources is an important element. Pu contaminated materials which are almost exclusively alpha emitters are widespread in nuclear reprocessing

facilities, yet these are difficult to detect by non-destructive or passive detection methods posing a problem for characterisation efforts.

This chapter looks at existing alpha particle detection methods, particularly through alpha-induced air-radioluminescence. It attempts to draw together the existing research on this subject and to lay out a path to progress the understanding and capability in this area based on the foundation of work carried out to date. The work is primarily focused on the research into and application of alpha detection technology for nuclear decommissioning, although it is possible that there could be applications for other areas such as nuclear safeguards and security.

2.3 Alpha Radiation

Alpha particles are comprised of two protons and two neutrons. They have a relatively strong positive charge and therefore interact strongly with molecules in the air as they are emitted from a radioactive source, transferring their energy within a range of a few centimetres depending on their initial energy. Their atomically large mass and charge also means that they are easily stopped in solid matter, for example by a sheet of paper or skin. Although the least penetrating form of radiation, if ingested alpha particles cause the most internal damage relative to absorbed dose due to their high linear energy transfer, making them hazardous to humans. Despite the biological hazard increasing from gamma to beta to alpha radiation, there are correspondingly less detectors available, and as some contamination isotopes may only be alpha emitters, this makes a new way to detect alpha more important [1].

Actinides, to which group the main isotopes found in nuclear applications belong, are primarily alpha emitters, giving off relatively weak beta and gamma radiation, which is also of low energy. Figure 2-2 shows a comparison of alpha, beta and gamma

emissions from two U isotopes widely found in the nuclear industry [5]. The main isotopes found in nuclear applications, which are predominantly alpha emitters, are ^{235}U , ^{238}U , ^{238}Pu , ^{239}Pu and ^{241}Am [24]. Alpha emissions are more likely from trans-uranic elements, those with a greater atomic number than U, for example Pu and Am, where the high atomic mass makes the isotopes unstable. Technology available at present is less effective for characterising actinides [15], which as the primary isotopes in nuclear applications, has implications for the nuclear industry, making advances in alpha detection highly desirable.

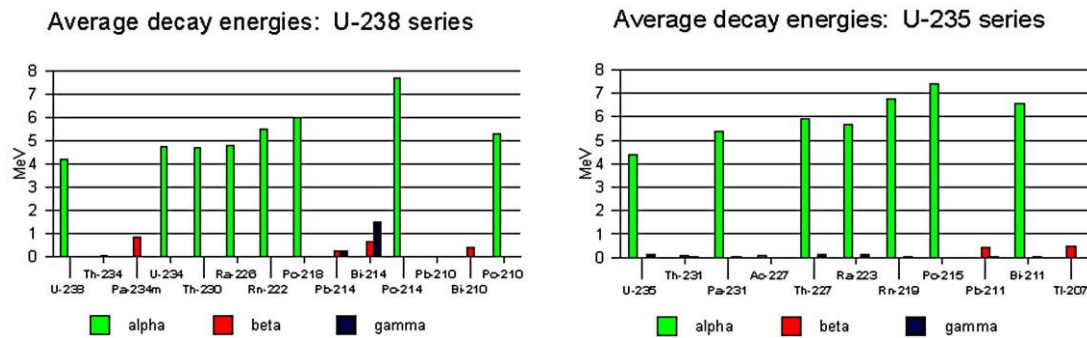


Figure 2-2: Average decay energies of U-238 and U-235 series. Source: WISE Uranium Project [25].

Due to the short range of alpha particles, traditional detectors which require direct interaction with the alpha particles must be used in very close proximity to a contaminated surface, around 1 cm [5]. This makes detecting alpha radiation time consuming, taking in the order of hours for one room [26]. It also requires the use of PPE to prevent ingestion by personnel in close proximity to alpha sources, including the danger of inhalation if disturbed, contaminated material becomes airborne. It may also be necessary to protect against exposure to other types of radiation which may also be present. Samples are taken from suspected areas and analysed in a vacuum for complete characterisation [5] which can take significant time and cost [27].

Due to these difficulties, and those in the development of direct alpha particle detectors, a new way to detect alpha radiation is being sought which can be accomplished at a distance using secondary effects, for example alpha-induced air-radioluminescence. In this chapter the authors review such alpha detection techniques and discuss further improvements and prospects for nuclear decommissioning applications.

2.4 Alpha-Induced Air-Radioluminescence

The most prevalent method of detecting alpha radiation at a distance is through the detection of the UV photons emitted by Nitrogen after receiving energy from alpha particle emissions. After emission from a source, an alpha particle's energy is transferred directly and via secondary electrons, to molecules with which they interact. When these molecules relax they may emit an Ultraviolet (UV) photon. Although the alpha particle and the secondary electrons they generate through ionisation have a range of only a few centimetres (depending on their energy), UV photons have a much longer MFP in air than alpha particles and therefore can be detected at a much greater distance from the source than a traditional detector would allow.

Researchers found the range of alpha particles with energy of 5.1 MeV to be 38 mm in air, with the area of highest intensity of radioluminescence scintillation within a radius of 10 mm from the source [13]. Others found by simulation that the range within which the energy of the alpha particle was transferred was approximately 5 cm for a 6.1 MeV source [26]. For a point source in space, the zone of alpha particles would be a sphere with a radius of the range of the alpha particle emissions. For a point source on a surface this would be a hemisphere with the same radius, see Figure 2-3 [17,28].

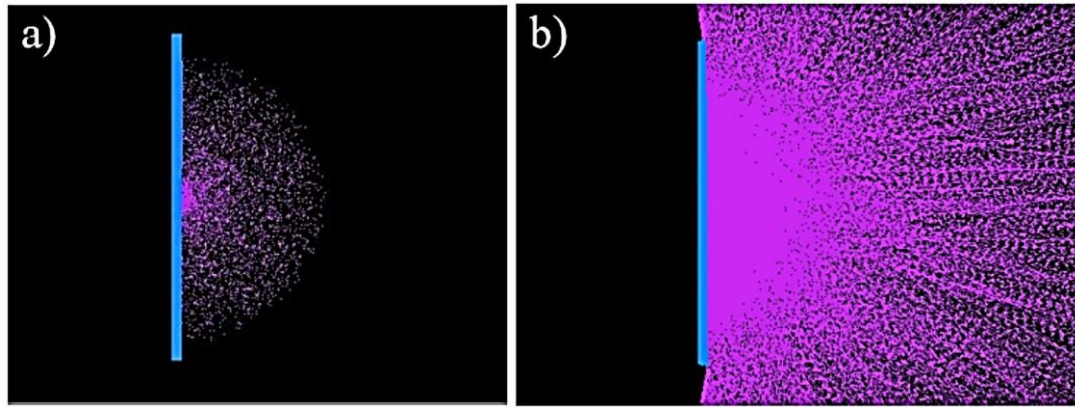


Figure 2-3: Model of: (a) Radioluminescence photons induced by alpha particles showing the hemisphere in which they are initially created by the alpha particles; (b) Showing the random directions in which the photons are emitted from the hemisphere in (a) and their longer path length—Using FRED Optical Engineering Software (Photon Engineering LLC) [17].

Reprinted with permission from the author.

The photons generated, similarly to the alpha particles themselves, form a hemispherical zone for a point source on a surface. This has a radius of many metres due to the longer travel of photons. The intensity of the radioluminescence decreases with an inverse square relationship to the distance from the source (see Figure 2-3) [25].

Although other gases present in air may also emit UV photons, Nitrogen which is the main constituent of air, has been proven to be the main emitter in the 300 to 400 nm wavelength range, in which 95 % of the radioluminescence intensity occurs [1,29]. Hence, research has been focused on this gas in particular. The radioluminescence has a discrete spectrum as can be seen in Figure 2-4, which shows the main intensity peaks of Nitrogen radioluminescence and their relationship to the 2P and 1N energy states from which they arise. Some gloveboxes may be Nitrogen or Argon filled as an alternative to air for operational purposes. An increase in the Nitrogen concentration has been shown to provide an increase in radioluminescence intensity, likely due to the reduction in Oxygen which quenches radioluminescence [30]. Argon may also provide

a more intense radioluminescence, though this requires further experimentation and verification.

Much of the radioluminescence seen in air and Nitrogen atmospheres is within the range of solar radiation wavelengths (see Figure 2-5). The intensity of daylight above approximately 300 nm is far greater than the intensity of radioluminescence due to the presence of an alpha source. Sunlight irradiance in 300 to 400 nm wavelength range reaches $(2-8) \times 10^{-2} \text{ W cm}^{-2} \text{ nm}^{-1}$, whereas the brightness of the peaks of Nitrogen radioluminescence are in the order of 10^{-10} to $10^{-7} \text{ W cm}^{-2} \text{ nm}^{-1}$ for sources within the $3.7 \times 10^7 \text{ Bq}$ activity range, and even at night the ambient light will be greater than the radioluminescence signal [1]. This provides a challenge to the detection of alpha-induced radioluminescence where a large background signal is present which must be removed by filtering, working in darkness or avoiding the range of sunlight by working in the UVC wavelength range (180–280 nm).

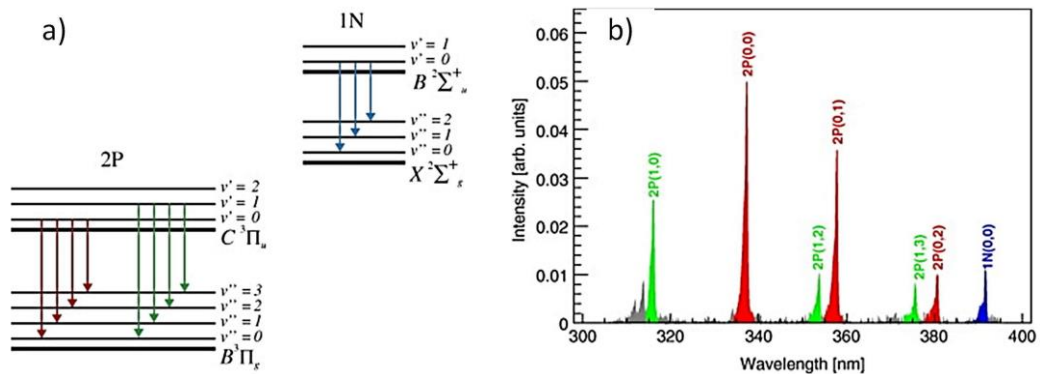


Figure 2-4: (a) Scheme of energy states of the 2P and 1N electronic-vibration band system of N_2 and N_2^+ ; (b) Nitrogen radioluminescence spectrum between 300 nm and 400 nm in dry air. The same colours are used in (a,b) for the corresponding spectral bands. Reprinted from [29] with permission from Elsevier.

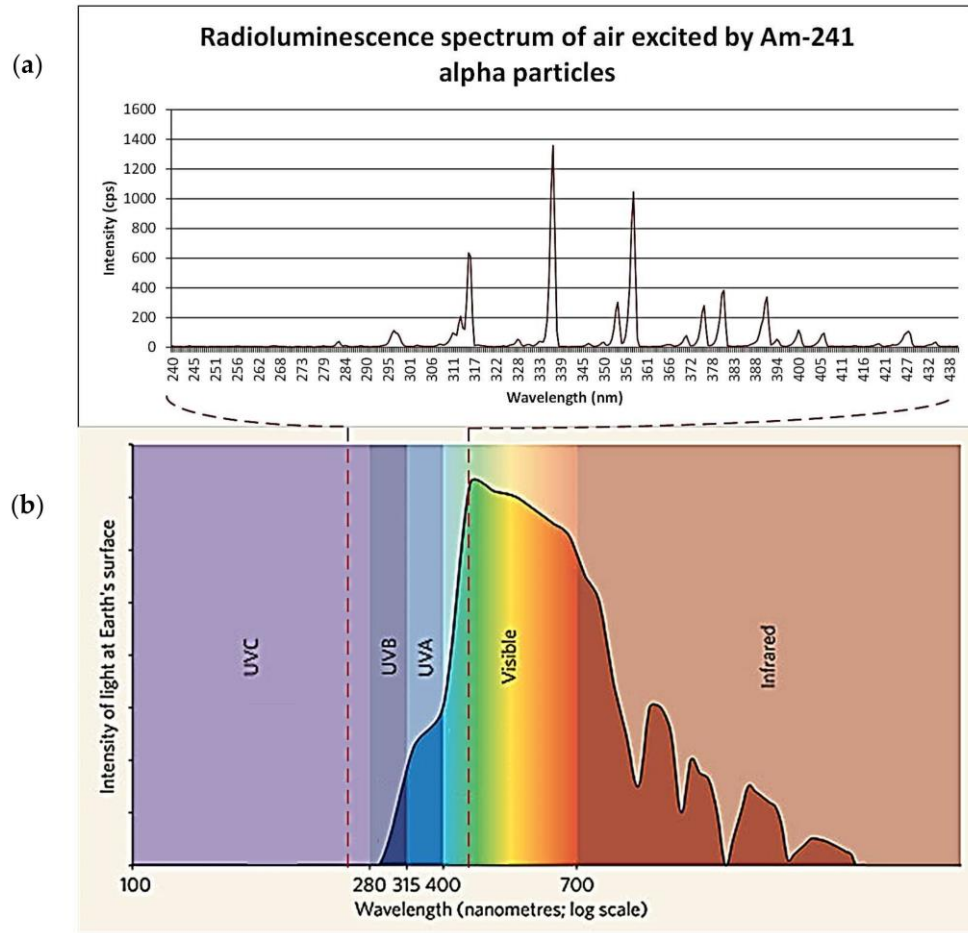


Figure 2-5: Comparison of the spectrum of alpha-induced photon wavelength in comparison with the spectrum of sunlight at the surface of the earth [18, 31]. Image (a) produced using data with the permission of the author [18]; Image (b) reprinted from [31] by permission from Springer Customer Service Centre GmbH.

Kerst et al. [32] investigated the effect of Nitrogen on radioluminescence in the UVC wavelength range. They note that although molecules in air can potentially emit light of below 300 nm, only N_2 can produce an amount which is detectable. They therefore tested a ^{210}Po source in a N_2 purged atmosphere and found increased radioluminescence in the sub-300 nm wavelength range due to an increase in NO luminescence, see Figure 2-6. This increase in radioluminescence in the solar blind region has implications in detection without the interference of background light if replicable in field conditions. However, little effect has been found on the CPS (counts

per second) recorded by a UVC detector (UVTRON, Hamamatsu) when N₂ was flowed over a ²¹⁰Po source [33]. This may have been due to using a flow rather than a purge.

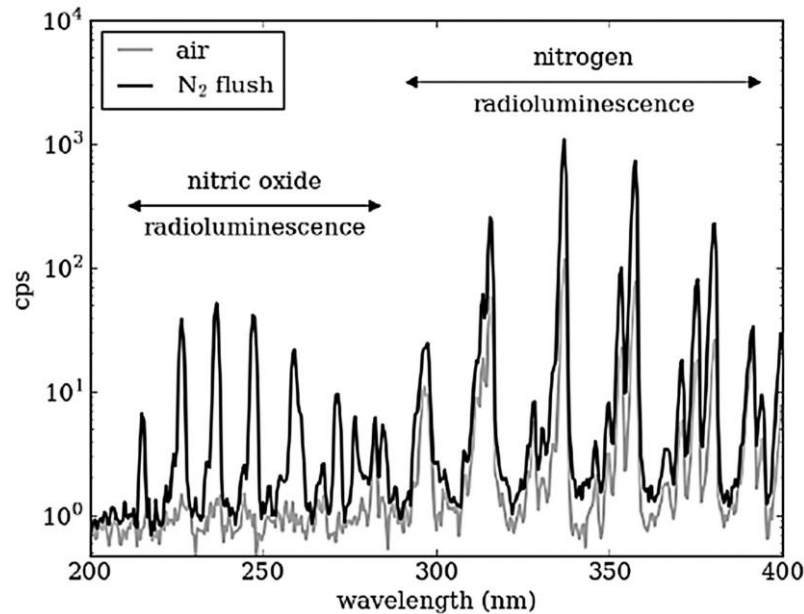


Figure 2-6: Increase in radioluminescence in the 200–400 nm wavelength range using an N₂ purge. Reprinted from [32] with permission from IEEE.

In calculating the number of UV photons produced in the process of radioluminescence, several results have been put forward, with values ranging from 20 to 400 depending on the number of alpha particles and the energy [1,17,28,34]. Two more recent pieces of research specifically looking at the radioluminescence yield of alpha particles, Sand et al. [34] and Thompson et al. [35], were able to correlate their findings with previous cosmic ray analysis of secondary electron radioluminescence, which would seem to verify their results. Sand et al. [34] concluded that there are 19 ± 3 photons per MeV of energy released from the source. This remains linear between 0.3 MeV and 5.1 MeV. Therefore a 5.1 MeV alpha particle would cause the emission of on average 97 photons. From their measurements, Sand et al. [34] found the efficiency for

conversion to luminescence from kinetic energy was 6.7×10^{-5} using 350 nm as a representative wavelength for all photons.

Thompson et al. [35] have developed a model which as part of the Geant4 simulation software framework, is able to predict the yield of air-radioluminescence photons produced by ionising radiation from alpha and beta radiation sources in the first negative and second positive excited states of N_2 . Their results are sufficiently close to those found in experimental methods, for example Sand et al. [34], for confidence in the predictive capabilities of the model. Thompson et al.'s [35] model predicted 18.9 ± 2.5 photons per MeV, whereas Sand et al [34] detected 19 ± 3 photons per MeV, showing a strong correlation between results from the simulation and results from observation. Thompson et al. [35] found that a linear correlation existed between alpha energy from sources below 5 MeV and the number of photons produced, also in agreement with existing observations.

It can therefore be asserted with some confidence that there are approximately 19 photons produced per MeV of alpha energy released from the source.

The energy of the photons produced is linked to their wavelengths which are in turn dependent on the gas in which the ionisation takes place. In Nitrogen this is well known and Figure 2-6 shows the peaks for a Nitrogen atmosphere. This is similar to air, where Nitrogen is the main component, although Oxygen quenches some of the Nitrogen radioluminescence, as can be seen by the difference between air and an N_2 flush.

Other atmospheres have also been tested. For example, Grum et al. [10] in research into corona discharge devices identified the emission spectra of corona discharges in Nitrogen, helium and air. In a Nitrogen atmosphere, they found that in the UVC range it is:

$$h\nu + n \rightarrow X \quad (2.1)$$

mechanism that is responsible for the emissions, rather than:

$$C3\pi u \rightarrow B3\pi g \quad (2.2)$$

which is the primary mechanism above 300 nm. Below 300 nm they also identified additional lines in the air spectrum that are not in the N₂ spectrum, possibly from contaminants or CO₂. In helium the spectrum below 300 nm shows only a weak emission at a wavelength of 249 nm. However, it shows a strong signal at 389 nm, whereas Nitrogen shows strong signals at 358 and 337 nm, and medium strong at 316 nm. If a gaseous atmosphere is to be used to enhance the radioluminescence signal, it would therefore appear that N₂ would be more beneficial than helium.

Thompson et al. [35], alongside developing a model of radioluminescence yield, also investigated the distribution of photons from alpha and beta sources using their simulation. They assert that an alpha source would be easier to locate due to the increased intensity of photons closer to the alpha source. Figures 2-7 to 2-9 show how the intensity of photons vary for three different sources, the first (Figure 2-7) being a 5.48 MeV ²⁴¹Am alpha source of simulated 1 kBq, the other two being primarily beta sources. Although in isolation it would appear that each provide a clear indication of the source location, if considered in a mixed radiation environment where there may be several ionising radiation emitters due to contamination, it becomes clear that the isolation of an individual area of contamination may be more easily accomplished for alpha emitting radioactive sources. Thompson et al. [35] suggest that by measuring the size of the corona, it might be possible to estimate the energy of the alpha emission

which may provide a means to identify the source material, although the difficulty of isotope identification is discussed later.

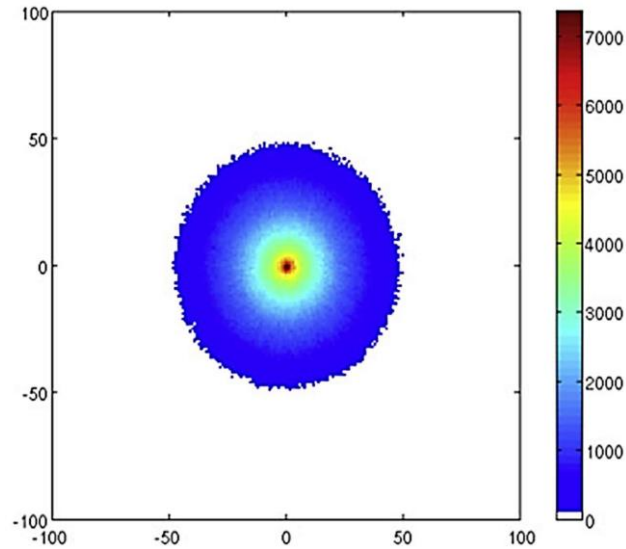


Figure 2-7: Number of photons emitted per mm^2 attributed to the 337 nm emission in a 200×200 mm area as observed from above a ^{241}Am source dispersed over a 2 cm radius circle on an Aluminium surface. The ticks give the x and y positions in mm. Reprinted from [35]

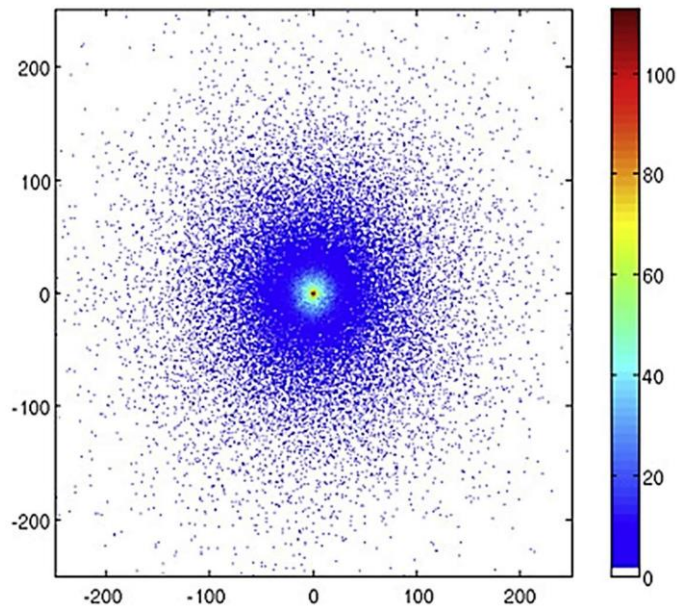


Figure 2-8: Number of photons emitted per mm^2 attributed to the 337 nm emission in a 500×500 mm area as observed from above a ^{60}Co source dispersed over a 2 cm radius circle on an Aluminium surface. The ticks give the x and y positions in mm. Reprinted from [35]

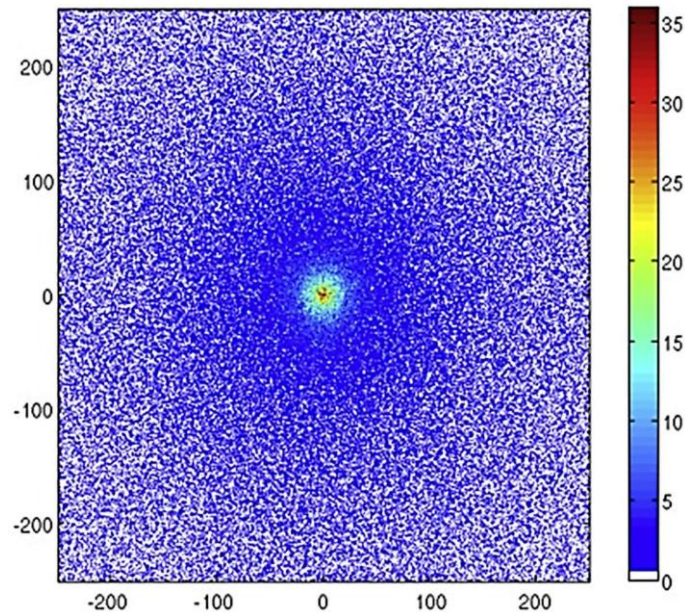


Figure 2-9: Number of photons emitted per mm^2 attributed to the 337 nm emission in a 500×500 mm area as observed from above a P-32 source dispersed over a 2 cm radius circle on an Aluminium surface. The ticks give the x and y positions in mm. Reprinted from [35]

It can therefore be seen from the research carried out to date that there are approximately 19 photons produced per alpha emission, 95 % of which are in the 300–400 nm wavelength range, which is within the solar radiation spectrum at the surface of the earth. The flight of an alpha particle depending on energy is approximately 35–50 mm. Within 10 mm of the source will be the greatest intensity of radioluminescence, with the photons traveling many metres in a spherical or hemispherical pattern, depending on the source geometry.

2.5 Advantages and Drawbacks of Using Radioluminescence

There are several benefits to detecting alpha particle emissions via radioluminescence from ionisation. The main benefit is that detection can be carried out with a greater distance between the source and the detector, reducing detection costs, time and risk to personnel, enabling automated or manual scanning. Photons have a much greater MFP

than alpha particles. In comparison to the 50 mm or so MFP of alpha particles themselves, the induced photons can travel 1 km at 200 nm and 10 km at 280 nm in typical atmospheric conditions [4]. As the photon flux drops off with an inverse square law relationship, the further away from the source that the detector is placed, the more difficult it is to detect the source due to the reduction in signal strength. As UV photons will pass through certain translucent materials, detection of alpha contamination can be carried out without breaching containment in instances such as glove boxes or sealed sample bags [5] although modification may be required by the addition of suitable materials.

The radioluminescence phenomenon will always be seen when alpha contamination occurs, and so can be used in all situations. Due to the distribution and reflection of photons, it also does not depend on a line of sight to the alpha source. For example the 'glow' may be visible behind an item in a glovebox. This glow can also be imaged and overlaid on a photo of the area in question, which gives a pictorial view of the contamination well suited to analysis by personnel who can then 'see' where the contamination is. This image could also be analysed to provide numerical data for the intensity.

Due to the short range of the alpha particles, the photon emissions are relatively local to the source allowing accurate location of the contamination. This also allows differentiation between alpha and other forms of ionising radiation, which occur over a longer range and therefore cause less intense radioluminescence [28]. Researchers found that the ratio of intensities between alpha, beta and gamma induced radioluminescence were $1:10^{-8}:10^{-10}$ respectively, allowing the much greater intensity of alpha radioluminescence to be detected in the presence of other radiation sources [1].

Although theoretically desirable, there are also considerable difficulties with using the radioluminescence approach. The main issue that needs to be overcome is separating the alpha-induced air-radioluminescence from background UV radiation, i.e., sunlight or background lighting. Although the Nitrogen radioluminescence has a distinct spectrum, see Figure 2-4, the main peaks of this spectrum are in the UVA and UVB bands of light (UVA 315–400 nm, UVB 280–315 nm wavelengths) (see Figure 2-5). Therefore, background light can strongly affect the ability of detectors to identify the relatively weak signal produced by alpha emissions within these wavelength ranges. This inhibits and restricts the use of many of the detectors trialed to date to darkness or carefully controlled lighting conditions, which is unfeasible for most practical decommissioning purposes where a wide range of different environments will be encountered.

UV radiation from the sun in the wavelength range of 200 to 280 nm, known as UVC, is absorbed in the atmosphere by Oxygen and ozone [36] therefore there is little background at the earth's surface in this wavelength range from natural light. Fluorescent lighting also emits very little UV light as this cannot be seen by the human eye and is therefore unwanted. Some fluorescent lamps may emit UVC at 254 nm which is the wavelength at which mercury fluoresces, as this is the mechanism through which fluorescent tubes operate [37]. So there is likely to be some background UV from interior lighting, but little of this will be in the UVC wavelength range for a properly operating lighting system.

Due to the low intensity of the UV radiation from the Nitrogen radioluminescence, a high signal-to-noise ratio is required in order to differentiate the signal from any background, and long collection times are needed, in the order of minutes to hours, to reliably detect the signal. Conversion efficiency is the ratio of the

energy of the particle transferred to the air during ionisation and the energy converted to radioluminescence. Conversion efficiency figures for the generation of air radioluminescence vary between 1×10^{-5} [1] to 6.7×10^{-5} [18]; 1.5×10^{-5} has been used as a conservative estimate in other work [28].

There are also issues with calculating the exact yield of this radioluminescence. Energy lost to the air has been used to calculate the yield, but due to internal absorption of the source and the complex mechanism of ionisation, it is not always possible to predict yield from a specific isotope via energy lost. As the nature of the radioluminescence does not depend on the isotope emitting the alpha particle, but depends on the energy levels of the gas atmosphere, this makes isotope identification at best complex and at worst impossible using this technique.

In 2013, Roberts [4] looked at the feasibility of using alpha-induced air-radioluminescence for the detection of radiation sources. Through a series of calculations and a number of Geant4 simulations, it asserted that a source with 10^{10} decays per second at a distance of 10 m, would produce a signal of 10's or 100's of photons per centimetre square. To verify the presence of the signal suggested by the calculations and simulations, experiments were carried out to detect a ^{210}Po source, using a photon counting module and bandpass filter. This verified the emission of photons in the solar blind range by an alpha source, but did not quantify the number of photons in this wavelength range. Although limited in its results in terms of quantifiable experimental data, this work was able to verify the presence of UVC photons and demonstrated an ability to detect these, albeit in dark conditions due to the photomultiplier having some ability to detect photons of above 280 nm. It concludes that it may be feasible to use this method to detect alpha or other ionising radioactive sources, however this would depend on the situation, and that further research would

be required, including determining the yield efficiency more accurately for this wavelength range [4].

One other consideration when trying to detect alpha induced radioluminescence photons is the transmittance of UV photons through visible light translucent materials. This is important in both optical elements of any detection system, for example lenses, filters and detector windows, as well as those found in field conditions, for example glove boxes or hot cell windows. The transmittance of a material will depend on the properties of that material and the wavelength of light trying to pass through. All forms of translucent materials have a transmission spectrum which determines how much of each wavelength of light is absorbed or allowed to pass through. This can be tuned by the addition of transition metal, rare-earth ions or nano-crystals to produce band pass filters, which can be useful in blocking out unwanted light.

Although limited in scope and the number of samples used, Lamadie et al. [15] investigated the transmittance of several materials. They determined that 1 mm thickness of Plexiglas would have a transmission of 91 % relative to air, 1 mm thickness of polycarbonate would have a 92 % transmission relative to air and that 1 mm thickness of triplex would have a 91 % transmittance relative to air. However, they do not take into account any specific wavelength differences. The images they present using their detection equipment in the UV range were carried out using a 10 mm thickness of Plexiglas, where they were able to image a source in excess of 1 MBq cm^{-2} at 1 m distance, closer for less active sources. Sand et al. [13] quote attenuation of 80 % by Plexiglas. However, they do not specify the thickness of the Plexiglas, which they refer to simply as a 'standard Plexiglas glovebox'. Others have shown various successes at imaging UV photons through Plexiglas, although the images were in the main indistinct [15, 38].

In the case of in situ materials, such as glove boxes and detector windows, the attenuation of UV photons can be a significant issue. As part of the research into a stand-off detector several of the researchers have looked into this issue and these results are included in this review.

For full characterisation, not only the presence but also the isotope is required. Although it is theoretically possible for the activity, or at least the emission rate, to be calculated from the intensity of the radioluminescence signal, the wavelength of the optical photons emitted are determined by the gas in which they occur, as opposed to the energy of the alpha particles. As yet, work has not been undertaken on isotope identification, and hence Section 2.6 looks at alpha particle detectors rather than systems which characterise the isotope.

2.6 Alpha Particle Detectors

This section explores the benefits and drawbacks of traditional detectors which are commercially available, and looks at the prototype and test detectors designed to detect and locate alpha sources through air radioluminescence. Some novel further ideas are also presented. The detectors included are designed to identify the location of an alpha emitter and not to characterise that source, hence carrying out part of the characterisation required for nuclear decommissioning, but not all.

2.6.1 Traditional Detectors

Currently, characterisation of sites in regard to alpha contamination is carried out by taking samples which are then analysed in order that the contamination can be identified and characterised. This process takes significant time as samples must be collected and recorded, sent to a suitable laboratory, analysed, and the results returned in a suitable

format [27,39]. Therefore it is desirable to have a less time consuming and labour intensive process to locate and identify alpha contamination. The detection of the alpha contamination is traditionally carried out using hand-held alpha radiation detectors.

Although hand-held alpha radiation detectors are readily available, these are in general intended for the immediate detection of alpha radiation for health physics purposes and not characterisation [40]. As these alpha particle detectors, which use a Geiger-Muller tube or more recently a scintillator, work through direct interaction with alpha particles the detector-source distance must be less than that of the range of the alpha particles [1]. This means that the detector must be positioned within a few centimetres of the source in order for alpha radiation to be detected. The benefits of these kinds of detectors are: fast results through the immediate detection of the presence of alpha particles (typically within seconds); good localisation of sources through close proximity requirement; portable; readily available; mature technology.

Although for certain detection purposes this is acceptable, there are drawbacks: proximity to the source provides a hazard for test personnel and requires the use of PPE; detectors may become contaminated if they inadvertently touch the source in hand-held applications; complex plant geometries may make contamination by touch more likely and scanning harder to achieve; time consuming to scan large areas; access issues (limiting penetrations to areas which require characterisation); use in areas of high radioactivity (including safety of personnel, levels of PPE required and contamination of equipment); limited collection of data not suited to isotope identification; no associated automatic mapping of contamination onto an image or map for location purposes.

Hence, it is desirable to find a new method of alpha particle detection which: can be carried out at a distance; is operated remotely; scanning based; completed on site;

portable; and possible through clear/translucent barriers (e.g., glove box sides or viewing windows). Therefore, a new way to detect alpha radiation has been sought through secondary effects of alpha particle emissions.

2.6.2 Alpha-Induced Air Radioluminescence Detectors

Alpha-induced air radioluminescence detectors may provide a way forward in overcoming the shortcomings of traditional detectors and there has been significant research in this area in devising a prototype system. Table 2-1 shows the results of various alpha particle detection research and is included to provide some comparison between the results of different research projects. As can be seen from Table 2-1 the differences in distances, sources, exposure times, conditions and detector methods makes comparison of the methods and results difficult in determining the most efficient system to date, but some broad conclusions can be made by a comparison in this manner. As of yet, these detectors are designed to locate an alpha source with various success, but identification of the source isotope has not as yet been achieved which would be required for full characterisation.

The remainder of Section 2.6 looks at this research in more detail, dividing the detectors by technology type.

Table 2-1: Summary of alpha particle detection research to date.

Authors Year [Ref]	Distance / Time / Activity (Where Known)	Source	Equipment	Conditions
Baschenko 2004 [1]	30 m / - / 3.7×10^7 Bq	^{239}Pu	Monochromator & PMT for spectrum Reflector & film for image	Darkness Presence of strong gamma source
Lamadie et al. 2005 [15]	1 m / 600 s / <1 Mbq. cm^{-2}	^{244}Cu	CCD, Fused silica objective lens	Through 10 mm Plexiglas, Darkness, Field Test
	10 cm / 3600 s / 30 kBq	^{241}Am	“	
	20 cm / 5 h / 3.88 kBq	^{238}Pu	“	

Giakos 2008 [41]	25 m / - / two 3.7×10^7 Bq sources	^{239}Pu	Spectrometer, ICCD camera, lenses, reflectors	Theoretical. Daylight. In presence of 18.5×10^7 Bq ^{60}Co gamma source.
Ivanov 2009 [42]	3 m / 600 s / 10^5 Bq	5 MeV alpha emitting, point source	“	Estimate of performance in daylight
Ivanov 2011 [43]	10000 s / - / 5×10^4 Bq		DayCor UV camera	Daylight
Leybourne et al. 2010 [44]	150 m / <1 min / 5 mCi (185 MBq)	^{210}Po	PMT, Filters	Field experiment
	150 m / - / 1 mCi (37 MBq)	“	“	Theoretical
Sand et al. 2010 [17]	0.4 m / - / 1.2 kBq, 620 CPS	^{239}Pu , ^{241}Am , ^{244}Cm	HAUVA (own design)	Spectral filtering
	0.4 m / - / 1 s, 100 kBq		“	Yellow radioluminescence or white LED light
	0.4 m / 1 s / 1 kBq	^{241}Am	„	‘Selected room lighting’
	0.2 m / - / 13 kBq	„	„	Coincidence filtering
Sand et al. 2013 [12]	- / >1 s / -	U, Pu	EMCCD	Darkness
Sand et al. 2015 [13]	- / 0.5 s / 0.52 GBq	Pu nitrate	„	Darkness, glovebox, quartz window
	- / 30 s / 4.0 GBq	Mox pellet	„	„
	- / 100 s / 0.52 GBq	Pu nitrate	„	„
	- / 100 s / 52.79 MBq	^{239}Pu planchette	„	„
Sand et al. 2016 [18]	1 m / 10 s / 4 kBq		PMT, optics, filter stack	UV-free lighting
	1 m / 10 s / 800 kBq		„	Bright fluorescent lighting
Inrig et al. 2011 [26]	1.5 m / 10 s / <37 MBq	^{241}Am	PMT, filter, optics	Artificial light (60 Hz)
Ihantola et al. 2012 [14]	0.157 m / - / 4200 Bq	^{241}Am	PMT, filter, optics	Light tight box, Nitrogen atmosphere
Ihantola et al. 2013 [5]	0.1 m / - / 50 Bq	^{241}Am	„	Red LED lighting
Kume et al. 2013 [16]	1 m / 30 s / 1.5 kBq	^{241}Am	PMT, lens, mirror	Darkness
	1 m / 20 s / 9 kBq		„	LED light–centre wavelength 635 nm
	1 m / 30 s / 1.5 kBq			Theoretical
Crompton et al. 2017 [33]	20 mm / - / 6.95 MBq	^{210}Po	Solar-blind UVTRON flame sensor (Hamamatsu UVTRON R9533)	Ordinary laboratory lighting.

2.6.3 Solar-Blind Detectors

In order to address the main obstacle to detecting radioluminescence, solar-blind detectors, those sensitive only in the UVC wavelength range, have provided the basis for prototype detector systems shown to be operable in normal indoor lighting conditions.

In 2011 Ivanov et al. [43] used an off-the-shelf, solar-blind, UV camera to locate alpha contamination in daylight conditions through air radioluminescence. They had estimated in 2009 [42] that they would be able to detect alpha radiation of 5 MeV energy with an activity between 40 and 100 Bq cm⁻² with a corresponding integration time of 600 s to 3600 s from a separation of 3 m between detector and source. The camera they used (DayCor SuperB UV, Ofil Ltd., Lawrenceville, GA, USA) is designed to show the corona and arcing of high voltage equipment for fault diagnosis [43]. It is ‘blind’ to UVA and UVB (400–315 nm and 315–280 nm wavelengths respectively), and only detects UV light of less than 290 nm (UVC). This removes the interference of the stronger background light, allowing detection of the much weaker air radioluminescence in daylight conditions.

They present an image of a 5×10^4 Bq alpha source with an integration time of 10,000 seconds (approx. 3 h). They also present images of background spots generated by noise, as a single frame and a sum of 7500 frames. This shows an apparently random distribution of these background spots over time, which the researchers were able to filter out to some degree for better sensitivity. They also presented a filtered image taken with a 500 s integration time.

Their use of cameras that are available off-the-shelf and are therefore mature technology is beneficial in terms of the reliability. As yet no one has put forward a tested method to quantify the intensity of the light captured by these images, however

this could potentially be used to determine the activity levels. This work shows that the approach of using solar-blind detectors in detecting air radioluminescence is viable in addressing the issue of background UV radiation interference, although Ivanov et al. note that there is future work to be carried out to quantify and apply their findings [43].

In 2017 Crompton et al. [33] were able to detect the radioluminescence from a 6.95 MBq Po-210 source from 20 mm distance using a solar-blind UVTRON flame sensor (UVTRON R9533, Hamamatsu, Hamamatsu City, Shizuoka Pref., 430-8587, Japan) in ordinary laboratory lighting. This sensor is designed to detect the UVC emissions from flames for fire detection purposes and is sensitive in the 180–260 nm wavelength range. The sensor was used with the manufacturer's off-the-shelf driver board configured to emit a pulse for each UVC photon detected. An average pulse rate of 0.3280 CPS was recorded, with a background pulse rate of $2.224 \times 10^{-3} \pm 0.7034 \times 10^{-3}$ CPS. A fused silica window was inserted between the sensor and source to prevent alpha particles directly impacting on the sensor. Although the distance between sensor and source is small, they assess that in this configuration the maximum detectable distance could have been 240 mm.

Crompton et al. [33] also tested flowing various noble gases over the source. They found that Xenon increased the CPS by 52%, P-10 increased the count by 32%, Neon by 26%, and Krypton 23%. Interestingly they found that Nitrogen had little effect on the CPS. However, they note that these results require replication for verification, especially in light of the difference between the increase in radioluminescence reported in a Nitrogen purge (Hannuksella et al. [30] and Ihantola et al. [5]) with the flow results presented by Crompton et al. [33].

Although the sensor used in Crompton et al.'s [33] research was only shown to work over a short distance in these experiments and its ability for locating the source

was not tested, they point out that these initial experiments indicate that this sensor may be viable for stand-off alpha detection if used with other elements in a detector system. This is due to its low background count and insensitivity to indoor lighting conditions. Also, that using a flow of gas which could be achieved through the deployment of a thin flexible pipe, which may be more easily provided in field conditions due to not requiring a gas-tight enclosure and the purging of air, could enhance radioluminescence for detection purposes. This presents a far from developed detector system, but does show a possible sensor which could be used as a foundation for the development of such.

Shaw et al. [36] note the limitations of using PMTs (photomultiplier tube) to detect UVC photons, and explore the background and function of new detectors in development, Geiger-mode avalanche photodiode (GM-APD) detectors. This semiconductor based alternative may make alpha induced air radioluminescence easier to detect than using CCD (charge coupled device) or PMT. They compared five different existing detection technologies, before detailing the GM-APD detector. In their tests this shows a better quantum efficiency at a wavelength of 270 nm (just inside the UVC range). Although their work does not include any testing for alpha detection, this provides an alternative detector technology which may prove useful in the detection of alpha induced radioluminescence. They also explore a number of possible applications of this technology, including the imaging of deep-UV (UVC).

The use of UVC detectors seems to somewhat overcome the issue of background interference from other light sources, however the low signal strength due to the smaller number of photons emitted in this wavelength range is an issue in terms of the distance at which these may work. Others suggest though that solar-blind detectors may not be completely 'solar-blind' and hence that the use of external filters

to ensure that there is no interference from longer wavelengths may still be required [36] although these would also attenuate the signal.

2.6.4 UVA and UVB Cameras

Other detectors trialled to date specifically focus on the main peaks in the Nitrogen radioluminescence spectrum, which occur at wavelengths between 310 and 400 nm, as 95 % of the intensity falls into this range [1]. Although in this range the number of generated photons is greatest, the intensity of UV radiation from other sources is much higher, i.e. sunlight and traditional artificial light. Therefore, these detectors must be used in complete darkness or with artificial lighting of specific wavelengths, even when filtering or background rejecting methods are used. This limits their practical application.

Work using camera-based systems has mainly focused on locating alpha sources rather than characterising them, with an overlaid image of the radioluminescence over a conventional image being the preferred method of demonstrating the presence of an alpha emitter. This results in images where contaminated surfaces seem to ‘glow’.

Lamadie et al. [15] used a CCD and objective lens to detect alpha sources using radioluminescence. The CCD was cooled with liquid Nitrogen and was backlit, which gave it a 60 ± 5 % quantum efficiency (QE) in the 300 to 400 nm wavelength range. This is in comparison to Sand et al. [13] whose EMCCD (electron multiplying CCD) achieved a maximum QE of 38 % in the Nitrogen radioluminescence wavelength range.

They noted that the luminescence was visible in what they termed a ‘bubble’ around the source with an approximate radius of the range of alpha particles emitted from the source, with the intensity reducing relative to the square of the distance from the source [15]. They found these ‘bubbles’ limited the separation distance between sources at which the two luminescence zones could still be distinguished, which was

greater than the resolution of the equipment used, and was between 30 mm and 50 mm depending on the energy of the alpha particles. They were also able to detect bulk contamination, showing that internal absorption that did not fully restrict the emission of alpha particles did not prevent detection.

They developed two equations to calculate the activity of the sample based on the signal intensity and the number of photons per alpha emission, both of which were verified by their experimental results.

The limitation of Lamadie et al.'s [15] work is that it required long integration times of between 1 and 5 h and was carried out in complete darkness. It does however provide advancement in the quantification and characterisation of the radioluminescence phenomenon.

In 2013, Sand et al. [12] tested an EMCCD device to carry out alpha imaging in a glove box with a quartz glass window. They were able to image two mixed fuel pellets (U and Pu), with a 60 s exposure time. The experiment was most likely carried out in darkness as they cite this as being beneficial.

Sand et al. [13] continued with this work in 2015 when they compared the efficacy of two low light cameras; an EMCCD and an intensified CCD (ICCD). They tested both the differences between the two cameras and also the effect of detecting several sources of different activity at the same time. Their samples were of various alpha emitting materials, and activities ranged from 106 kBq to 4.3 GBq.

Both Sand et al.'s [13] systems are sensitive to natural light (visible and UV) and therefore tests were carried out in near darkness. Testing was carried out in a modified glove box where one of the glove ports had been replaced with a quartz glass window to allow a 90 % transmittance of photons, as compared to approximately 80 %

attenuation by standard glove box Plexiglas. They then overlaid their optical results onto a conventional image.

Their images show that although the higher activity sources were detected, those emitting similar radioluminescence intensities to the low background light were undetectable to both systems. They were able to achieve a resolution of better than 1 cm between sources. They also found that high intensity sources could mask lower intensity ones and suggested re-imaging after the removal of high intensity sources to check for sources of lower intensity, using longer exposure times or reduced background lighting. Sand et al. [13] conclude that the ICCD gave marginally better results in the field than the EMCCD, partially due to its greater field of view.

Pineau et al. [45] (patent registered) put forward a proposed stand-off alpha detection system which is broad-ranging in its description, and as such all avenues of operation it describes may not necessarily have been shown to work. Their main assertion is to fill the environment containing the source with a scintillating gas, which may contain Nitrogen. As Nitrogen has been shown to be the main radioluminescence emitter in the UV range, this is consistent with other findings. This could be in an enclosure which is placed over the area to be investigated, which will retain the scintillation gas and has a window transparent to UV photons. However, the flow of gas used in other work [33] could be easier to apply in the field than the need for a gas-tight enclosure to be deployed in potentially difficult to access or contaminated areas.

Pineau et al.'s [45] detector is described as being a CCD type detector, connected to a ST 138 type controller. Due to the small number of photons produced, the system will integrate a number of images, therefore increasing the detection time. They suggest using a wavelength range of 200–400 nm. The device may also have a camera able to take a visual image over which to overlay the image of the alpha induced photons. Due

to the possible interference of light in the visual spectrum, they suggest using the system in darkness or using filters to attenuate light outside of the UV spectrum. No results are presented in the effectiveness of this system, however, for a patent to be applied for it may be assumed that they were confident that this system would work, and tests may have been successfully carried out.

Haslip et al. [46] use a comparison of the alpha induced Nitrogen radioluminescence signals of four wavelengths; two wavelengths where Nitrogen radioluminescence peaks, and two where it does not which present the background signal. A telescope is used to collect the signal, which is amplified by mirrors and focused on six UV-sensitive cameras. This is achieved through the use of beam splitters and wavelength selective filtering. Images from these six cameras are collated by a microprocessor proving an aggregated image to the operator which is in almost real-time. Although this system is not able to reject daylight, it can be used at night where there is still a significant amount of background UV radiation, or in the presence of street lighting.

In 2008 Giakos [41] proposed a stand-off alpha detector architecture using a spectrometer and ICCD camera, with a focusing assembly of lenses and reflectors. Their calculations indicate that two 3.7×10^7 Bq ^{239}Pu sources could be detected at 25 m, even in the presence of an 18.5×10^7 Bq ^{60}Co gamma source. They also suggest that the use of an active system using a Raman lidar system along with the passive radioluminescence detector, would not only be able to determine the presence of a radiative source, but also indicate its biological hazard by determining the energy loss associated with the detected light through the specific spectrum. The calculations are presented in their paper to show how the architecture was devised, but there is no evidence that this

system was tested and therefore if it was successful or not, or any limiting factors found during any experimental trials.

2.6.5 UVA and UVB PMT Based Detector

Due to the ability to more easily quantify the signal intensity, other prototypes utilise a PMT to detect the radioluminescence. In 2010 Leybourne et al. [44] reported their prototype detector was capable of detecting a Po-210 source (37 MBq) at 150 m distance from the detector, outdoors. Using optical filtering, telescope optics for collection, and a PMT, they were able to detect the presence of an alpha emitting source on the surface of any one of three, 55-gallon drums spaced 10 m apart at approximately 150 m distance. This was achieved in less than 1 min of data acquisition time for each source. Although not specifically stated, it can be inferred from the text that these experiments were carried out at night as there is reference to ‘heavy traffic’ and ‘other surrounding outside illumination’ causing interference. However, even at night there is significant UV radiation outdoors.

Leybourne et al.’s [44] filtering was able to attenuate background UV radiation and provide a sufficiently high signal-to-noise ratio to differentiate the relatively weak UV radioluminescence. They also noted an inverse squared relationship between the intensity of the UV photon signal and distance, as would be anticipated in a spherical (or hemispherical) isotropic photon emission zone around a point source.

The result of Leybourne et al.’s [44] work is very positive in terms of indicating that it is possible to detect alpha emissions through air radioluminescence in the presence of significant UV background. However, there are several drawbacks and limitations to the work. A relatively crude approach was taken for identifying the alpha source, in terms of a resolution of 10 m between sources (i.e. the distance between the drums) and the variability of the counts which show little more than the presence of a

single or double source rather than anything about the nature of the source. It is possible that the experiments were carried out at night, to reduce the background UV that the device was required to reject. There is little information on the equipment specification or models used to carry out the experiment, meaning that it could not be replicated to check the accuracy of the work. This includes the bandpass of the filtering system. However, whilst limited, this work does show that there are approaches to this method of alpha particle detection which may prove viable in the field.

Baschenko [1] used a monochromator and PMT in photon counting mode to determine the spectrum, and low light sensitive film to image the source. They found that the ratio of intensities between alpha, beta and gamma induced radioluminescence were $1:10^{-8}:10^{-10}$ respectively, allowing the much greater intensity of alpha radioluminescence to be detected in the presence of other radiation sources. This has two implications. The first being that this technique can be used to combat exposing personnel to beta and gamma radiation, which may also be present within the range of traditional alpha particle detectors. The second is that the different types of radiation do not interfere with the alpha detection, making it suitable for mixed radiation environments normally seen within the nuclear industry.

Whilst characterising the alpha induced radioluminescence, Baschenko [1] found that 95 % of this was in the 310 nm to 400 nm wavelength range and was due to the 2^+ Nitrogen transition system. They calculated that there were approximately 30 UV photons emitted per alpha event, with 2.5×10^{-5} of alpha particle energy being transformed to photon energy. They also assert that alpha particles may be emitted in a cone shape with an angular distribution which is proportional to $\cos^2(\theta)$, where θ is the angle between normal to the surface and the flight of the alpha particle, although this

conclusion is not supported by other literature which finds the emission of photons is isotropic [34] and therefore is likely to be a misinterpretation or anomaly in the results.

Baschenko [1] used these results to calculate a possible detector set up. From calculations of the effectiveness of this system, they were able to determine that this would not be suitable for use out of doors as background UV would always exceed the required level, even at night.

Other work of Sand et al. [17] focuses on two potential methods of detecting radioluminescence; spectral and coincidence filtering. In 2010 Sand et al. [17] and Hannuksela et al. [30] tested both these methods. They compared background lighting to the radioluminescence signal using a beam splitter and interference filters in a device they named Handheld Alpha UV Application (HAUVA).

Noting that cameras require relatively long integration times, Sand et al. [17] and Hannuksela et al.'s [30] spectral filtering detection system uses two PMTs, which allows detection using an integration time of approximately 1 s for a 100 kBq source at 400 mm distance from the detector. This was achieved under artificial background lighting conditions which did not produce UV. Using a 40 nm bandpass filter, the signal was first filtered into the peak air radioluminescence wavelength range, 300–340 nm (where 337 nm is the most intense peak of the spectrum). The signal was then split, with the background portion being passed through a further 15 nm bandpass filter giving a 299 to 303 nm wavelength range.

Using two PMTs and a time correlated single photon counting unit Sand et al. [17] and Hannuksela et al. [30] verified that all photons from a single alpha decay were emitted in one 5 ns time window, as found in earlier work. This time period was sufficiently short to make a background count event at the same time as an alpha induced photon improbable. Using coincidence filtering, they were able to detect

radioluminescence against background light which was 500 times more intense than the radioluminescence. At this stage in their work, they quote a value of 400 photons per 5 MeV alpha emission. However this is reduced in later work to 20 photons per MeV of alpha energy, more in line with others' findings.

Sand et al. [17] and Hannuksela et al.'s [30] optimised optics, designed with a large collection angle to collect the greatest number of emitted photons, have a collection efficiency of 0.12 % at 400 mm, and they noted how this dropped off rapidly from 300 mm onwards, showing the importance of distance to source. They also found a rapid drop in signal intensity when the source was moved 20 mm to the side, giving a positive indication for source location possibilities.

By using a Nitrogen-only atmosphere and a 10 kBq ^{241}Am source, Sand et al. [17] and Hannuksela et al. [30] found that the detector CPS increased to 650 CPS, from 150 CPS in normal atmosphere. They attributed this increase to the removal of the quenching effect of Oxygen.

Building on their earlier work, in 2016 Sand et al. [18] published the results of alpha induced radioluminescence detection experiments carried out in bright lighting conditions. Using the same set up with two different equipment options, they were able to distinguish a 4 kBq source at 1 m in 10 s under UV free lighting, and 800 kBq under bright fluorescent lighting.

The general set up for Sand et al.'s [18] experiments comprised of a telescope, utilising two lenses to focus photons onto the eyepiece. This light passes through a filter stack before being focused onto the window of a PMT. The PMT is used in photon counting mode to determine the intensity of this signal. Two different filter stacks and PMTs are used. The first is a PMT with an ultra-bialkali photocathode which is sensitive in the near UV range. The associated filter stack is sensitive at a central wavelength of

335 nm. This was tested under yellow lighting conditions. The other set up utilises a solar blind PMT which has a caesium-telluride photocathode, with a filter stack centred at 260 nm, which was tested under fluorescent lighting conditions.

Sand et al. [18] recognize the limitations of their systems, in that they are not suited to imaging due to utilising telescope optics, and that scans are time consuming due to the narrow field of view. Due to the differing field environments, each site would have to be surveyed in advance to determine if these detector systems were suitable for that particular site. They also note that solar blind camera detection methods can only be used in open spaces, however, the reasoning behind this statement is not qualified.

Kume et al. [16] build on the work of Lamadie et al. [15] and Chichester and Watson [28], whom they consider to have both developed ‘convenient’ systems for stand-off alpha detection, by addressing the issue of noise generated by a high gamma radiation background which create a low signal to noise ratio. They note that Ihantola et al. [5] have gone some distance in noise rejection by using time-coincidence, but that this has not completely removed the background noise generated by gamma-rays. Their solution is an ‘alpha camera’ which utilises a lens and mirror to focus the UV photons onto the UV detector, a PMT with a response in the range of 300–650 nm, peaking at 350 nm (35 % QE). Lead shielding around the PMT and mirror reduces the influence of gamma-rays on the system. A CCD camera, also within the confines of the Lead shield, provides a visual image over which the results of the PMT can be overlaid to provide a visualisation of the alpha contamination’s location.

One limitation of Kume et al.’s [16] work is that this detector currently works exclusively in dark conditions. Their proposed resolution to this issue for field operations is to use a coating on the lens of their system to filter visual light. There is no discussion on the difficulties that this may present due to the attenuation of the UV

light that is likely to occur, or to the wavelength range of the light attenuated by the filter, or what the nature of this coating will be. In practice this may be a more significant issue than they suggest.

Inrig et al. [26] used a position sensitive PMT with UV filters and a series of six lenses to detect a 1 μCi (37 kBq) source from 1.5 m distance with a 10 s integration time. This was accomplished in a windowless room with dim lighting by using an algorithm and the known frequency of oscillation of the electricity supply to the lighting in their experimental environment to reject any unwanted light. They were able to image the alpha sources, although the resolution of the images was poor. This method may be suited to internal environments without windows where the frequency of electronic supply oscillation is known. However, it is possibly not well suited for general field operations.

In 2012 Ihantola et al. [14] used coincident spectrometry of gamma radiation and alpha-induced radioluminescence to enhance alpha detection in areas of high activity. Radioluminescence photons from an alpha emission trigger the operation of a gamma detector. Hence only gamma photons which occur in the presence of alpha induced photons are detected. This ensures that the detector is focused on the alpha emitter and not other gamma emitting sources which may produce photons of a higher energy than the alpha emitter and so mask the alpha source. This was undertaken not only to locate the source, but also to characterise the source and determine the isotope, which cannot as yet be achieved with alpha radioluminescence alone. The alpha detector, comprised of a collection lens and PMT, was able to identify a 4.2 kBq source from 157 mm away in both a Nitrogen or air atmosphere. In Nitrogen the intensity of the signal was 150 times the background, in air 30 times. The 50 mm field of view provided by their test equipment means that a very localised analysis can take place of

the alpha emitter. It is also possible to detect sources in sealed containers if the material of these is transparent to UV radiation, where UV photons will escape, but alpha particles will be stopped by the container.

Their experiments were carried out in the dark, and Ihantola et al. [14] suggest the use of filters for daylight working. Although the system worked, they conclude that the UV system was better for locating the source and the gamma detector for identifying the isotope, and suggest the two could be separated for better efficiency. In 2013 this work was continued using dim red LED lighting which allowed a level of illumination sufficient for working and for imaging of the set up [5]. They note during this work that the coincidence filtering method works better with a high gamma background and integration times of minutes or hours. This method allows an avenue for the identification of the isotope as the gamma emissions are more suited to this type of analysis than alpha induced radioluminescence.

There are limitations to this work of Ihantola et al. [14]. Detection of the alpha-induced radioluminescence photon suffers from the same issues as with other detectors, primarily the interference of environmental light sources. However, Ihantola et al. [14] found that this coincidence spectrometry technique is ten times faster than a conventional gamma spectrometer, and from this it seems that their assertion that it is a step forward is not unsubstantiated.

All of the above research results confirm that it is possible to detect alpha induced radioluminescence in a number of ways and situations, but as these require a background of no, low or special light they are unsuitable to be used in the field at present due to the difficulties in controlling the lighting conditions.

2.6.6 Other Detector Types

Although in the main recent detectors have focused on the detection of Nitrogen radioluminescence photons, this is not the only possible secondary effect of alpha particle emissions which could prove suitable for the detection of alpha contamination.

Sprangle et al. [47] put forward an alternative method of stand-off radiation detection through the use of an ionising laser and a probe beam. Although their work is specifically for gamma detection, they state their intention at some future time to test their concept using an alpha source to reduce the safety issues, though no evidence of this is available to date. Hence this method may be suitable for alpha detection. Ionising radiation produces free electrons in air. These attach themselves to Oxygen molecules and form O_2^- ions in greater concentration to free electrons. A high powered laser, focused close to the radiation source is used to photo-detach the negative ions, which initiates an avalanche ionisation process. A probe beam can then be used to detect the changes in electron density caused by the avalanche ionisation, and the presence of radioactivity determined using measurement of the frequency modulation. The main advantage of this system is that it would be able to detect ionising gamma radiation from distances greater than 100 m.

Sprangle et al.'s [47] paper highlights a potential design concept for a gamma detector, which has two drawbacks when applied to alpha detection. This is a design concept which has not as yet been proven for gamma detection for which it was designed. In addition, an examination of the possible feasibility of using this design for alpha detection is not presented in this paper. For example the much shorter MFP in air of alpha radiation in comparison to gamma radiation is likely to produce a smaller ionisation 'bubble' which may present challenges in focusing the laser sufficiently close to the alpha source without prior knowledge of its whereabouts. It may also find the

materials used for shielded windows challenging, for example in glove boxes or hot cells. However, this does present a possible alternative method of alpha detection at further distances, which may merit further consideration.

In order to address the propagation loss at a distance from the source to the detector, Yao et al. [48] used a collimated beam emission from a Nitrogen laser at a wavelength of 337 nm to further excite alpha ionised air molecules from the $B^3\pi$ to $C^3\pi$ state. The absorption of the energy required was detected and from this the presence of alpha radiation was identified. This detector was successful in detecting a 1.48 GBq source at a maximum standoff distance of 10 m. They found that the detection signal was not sensitive to the distance between the detector and source, as it is with the photon detector methods. In their tests they were able to determine the relative intensities between two sources of different activities. They also note that due to the longer carrier lifetime in the $B^3\pi$ band compared to the $C^3\pi$ band, the population of carriers in the $B^3\pi$ may be an indication of the intensity of the radiation causing the excitation.

Although the work of Yao et al. [48] was successful in identifying the presence of an alpha source its main drawback is the required detector configuration. It requires an emitter and detector diametrically opposite each other in line with the alpha source. This means that both sides of the alpha source need to be accessible, which may not be possible for surface contamination, or in other hard to access areas. It would make scanning difficult to conduct, as the detector alignment would need to be parallel to any source, rather than perpendicular (see Figure 2-10). As the distance from the source to the laser or detector has no effect on the signal it would not be possible to determine the position of the source between the two, and direction to the source would be difficult to determine. Hence, it would be difficult and time consuming to find the source of the alpha emissions.

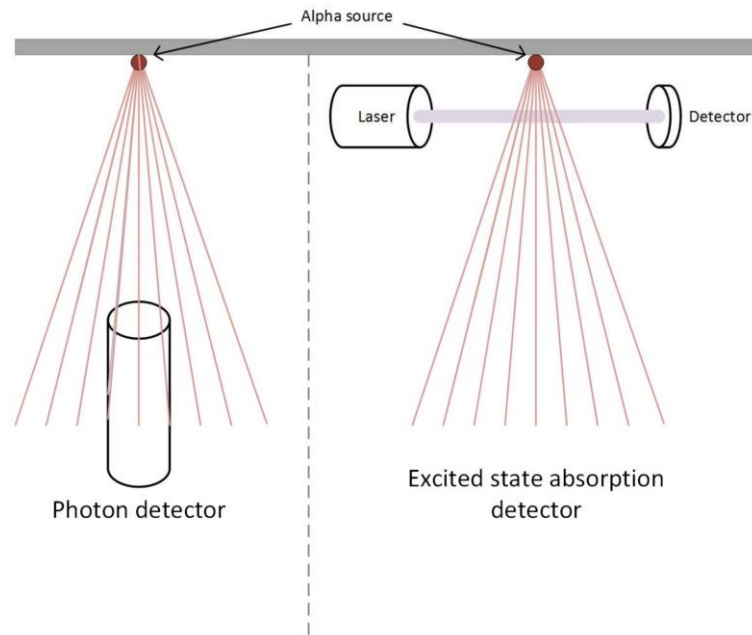


Figure 2-10: Deployment of photon v. excited state absorption detector systems.

Baschenko [1] suggests a similar alternative method, using a laser of specific wavelength which would affect air molecules already excited to a certain energy state due to alpha ionisation. This is the same as they approach of Yao et al. [48], but Baschenko [1] aims to detect the change in the number of photons that are emitted due to the increase in energy created by the addition of the laser energy to the already excited Nitrogen molecules, rather than changes to the laser probe signal. Baschenko [1] has not tested his approach and merely mentions that this may be theoretically possible, whilst noting that there would be significant technical difficulties in using this approach.

Allander et al. [49] developed a system for detecting the ion pairs produced by alpha particle ionisation of the surrounding air, which they call the LRAD system (Long-Range Alpha Detector). It utilises an air current or an electric field to transport the ion pairs to a collection grid where they are detected as an electric current, the current being proportional to the activity and therefore allowing a measurement of this. However, these require either that the potentially contaminated object is placed inside

a chamber where filtered air can flow over it to carry the ion pairs to the grid, or for the detector system to be introduced into an existing pipe where an air flow can be used to measure any contamination inside the pipe. Both of these have implications for the ease of use in the field, and the initial setting up of the system, including moving and cutting into potentially contaminated materials. A third method allows for the detector to be placed over a potentially contaminated surface (for example, soil or a concrete floor) and an electronic field be used to detect the ion pairs. The main drawback of this system is that the detector could come into contact with contamination, thus becoming contaminated itself, and still requires the operator to be in close proximity to the contamination to set up the device. However, in processing samples, especially in large quantities, and for internal pipe examination, these methods could prove superior to traditional techniques. Certainly radioluminescence would be harder to detect within a pipe without special deployment equipment.

2.7 Future Prospects for Alpha Induced Radioluminescence Detection

Initial work in the detection of alpha contamination through Nitrogen radioluminescence has concentrated on the main peaks of the radioluminescence spectrum, which occur in the 300 to 400 nm range. This leads to background UV radiation from the sun or artificial lighting interfering with the detection of the alpha induced radioluminescence by masking its much weaker signal. Filtering of the wavelength of photons detected allowed for the imaging of alpha sources in dark or special background lighting conditions, but not as yet in daylight. By moving away from the UVA and UVB range into the UVC range, a possible route to overcoming this limitation becomes apparent. Although the peaks of intensity in this band appear to be lower, there is not the competition from sunlight and artificial light, improving the

signal to noise ratio. This would potentially make detection possible on site in nuclear installations to provide characterisation for decommissioning and other purposes.

A detailed analysis of the spectrum of UVC is required, including identification of any significant peaks which may provide the best chance of detection. Other gases may provide a better scintillation atmosphere, including in the UVC wavelength range and should be investigated. Tests carried out in the 1960s provide some information regarding the effect on wavelength of emitted light in various gas environments, for example, see Morse et al. [50]. However, these require further investigation to apply them to enhancing the scintillation for specific required wavelengths.

Other beneficial future work would include the further testing of UVC/solar blind detectors to determine their efficacy in detecting alpha induced radioluminescence. A review and testing of currently available UVC detection technology would allow an assessment which could be utilised to develop a new UVC detector specifically for nuclear decontamination purposes.

Putting together a number of effective techniques to provide a multi-stage detector may be the route forward. These other possible techniques include but are not limited to: data processing algorithms, collection optics, superposition and amplification, and the use of light reactive materials. A multi stage detector may provide a more efficient and robust detector for use in the field. Coincident and background attenuation techniques are the subject of continuing experimentation and could be expanded, as could active detectors of the kind as put forward by Baschenko [1] and Yao et al. [48].

Transmission through translucent materials for different wavelengths requires more investigation for a completely suitable field detector to be produced. The limited research carried out to date does not contain sufficient detail or analysis of the phenomenon to determine how much of an issue this will be for detection in the field,

and how this can be addressed. Tests to show both the internal and external transmission would be useful, for conditions where the surface reflection of the glass may or may not be relevant. In lenses and filters the internal transmission is more relevant as an anti-reflective coating can be used. This may not be possible for gloveboxes and hot cell windows, hence the external transmission may be more suitable. It may also be beneficial to test transmission of existing materials in the field where the age of the materials may also prove influential as some of the nuclear sites for decommissioning are of a substantial age. An understanding of the transmission of these materials may also be beneficial in determining if contamination is on the interior of the translucent material or at a distance which has not as yet been addressed, most likely due to researchers already knowing the location of the contamination in test situations.

Although there is a great deal of existing research and information, the differences in distances to source, detectors, sources and other conditions makes an assessment of progress difficult. A systematic testing regime with single variable differences between tests would provide a more easily accessible and comparable set of results, in terms of effect of yield on different conditions (gases, translucent materials, reflection, etc.) and the efficacy of different detector types.

Work to date has provided a sound basis for continuation, with a clear route along the UVC wavelength path, possible benefits from the identification of an alternative radioluminescence gas, and routes using optics and other methods to optimise the collection, processing and detection of alpha-induced air-radioluminescence photons. This work will lead to the development of an alpha detection system that can be used on site for nuclear decommissioning purposes.

Chapter 3

Experimental approach and set up

Following a review of the existing research to date, application of the knowledge gained to the aims of the work led to the resolution of various important decisions regarding approach, equipment selection, and experimental methods. This included initial testing to assess the potential of the approach and equipment before experimentation with an active alpha source.

3.1 Approach

Although the majority of alpha-induced radioluminescence is emitted in the 300 – 400 nm wavelength range, detection is greatly affected by interference from natural and artificial light. It was clear from the existing literature that despite efforts to filter or subtract this light, in the UVA and UVB wavelength range, background was the major stumbling block to detecting alpha-induced radioluminescence. All detectors successfully tested to date utilising this wavelength range required darkness or special lighting conditions to operate effectively.

If the background could be discounted in some way without the need for filtering or subtraction, then the task would be simplified to developing a configuration of detector which is sensitive enough to detect the radioluminescence signal. Two attempts to detect alpha-induced radioluminescence in the UVC wavelength range had promising results opening up the possibility that detecting only the UVC part of the radioluminescence may be a way forward for a stand-off alpha detector [43, 44]. Although neither pieces of research themselves offered a means to a field ready detector, the imaging of UVC by a CCD camera and the use of a UVC sensitive MFP in dark conditions indicated that if a suitable UVC sensor could be found, and based on this a suitable UVC detector system could be developed, that this may lead to a resolution of the issue of background interference. Although simplifying the problem, the resolution would need to overcome the considerations in the UVC wavelength range (see Chapter 1 section 1.8: *Underpinning science*) in terms of small signal strength along with transmittance through translucent materials, such as glass and plexiglass. And a truly solar-blind sensor would be required to completely reject the significantly larger background signal.

3.2 Equipment selection

3.2.1 UVTRON sensor

In searching for a potential solar-blind sensor suitable for a detector system capable of being used in the field, the following considerations were identified as important: wavelength range; size of sensor and associated electronics; availability; robustness; sensitivity; reliability; dark count. These considerations were important to develop a reliable detector with the following attributes: solar blind and therefore can be operated in normal lighting and daylight conditions; easily portable and can access limited

spaces; reliable and robust, able to withstand being moved between deployment locations; good availability for future development; and sensitive enough to detect the UVC radioluminescence from a distance with a good signal to noise ratio.

The most important factor was wavelength range, as the UVC part of the spectrum had been selected following the review of existing literature. MFPs, as generally used in light detection and as used in Leybourne et al's work [44], even when described as 'solar-blind' tend to be used with monochromators as they have a decreased sensitivity in the solar wavelength range, but are not completely insensitive to it. This makes the set up large and expensive, or subject to background light interference. ECCD are also used in the UV wavelength range, but are sensitive to heat and require cooling to reduce the dark count [43]. Both these devices are designed to quantify and characterise light, over and above pure detection. An alternative device was sought which would overcome the limitations of these devices, more suited to a detection role than requiring precise quantification.

UVC emissions from flames and electrical discharge are routinely detected for safety and maintenance purposes. Sensors designed to detect these are intended to be used in daylight conditions and are therefore truly solar-blind. The UVTRON by Hamamatsu (Japan) is one such family of these sensors. They are designed to be used in fire detection systems for commercial warehouses etc. where their high-speed response may be more suited than other fire detection methods, such as smoke or heat detectors. They are small and robust, are a mature technology and available off the shelf, meeting the identified considerations of a suitable sensor for these experiments.

Alternative UV flame sensors were considered. These include for example the F4-UV produced by 3M. Although the sensor within this system is solar-blind, it comes in a housing with a readymade user interface, making it larger than the UVTRON (101.6

x 117 x157 mm) and less easily adaptable [51]. The Honeywell FLS 100 UV is another solar blind UVC flame detector. It also comes in a housing, of dimensions 125 x 80 x 57 mm, with built in electronics. The cost of this is around £1000, making it much more expensive than the UVTRON as well as significantly larger [52]. These two examples typify the alternative UVC flame sensors on the market, which are supplied in housings which also contain the sensor and electronics, and therefore are significantly larger, more costly and less flexible than the UVTRON. The UVTRON offers an adaptable sensor which can be repurposed for radioluminescence detection, has a proven track record and was the clear choice for this work. Photodiodes were also considered, but these have a very small active area and peak at the top end of the UVC wavelength range (265 nm) making them less solar-blind than the UVTRON. Having considered alternative flame sensors and UVC sensors, the UVTRON was determined as having the best potential for this application.

3.2.1.1 How the UVTRON works

The UVTRON uses the photoelectric and gas multiplication effects to detect a photon in the UVC wavelength range. The electrodes are housed in a fused silica glass cylinder which contains an ionising gas. Fused silica is required as this attenuates UVC photons less than normal glass, transmitting over 90 % of UVC photons for thicknesses of up to 10 mm compared to much less than 10 % of UVC photons transmitted through optical glass [20] (see Chapter 1 section 1.8 *Underpinning Science*). The cathode is made of Ni which is sensitive to photons only in the 185 – 260 nm wavelength range. (A Mo cathode version is also available which is sensitive in the 185 – 300 nm wavelength range, but this is therefore sensitive to daylight).

When a photon of the correct wavelength hits the cathode, an electron is emitted. A high voltage between the electrodes accelerates this electron through the ionising gas to the anode. As it travels it ionises the gas, causing more electrons to be produced, which are also accelerated towards the anode. This results in a cascade effect. The moving electrons cause a current at the anode which is emitted as a pulse. This pulse is of a very short duration, 10 μ s FWHM (full width half maximum), with a maximum which was observed at approximately 12 V. The UVTRON has a minimum quenching time of between 1 to 3 ms, depending on the quenching circuit used.

3.2.2 UVTRON – model R9533



Figure 3-1: UVTRON R9533 – courtesy of Hamamatsu Photonics K.K.

The R9533 model (see Figure 3-1) was selected from the UVTRON range of sensors as it is sensitive only in the 185-260 nm wavelength range (see Figure 3-2) and is the most robust of the UVTRON range of flame sensors. The electrodes of the R9533 are capable of resisting mechanical shocks 10 times greater than other UVTRON models (excluding the R9454 which is similarly optimised). Other UVTRON models were tested during the work for a comparison of sensitivity to the R9533.

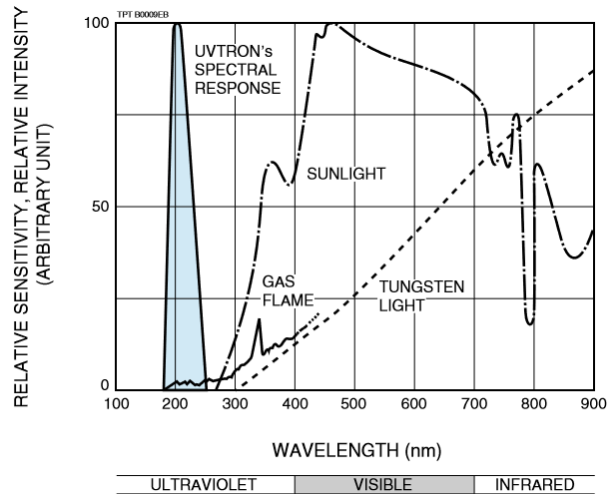


Figure 3-2: Comparison of UVTRON spectral response to sunlight, gas flame and Tungsten light - courtesy of Hamamatsu Photonics K.K. [53]

The UVTRON R9533 is relatively small, measuring 13 mm in diameter and 20 mm in length (36 mm including connection pins) and weighs approximately 2.5 g. (see Figure 3-3).

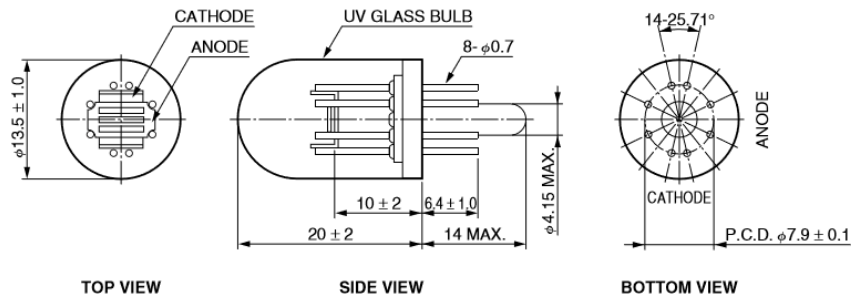


Figure 3-3: UVTRON R9533 size specification - courtesy of Hamamatsu Photonics K.K. [54]

The R9533 also has a wide field of view (see Figure 3-4).

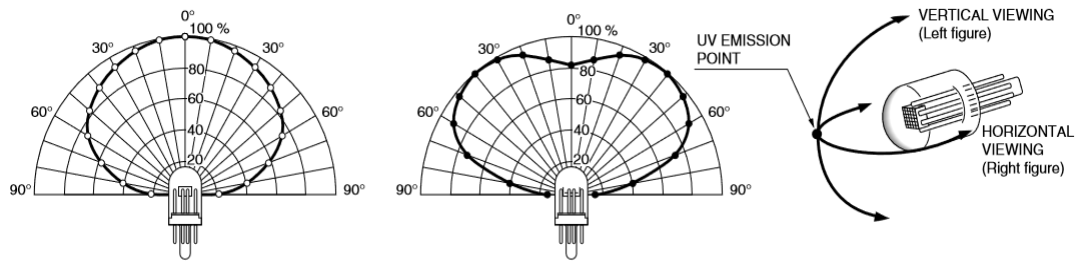


Figure 3-4: UVTRON R9533 field of view - courtesy of Hamamatsu Photonics K.K. [54]

It is a readily available, COTS item, and a predesigned optimised driving circuit (C10807, Hamamatsu) is similarly available to purchase.

3.2.3 Driving circuit

The C10807 driving circuit (see Figure 3-5) is optimised to work with the R9533. It provides the high voltage required for the gas multiplication effect and conditions the output pulse to a 5 V, 10 ms square wave, as compatible with general electronic circuitry.

When UVC is incident on the UVTRON, it outputs a 10 μ s pulse from the cathode, which is detected by the driving circuit. The frequency of these pulses from the UVTRON varies according to the amount of UVC light incident on the sensor. This is processed by the drive circuit electronics and a 10 ms pulse is output (see Figure 3-6). This pulse duration can be extended to greater than 10 ms by the addition of a capacitor to the drive circuit. Dependent on the application, the extension to the pulse time may be beneficial, for example when the pulse operates a buzzer for fire alarm purposes.

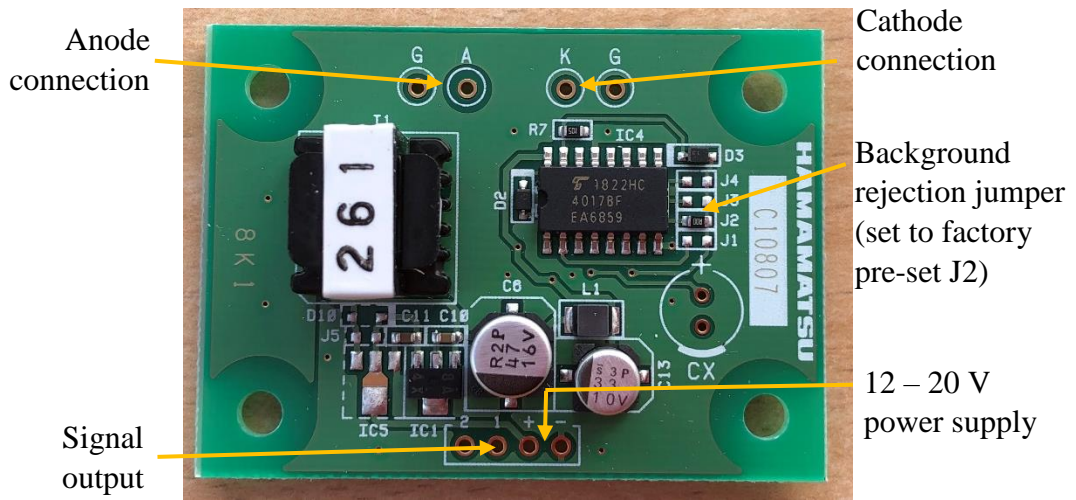


Figure 3-5: Photograph of UVTRON driving circuit (Hamamatsu, C10807) – with factory pre-set background rejection jumper.

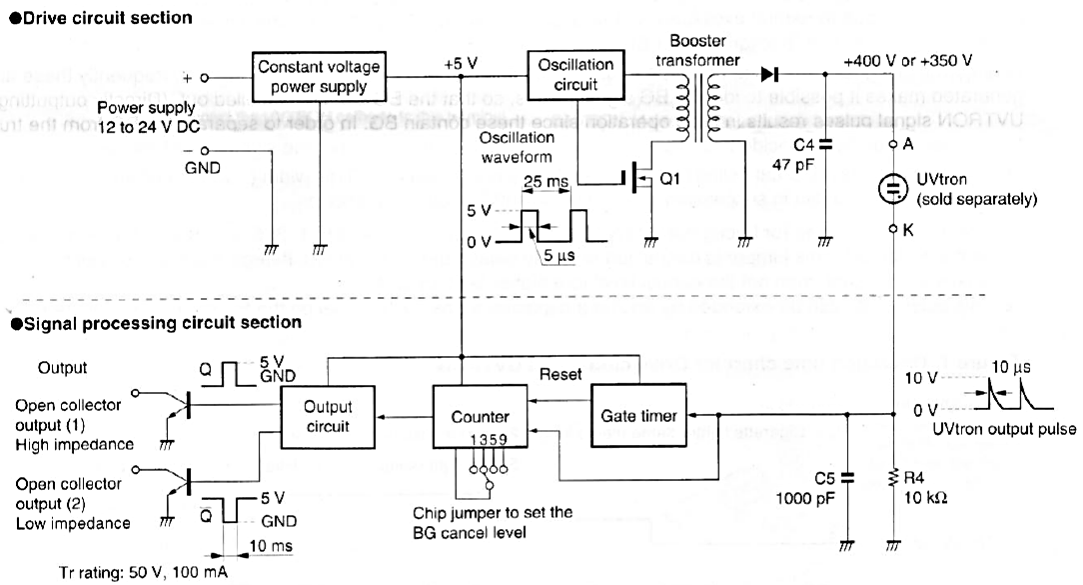


Figure 3-6: Circuit configuration diagram (Hamamatsu C10807) - courtesy of Hamamatsu

Photonics K.K. [55]

Although the UVTRON is already low in background count, this can be further reduced using the option to select the number of pulses received from the UVTRON

before a pulse from the driving circuit is emitted, to either 1, 3, 5 or 9 pulses. This is to allow flexibility in background rejection to prevent false alarms in fire detection applications. In the J2 position, which is the factory pre-set (see Figure 3-5) the driving circuit must receive three pulses within 2 seconds before an output pulse is generated. The majority of experiments in this work required a greater sensitivity to UVC and hence the jumper was moved to J1 to provide a pulse without background rejection from the driving circuit. Unless otherwise stated from hereon, the jumper was in the J1 position.

The minimum time between pulses is 25 ms, giving the driving circuit with no background rejection a maximum output of 40 pulses per second. In practice, the maximum reached was 38 CPS. Figure 3-7 shows the timing of the pulses (with background rejection set to 3 pulses), including the increase in pulses from the UVTRON dependent on the amount of incident UVC, and the output of the driving circuit.

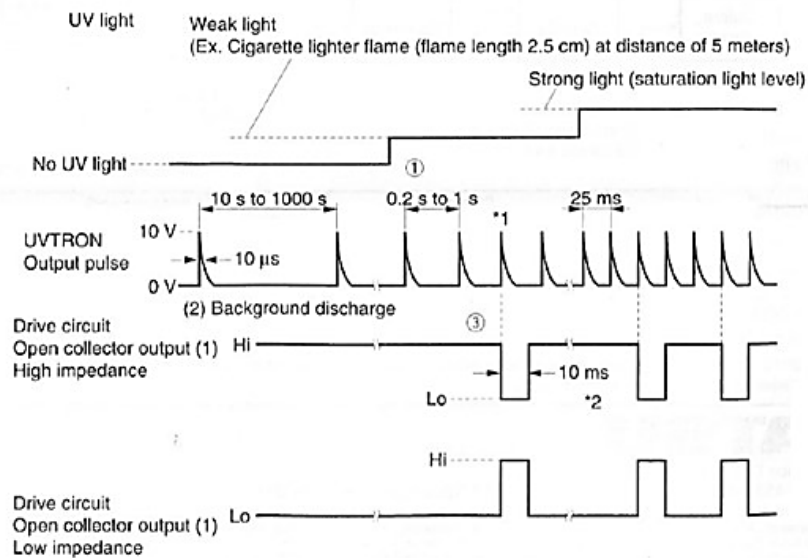


Figure 3-7: Operation time chart for Drive circuit and UVTRON - courtesy of Hamamatsu Photonics K.K. [55]

3.2.4 Counting device – the Arduino Uno



Figure 3-8: Photograph of Arduino Uno

The Arduino Uno (see Figure 3-8) was selected as the counting module. It is a reliable microprocessor board based on the ATmega328P microcontroller. It was selected as it fits well with the UVTRON system, matching it in terms of being small, robust, reliable and simple to use. The Arduino board is 68.6 x 53.4 mm. The output pulse of the driving circuit, 5 V, 10 ms, square wave, can be input to one of the input pins on the Arduino board and can be read directly without the need for any other processing. The board can also provide the 5 V reference voltage required to stabilise the output pulse from the UVTRON, removing the need for a separate voltage supply. The Arduino can be powered from a computer using a USB cable which also carries the collected data (number of pulses per second in this application) back to the computer, removing the need for an additional power supply. The software required to program and operate the board is open source, meaning that any computer with internet access can quickly be set up to use the UVTRON system, without the need for specialist software. Programming is easy with support from online tutorials and a user forum in case of

issues. The Arduino Uno also has sufficient inputs and outputs to give the facility to control other equipment, for example, motors for an automated scanning platform, if required. It is easily available and low cost, providing the features required without the need to purchase a system with extra, but unrequired functionality, such as a counting module as may be used with a MFP.

3.3 Experimental set up

The R9533 UVTRON was connected to the C10807 driving circuit as per manufacturer instructions (see Figure 3-9). The Arduino 5 V output was connected via a 1 k Ω resistor to the driving circuit output.

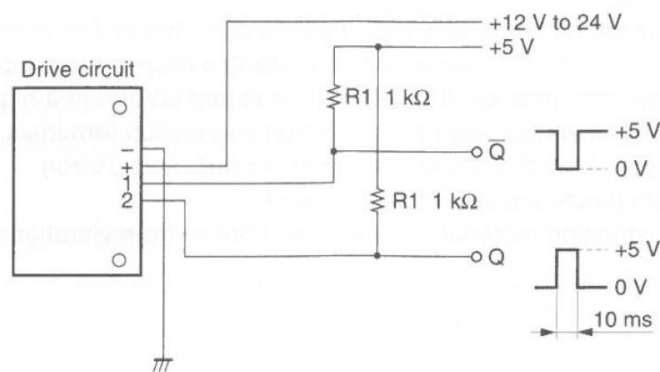


Figure 3-9: Driving circuit power and output connections - courtesy of Hamamatsu Photonics K.K. [55]

The 5 V, 10 ms output pulse was directed to an input pin on the Arduino Uno board. The Arduino counted the number of pulses in each second, relaying this value to a laptop second-by-second on a real time basis. This data was manually transferred to a spreadsheet for analysis, or to Matlab to produce plots. From this an average CPS could be calculated, or counts in a set time period could be calculated, for example the number of counts in an hour, through the addition of the counts in each second of the experiment.

For experiments where the output pulse characteristics were required, the direct output from the UVTRON and the conditioned output from the driving circuit were connected to an oscilloscope so that the pulse shape could be seen and measured. Figure 3-10 shows the pulse shapes recorded in different gas atmospheres (see Chapter 5; *Gas flow to enhance the detection of alpha-induced air radioluminescence based on a UVTRON flame sensor for gas atmosphere experiments*).

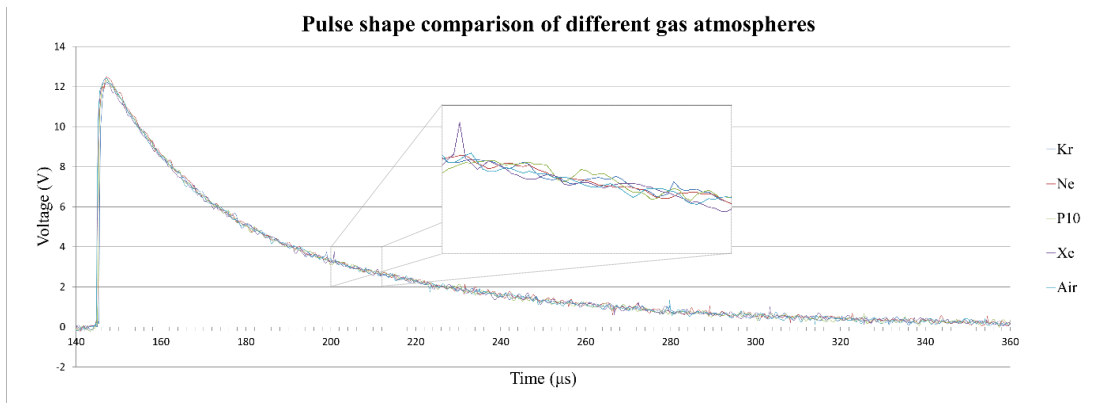


Figure 3-10: Examples of typical pulse shapes from the UVTRON before processing – with an enhanced view of the 200 – 210 μs time period

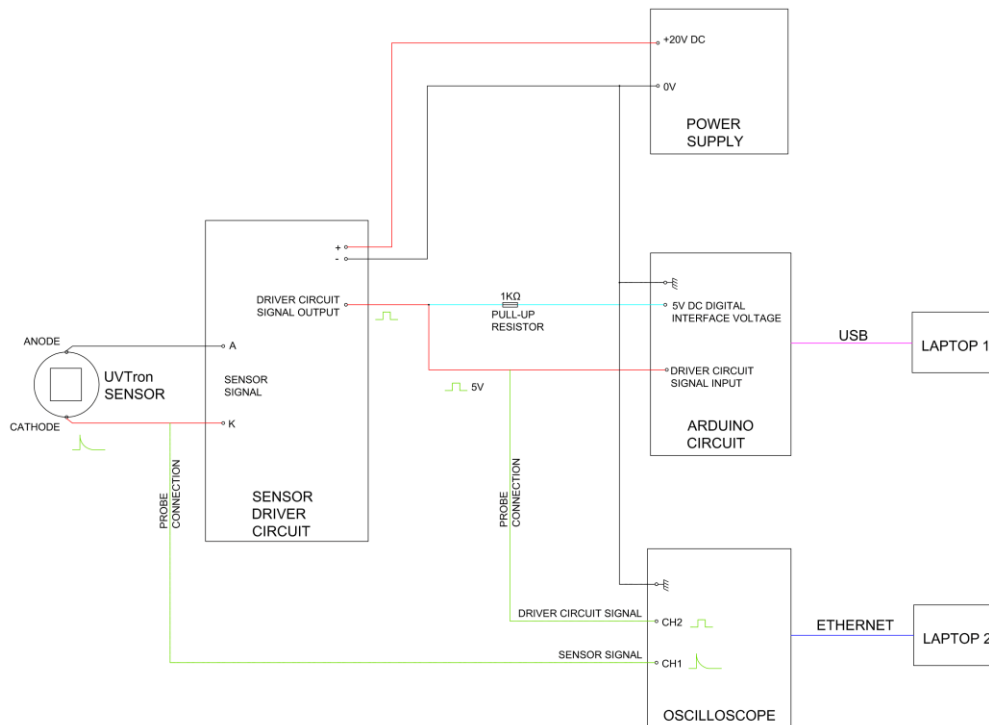


Figure 3-11: Full equipment set up connections schematic – with oscilloscope

Figure 3-11 includes the full schematic with both the Arduino and oscilloscope connections shown.

The UVTRON was mounted on the exterior of a plastic project box using an E678-8F socket (Hamamatsu), with the Arduino Uno and driving circuit housed inside the project box (see Figure 3-12).

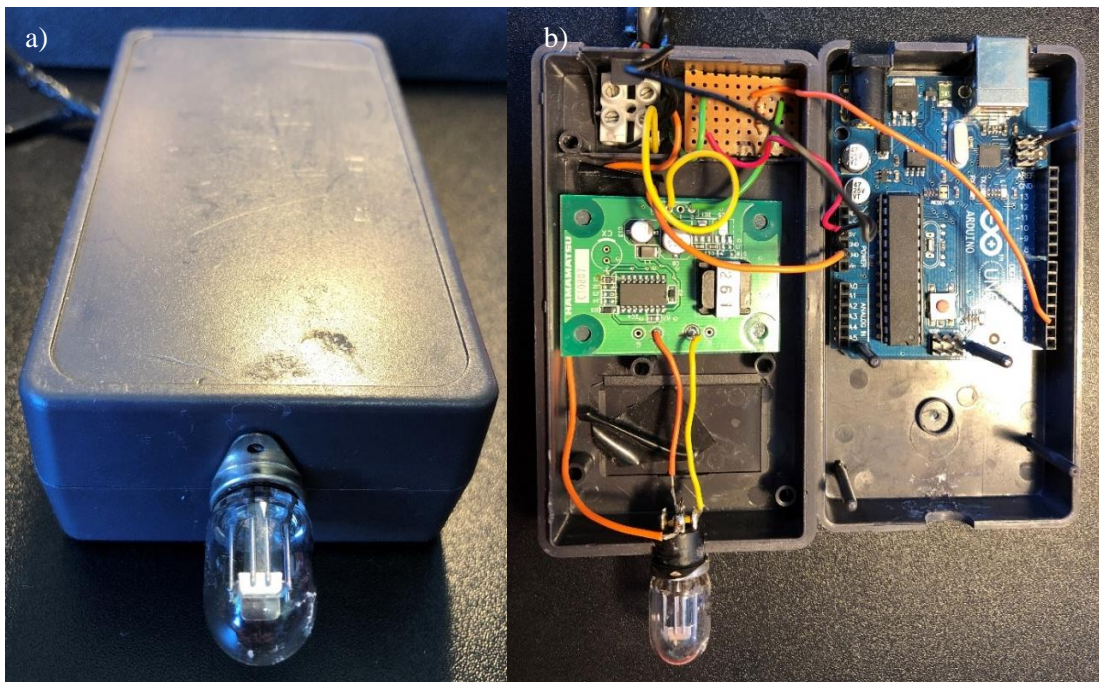


Figure 3-12: Photograph of project box housing electronics a) box closed b) box open to show the driving circuit, pull-up resistor and Arduino Uno.

A UVC emitting light source was used at the commencement of all experiments to ensure that the equipment was working correctly. This was required due to the infrequency of background pulses to verify that a pulse was being received by the laptop.

3.4 Preliminary testing

As data supplied by the UVTRON manufacturer is intended for flame detection purposes, and therefore likely includes a safety margin, it was first necessary to establish if the sensor had potential in this alternative application. These initial experiments were carried out without the presence of an active alpha source for safety reasons. A small UVC light source (L9657-03, Hamamatsu) was used to represent the UVC radioluminescence in these tests.

3.4.1 Distance test

The first test of the UVTRON was carried out using an oscilloscope to monitor the output pulse and a manual record of pulse frequency was taken at different distances between the UVTRON and the UVC light source. The UVTRON and associated electronics were placed on a moving platform (see Figure 3-13) so that the distance between the light source and the UVTRON could easily be increased. The background rejection of the driving circuit was set to 3 pulses received from the UVTRON before a pulse was emitted, which is the default factory setting. (Later this setting was reviewed and changed to 1 pulse when the low background of the UVTRON had been established.)

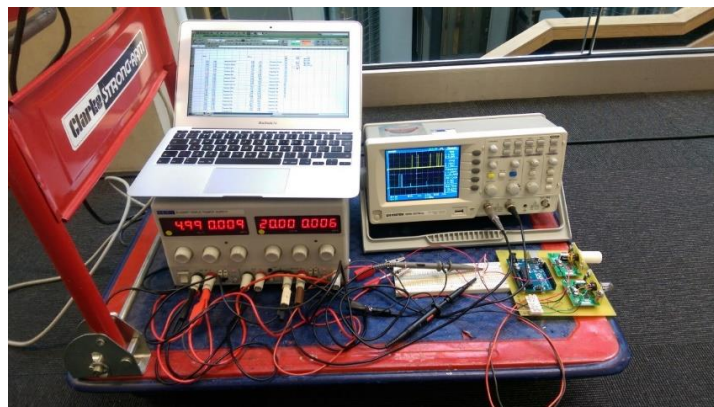


Figure 3-13: Equipment on trolley carrying out distance testing using a UVC light source

The average frequency was recorded at increasing distances, with 1 m between observations. This was plotted on a graph to show the drop-off in pulse frequency by distance (see Figure 3-14). The furthest separation achieved was 27 m, where a signal was still observable, though very weak by this point (The 27 m limit was imposed by the maximum length of the space where testing took place).

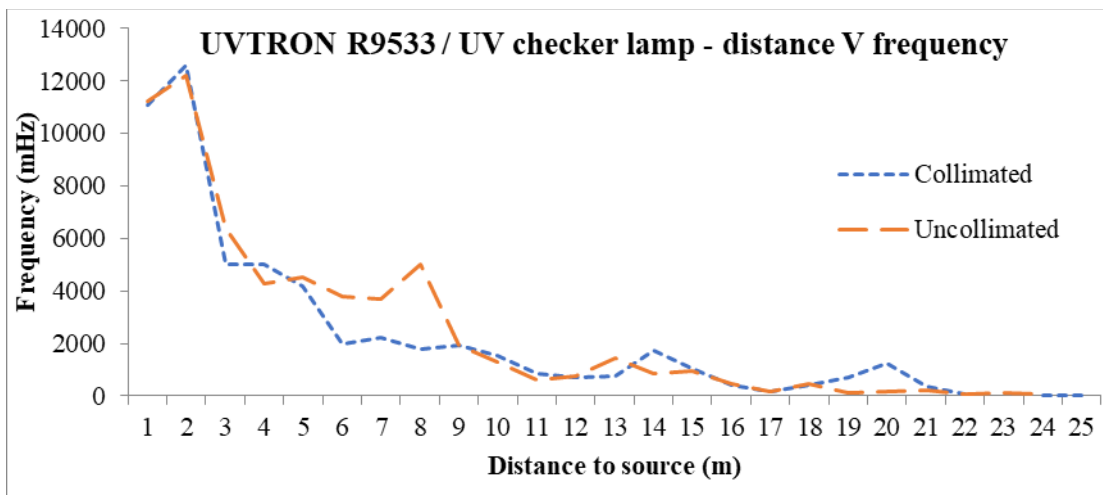


Figure 3-14: Graph showing signal frequency of UVTRONs v distance between UVTRON and UVC light source

At each point, the UVC light source was covered to block the signal reaching the UVTRON and a decrease in count was observed. The frequency of pulses reduced to zero when the light from the UVC light source was blocked. This was the first indication of the low dark count of the UVTRON and its lack of response to daylight and indoor lighting conditions.

3.4.2 Pulse characteristics

The direct pulse from the UVTRON and conditioned pulse from the driving circuit were compared, in terms of amplitude, duration, frequency and shape. The trigger point was set so that one or both of the pulses would trigger the oscilloscope, and these two sets

of results were compared. It was found that both pulses occurred together in all instances, with the conditioned pulse (green square wave) emitted slightly after the direct pulse (yellow peak) – see Figure 3-15.

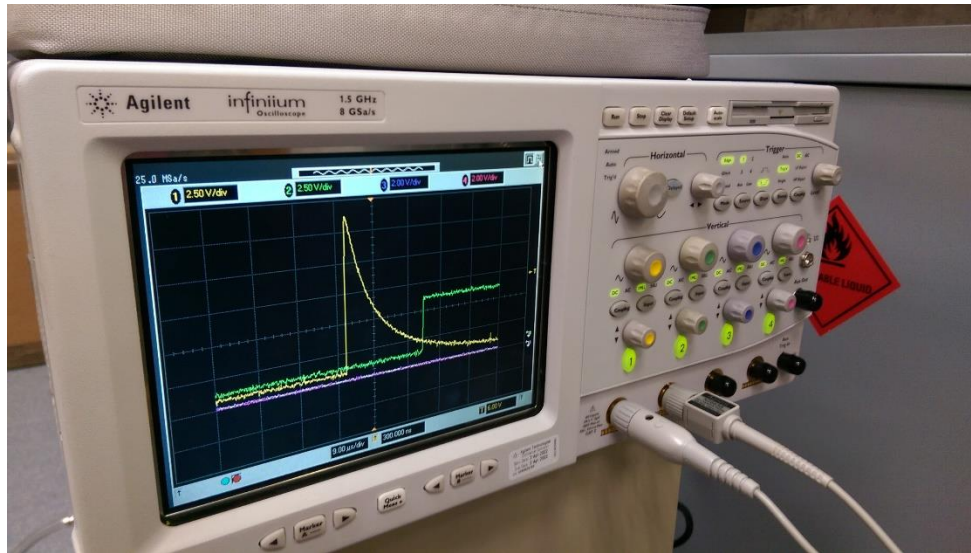


Figure 3-15: Photograph showing conditioned pulse in green and direct pulse in yellow from the UVTRON

The direct pulse had an amplitude of around 12 V, and a duration of approximately 10 μs (FWHM). The conditioned pulse occurred approximately 100 μs after the leading edge of the direct pulse, and was 5 V in amplitude (as expected with the 5 V reference voltage applied to the output). The direct pulse varied slightly in amplitude and duration. From this, it was verified that the two pulses occurred at the same time and with the same frequency. The Arduino is not capable of detecting a pulse of the duration of the direct output, therefore the conditioned pulse was used for counting purposes. The direct pulse was observed and recorded during experiments to see if differences in the stimuli affected the pulse shape.

3.4.3 Background test

The effect of natural and artificial light was observed, with a virtually zero count being seen when the sensor was placed in artificial lighting, either in the centre of a room or when placed in close proximity to and facing double glazed windows. This is in line with the anticipated negligible or zero levels of UVC expected from natural and artificial lighting. This preliminary observation was later quantified by further background tests (see Chapter 8 and Chapters 4, 5, 6 and 7 for background quantification).

Outdoor tests were carried out at a later date to see if the attenuation of UVC by window glass caused the very low background count and if direct sunlight would affect the UVTRON pulse count (see Appendix D). These tests were inconclusive, but indicated that temperature and not ambient light may determine outdoor background readings.

3.4.4 Source location testing

Once it had been established that the UVTRON may be sufficiently sensitive and had excellent background rejection, tests were carried out to determine if the UVTRON was capable of locating a source during an automated scan. In order to achieve the maximum benefit from a stand-off detector, removing the operator from the locality and reducing the time required to operate the detector can be achieved by automating the system to scan an area without the intervention of the operator. The operator is then only required to set-up the equipment and collect the data. Scans can be carried out over a long period of time, hours or days, meaning larger areas can be scanned, or longer dwell times can be used to increase accuracy. The latter is especially beneficial in applications where there is a very small signal strength as long count durations can be required to achieve a statistically significant result.

A collimated scanning platform was designed and built, which would scan an area and record the output pulse at equidistant points over that area (see Figure 3-16).

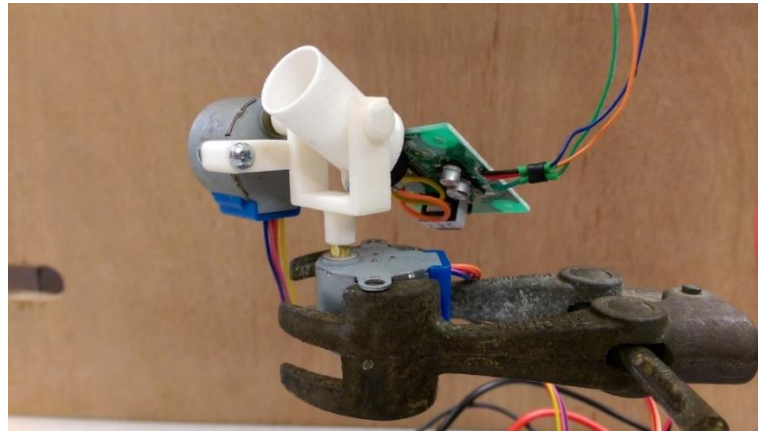


Figure 3-16: UVTRON scanning platform – showing collimator and driving circuit.

Using the equation;

$$\theta = \tan^{-1} \left(\frac{x}{S} \right) \quad (3.1)$$

where x is the distance between scanning points on the surface being scanned, S is the perpendicular distance from the detector to the surface and θ is the angle of the detector in relation to S , it is possible to calculate the angles of motion for the detector which will provide equidistant points on the surface being scanned. However, this does require a knowledge of the value S which may not be known in a real-world setting. Hence it was decided to use 10° increments in the horizontal and vertical direction for each of the count points. Integration time was 10 s at each point. The UVTRON has a wide field of view (see Figure 3-4) so a collimator was used to narrow the field of view for these tests.

The results are shown below (Figure 3-17). The double hotspot occurred because the UVTRON has a dip in sensitivity in the 0° position in one orientation (Figure 3-4). The UVTRON was reoriented by 90° to remove this dip in sensitivity (Figure 3-17 c).

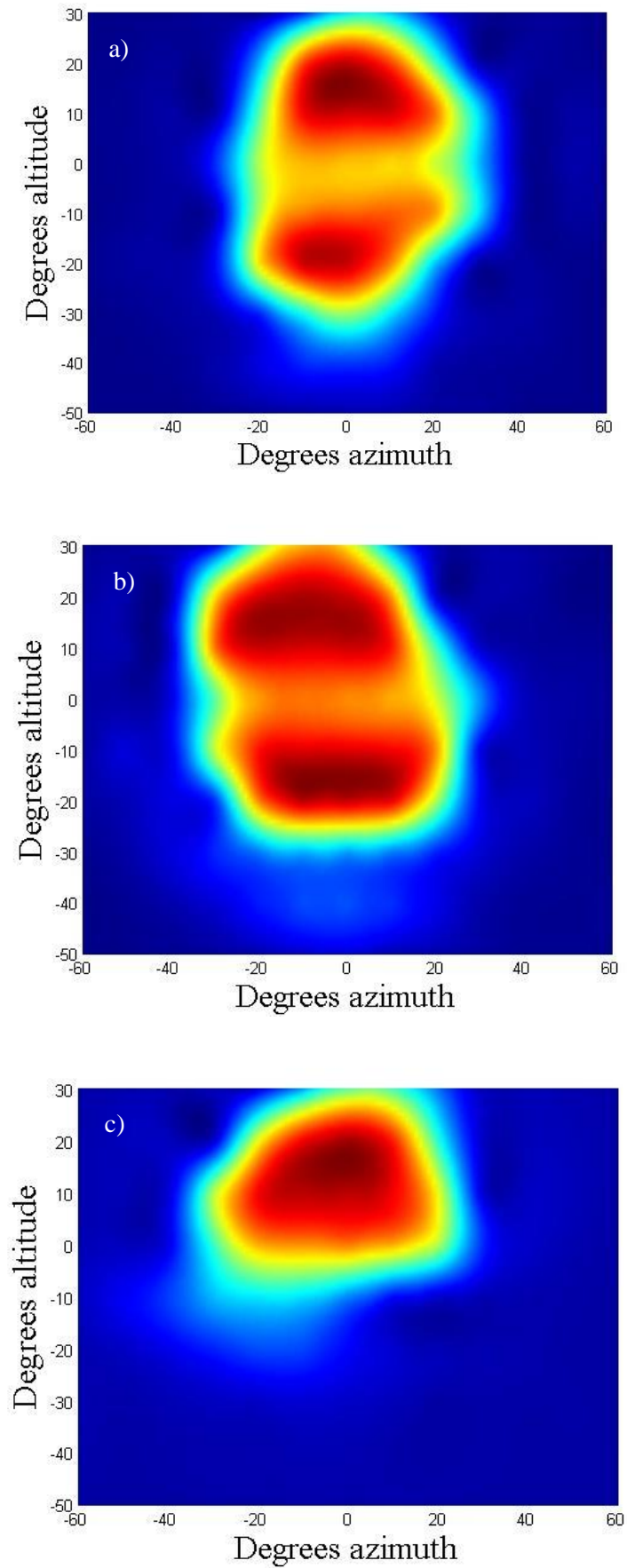


Figure 3-17: Plots of scan data showing location of UVC source.

It can be seen from the scans that the UVTRON can indicate the location of a source of UVC photons when used in conjunction with a scanning platform. As the UVTRON will likely be included in a detector where automated scanning is used to minimise operator time, it is important that this was part of the initial testing.

3.5 Conclusions of initial testing

These successful initial test campaigns indicated the potential of the UVTRON for the detection of alpha-induced radioluminescence in the UVC wavelength range, and so a series of experiments using an active alpha source were carried out at the National Physical Laboratory (NPL) in Teddington, National Nuclear Laboratory (NNL) in Cumbria, and Lancaster University's Engineering Department, Physics Department and Lancaster Environment Centre (LEC).

The aim of these tests was to first ascertain that detection of a UVC bulb and the UVC from a flame would translate to the detection of UVC radioluminescence from an alpha source by the UVTRON. If so, characterisation of the UVTRONs response to this radioluminescence would be carried out. This would include the amount of UVC detected in comparison to background readings, how sensitive the UVTRON was to alpha-induced radioluminescence and could a maximum distance in relation to activity be established. As it was known that the amount of radioluminescence in the UVC wavelength range was small, enhancement of the signal was also investigated, with the effect of a gas atmosphere on the number of radioluminescence photons in the UVC wavelength range explored. In the field the detector may be exposed to mixed radiation, and so the effect of gamma and beta radiation on the UVTRON also required investigation, with the use of shielding possibly proving to be required in a prototype detector system.

Five main groups of experiments were carried out in total, with additional tests completed as required to complete the investigations. The first set, carried out at NPL, were to establish that the UVTRON was capable of detecting alpha-induced radioluminescence in the UVC wavelength range and to quantify this where possible, with the output pulses investigated from both the UVTRON and the driving circuit (Chapter 4: *First results of using a UVTRON flame sensor to detect alpha-induced air fluorescence in the UVC wavelength range*). The second set, also carried out at NPL, were to establish the effect of a gas flow over the source on the detectable UVC (Chapter 5: *Gas flow to enhance the detection of alpha-induced air radioluminescence based on a UVTRON flame sensor*). The following two sets of experiments carried out at the NNL and Lancaster University (Engineering department, Physics department and LEC) investigated the effect of gamma and beta radiation on the UVTRON and associated electronics (Chapter 6: *The effect of gamma and beta radiation on a UVTRON flame sensor: assessment of the impact in implementation in a mixed radiation field*). The final set of experiments, carried out at NPL, followed the results of the work on gamma and beta radiation to test a collimated UVTRON when exposed to alpha, beta and gamma sources, individually or in combination (Chapter 7: *Performance characteristics of a Tungsten collimator and UVTRON flame sensor for the detection of alpha-induced radioluminescence; Impact of UVC reflecting mirror and the effect of beta and gamma radiation sources.*).

Chapter 4

First Results of Using a UVTRON Flame Sensor to Detect Alpha-Induced Air Fluorescence in the UVC Wavelength Range

Anita J. Crompton, Kelum A. A. Gamage, Steven Bell, Andrew P. Wilson, Alex Jenkins and Divyesh Trivedi

Reprinted from Sensors, 17(12), 2756; November 2017, with permission from Sensors.

4.1 Abstract

In this work, a robust stand-off alpha detection method using the secondary effects of alpha radiation has been sought. Alpha particles ionise the surrounding atmosphere as they travel. Fluorescence photons produced as a consequence of this can be used to detect the source of the alpha emissions. This paper details experiments carried out to detect this fluorescence, with the focus on photons in the ultraviolet C (UVC) wavelength range (180–280 nm). A detector, UVTRON R9533 (Hamamatsu, 325-6, Sunayama-cho, Naka-ku, Hamamatsu City, Shizuoka Pref., 430-8587, Japan), designed

to detect the UVC emissions from flames for fire alarm purposes, was tested in various gas atmospheres with a ^{210}Po alpha source to determine if this could provide an avenue for stand-off alpha detection. The results of the experiments show that this detector is capable of detecting alpha-induced air fluorescence in normal indoor lighting conditions, as the interference from daylight and artificial lighting is less influential on this detection system which operates below the UVA and UVB wavelength ranges (280–315 nm and 315–380 nm respectively). Assuming a standard $1/r^2$ drop off in signal, the limit of detection in this configuration can be calculated to be approximately 240 mm, well beyond the range of alpha-particles in air, which indicates that this approach could have potential for stand-off alpha detection. The gas atmospheres tested produced an increase in the detector count, with Xenon having the greatest effect with a measured 52% increase in the detector response in comparison to the detector response in an air atmosphere. This type of alpha detection system could be operated at a distance, where it would potentially provide a more cost effective, safer, and faster solution in comparison with traditional alpha detection methods to detect and characterise alpha contamination in nuclear decommissioning and security applications.

4.2 Introduction

The ability to detect alpha emissions from nuclear materials is important in nuclear operations, nuclear decommissioning, and nuclear security applications. Due to their positive charge, alpha particles travel only a short distance after emission from nuclear materials, typically around 50 mm through air depending on their energy. This is due to their interactions with atoms in the surrounding atmosphere. Therefore, detectors which require direct contact with alpha particles need to be in close proximity to any surface or object to determine if alpha contamination is present, at a distance of less

than the MFP of the alpha particles. This causes a number of issues, as documented by other researchers [1, 5, 39]. As objects to be monitored may be in a mixed radiation environment, personnel carrying out detection activities may require PPE and have limited time in which they can safely operate. Large structures or complex geometries take significant time to monitor in such close proximity. A stand-off detector, where a significant distance between the detector and surface can be achieved, can reduce the time taken for monitoring whilst distancing the operator from the radioactive environment.

As an alpha particle travels it ionises the air, transferring energy to the atoms and molecules in its path, mostly due to its positive charge. These excited atoms may emit an optical photon to return to a stable state and these photons have a MFP in the order of kilometres [29,35]. So in theory they could be detected from a significant distance, much further than direct alpha particle interaction detectors could achieve.

Although there have been experiments and several prototype detectors which have utilised this effect for stand-off alpha detection [1, 13, 15, 17, 30, 56], there are significant difficulties with this approach. The main issue is the interference of light (natural or from lighting equipment), which is typically present at a much greater intensity compared with the signal from alpha-induced fluorescence. Operating in dark or special lighting conditions alleviates this problem somewhat, as can be seen by the success of Sand et al.'s detector system under special lighting conditions [18], where UV-free lighting sufficient to see was used to operate the equipment with a filtered PMT. Although where special lighting can be used this detector has positive results, it is not possible to always specify lighting conditions in the field. The variability of lighting levels over short time periods, especially from natural light sources, means that subtracting the background is a very difficult option and although a patent has been

filed for such a detector [46], this requires the use of six separate cameras sensitive at six different wavelengths, and details on the testing of such a device are absent in the available literature. Although filtering can be used, it causes an unwanted attenuation of the desired signal along with the undesired background light, especially in the ultraviolet (UV) wavelength range, and special materials are required, for example fused silica. Although Sand et al. use filtering of a specific bandpass which coincides with a peak of 334 nm, the main peak from Nitrogen fluorescence, they still require special lighting conditions to determine the signal from the background. Ivanov et al. had some success in using a solar-blind CCD (charge coupled device) camera [43] which could image UV fluorescence in daylight without the need for specific filtering. However, this is limited by the time taken to carry out imaging, process it, and then analyse the results, meaning that a solar-blind CCD camera would have limited applications in the field or for scanning purposes. Although there are 'solar-blind' detectors available, for example the Hamamatsu R7154P high sensitivity solar-blind photocathode (160–320 nm), upon testing this proved not to be completely solar blind, although it was much less sensitive above 320 nm. Hence, these are still affected by background light and not sensitive enough to determine the alpha-induced fluorescence from background in normal lighting conditions.

Therefore, this research has focused on a detector which is less affected by natural and artificial light than other stand-off detectors available to date: the UVTRON by Hamamatsu. This detector is designed to detect UVC emissions from flames for use in fire detection systems and to have a negligible background count in normal indoor lighting. Experiments were carried out to determine if the UVTRON was able to detect the UVC fluorescence photons generated by an alpha source, and the effect of different gas atmospheres on this detection.

4.3 Materials and Methods

Experiments were carried out at the National Physical Laboratory in Teddington, Middlesex. The set up for the experiments was as follows (see Figure 4-1).

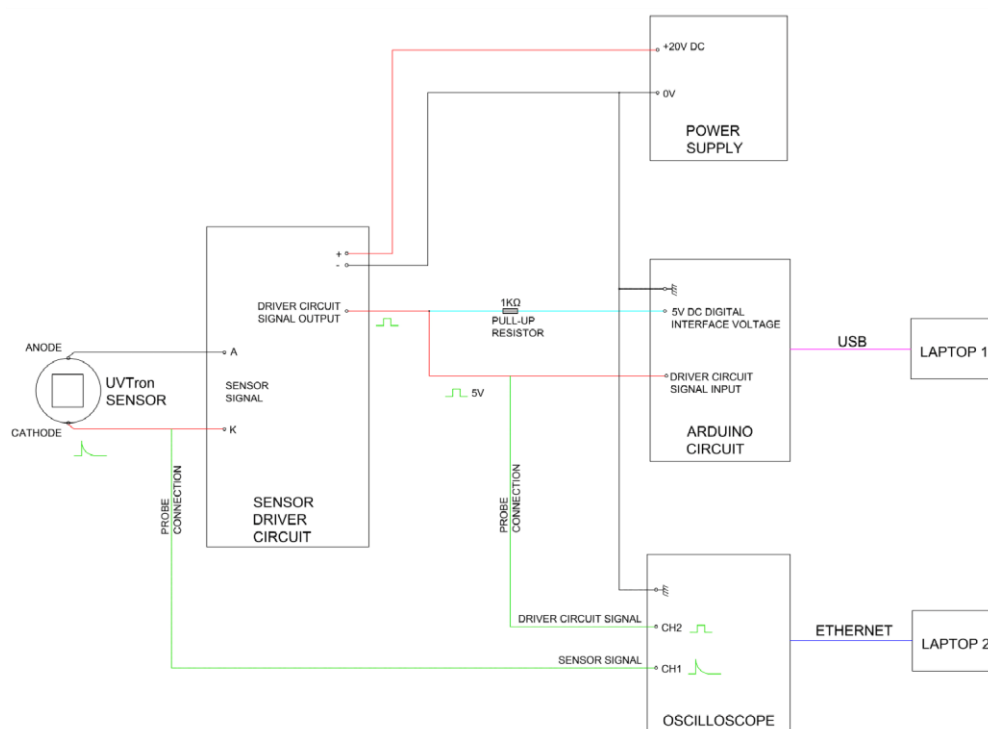


Figure 4-1: Schematic of equipment set-up.

A ^{210}Po source of 6.95 MBq (see Section 4.3.2, *Source*) was placed in close proximity to the UVTRON detector (Hamamatsu, R9533, see Section 4.3.1, *Detector*), with an approximate separation of 20 mm between the source and detector, unless stated in the results. Experiments were run with the source inside a gas flow box with a fused silica window (see Section 4.3.3, *Gas Flow Box and Gas Flow Set-up*), unless stated in the results (Figure 4-2).

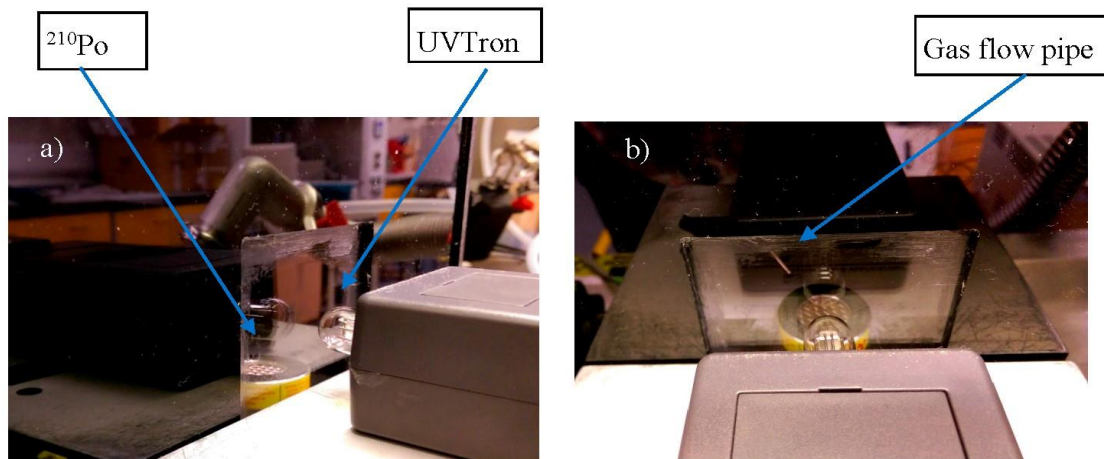


Figure 4-2: Photographs (a, b) showing the ^{210}Po source inside the gas flow box (silver disk with mesh surface and yellow edge) and the UVTRON (small glass bulb), attached to the grey box housing the detector electronics. In photograph (b) the tube through which the gas was flowed over the source can be seen above and to the left of the source.

The output from the UVTRON was recorded directly using an oscilloscope (Infiniium 54845A, 8 GSa/s, 1.5 GHz (Keysight Technologies, Santa Rosa, CA, USA) which recorded the shape of the direct pulse. The output of the UVTRON driver (C10807, Hamamatsu, Hamamatsu City, Japan) was connected to an Arduino Uno which counted the number of output pulses per second. A second channel on the oscilloscope was also connected to the output of the driver circuit which recorded the time and shape of the driver output pulse. Hence the direct pulse from the UVTRON and the processed pulse from the UVTRON driver circuit could be compared.

Where the effect of gas atmosphere was tested, the gas flowed across the surface of the source from a pipe placed above the source (see Figure 4-2 b). The gas flow rates are stated for each gas tested in Section 4.3.5.

The lab in which the experiments were carried out had no windows and conventional strip lighting. This lighting remained on for the duration of all experiments.

4.3.1 Detector

UVTRON detectors utilise the photoelectric effect and gas multiplication to generate an output pulse when a photon is incident on the photocathode. The UVTRON used in this research (the R9533) has a Ni cathode which is insensitive to photons with a wavelength of greater than 260 nm. This makes it effectively solar blind (see Figure 4-3).

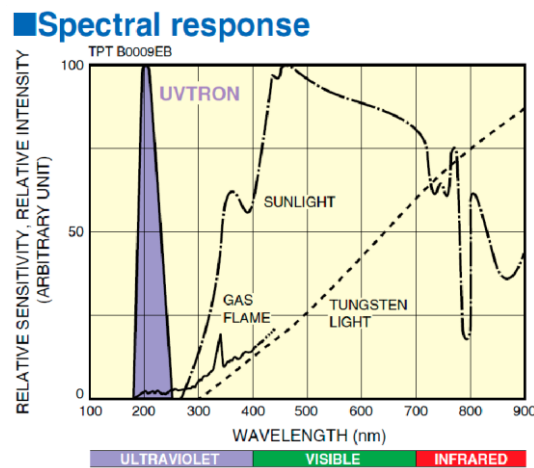


Figure 4-3: Spectral response of UVTRON in comparison to sunlight, Tungsten light, and gas flame [53].

Photons within the 180–260 nm range when incident on the photocathode of the UVTRON cause an electron to be emitted through the photoelectric effect. An electric field generated by a voltage differential between the cathode and the anode causes this free electron to be accelerated through the gas contained within the UVTRON. As the negatively charged electron passes through the gas it interacts with the gas molecules and transfers energy, causing ionisation and creating ion pairs. The gas atmosphere within the UVTRON bulb enhances this ionisation process. The positive ions created are attracted to the cathode, whilst the negative free electrons are attracted to the anode. As each free electron is generating further free electrons there is an avalanche reaction which causes an exponential increase in the number of free electrons incident on the

anode. This generates a signal which is interpreted by the driver circuit and a pulse is output by the driver circuit when this avalanche phenomenon occurs.

The detector used for these experiments, R9533, is one example of one model in the UVTRON range. It was selected due to its robust nature and the availability of an optimised off-the-shelf driver circuit.

4.3.2 Source

A sealed ^{210}Po source was selected for these experiments as ^{210}Po decays through alpha emission only, with a very low X/ γ emission intensity (see [57] for a ^{210}Po nuclide table). This was to eliminate the possibility of other radiations from the source generating a response from the UVTRON, either through direct interaction or secondary effects. This source had an activity level of 6.95 MBq at time of use (29 August 2017). The source can be seen in the photographs of Figure 4-2.

4.3.3 Gas Flow Box and Gas Flow Set-Up

In order to provide a support for the source and to allow the testing of different gas flows, a box of dimensions $260 \times 234 \times 230$ mm was constructed of 5-mm-thickness black Perspex. The box size was determined by the dimensions of an optional hemispherical reflector, which was not used in these experiments as the signal was sufficient for the detector to record an output.

The box has a 75×75 mm window of 2-mm-thick synthetic fused silica (Spectrosil[®]) (see Figure 4-2). Fused silica is preferable to ordinary glass as it allows UVC to pass with minimal attenuation (see Figure 4-4). This material is specifically designed for deep UV (UVC) optical applications.

Typical Transmission Spectrum

Sample thickness 10mm

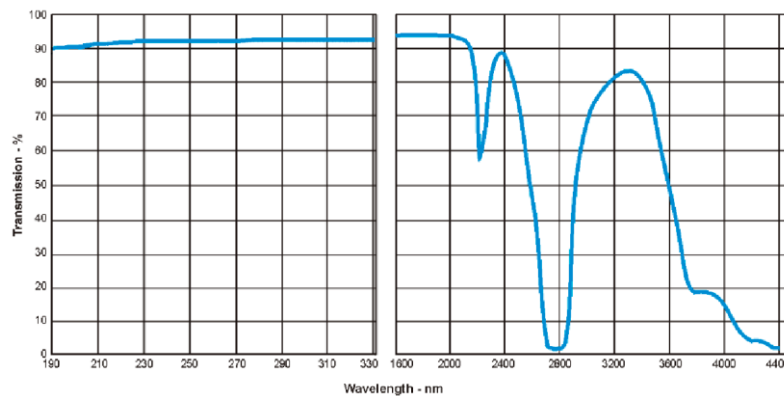


Figure 4-4: Transmission spectrum of fused silica window material [58].

The lid was placed on the box during gas experiments, but does not provide a gas tight seal. The gas flowed over the source in an air atmosphere using a small flexible pipe of 1 mm bore diameter (see Figure 4-2b).

4.3.4 Measurement

The pulses emitted by the UVTRON device driver (Hamamatsu C10807) each second were counted (CPS). The driver which both powers the UVTRON and processes the output signal. The UVTRON driver outputs a 5-V square wave on each detected avalanche event from the UVTRON, and the number of these per second was counted by the Arduino. The Arduino is unable to count the pulses directly from the UVTRON as they are of 10- μ s duration, too short for the Arduino to detect. Therefore, an oscilloscope was used to verify that each pulse directly from the UVTRON was accompanied by a square wave pulse from the driver circuit. It was then manually verified by observation that each of these pulses correlated to a count from the Arduino. Hence, the CPS of the Arduino was verified. The time delay between the two pulses was recorded for comparison to outputs using other UVC sources (e.g., UVC bulb, flame).

The direct pulses from the UVTRON were recorded via the oscilloscope in order that pulse characteristics, i.e., shape, height, duration, could be determined and any difference between those resulting from an alpha source as compared to a UVC bulb or other UVC source could be identified. The 5-V square pulse from the UVTRON driver circuit was also recorded using a second channel on the oscilloscope. The oscilloscope was set to a sample rate of 20 MHz, and 1800 acquisition points, with a trigger level of 6 V to ensure that the direct UVTRON pulse which was approximately 12 V triggered each recorded event, rather than the UVTRON driver which outputs a pulse of 5 V. However, both pulses were displayed and recorded as the trigger determines the time at which the output is measured for all channels in use (one for the direct UVTRON output, the other for the driver output).

4.3.5 Gases

In order to determine the effect of different gases on the fluorescence count, five different gases were flowed over the source. The gases are as listed in Table 4-1 below

Table 4-1: Table of gases.

Gas	Symbol	Purity	Approximate Flow Rate mL/min
Nitrogen	N ₂	N5.0	65
Xenon	Xe	N5.0	50
P10	10% CH ₄ /90% Ar	±5%	60
Krypton	Kr	N5.0	55
Neon	Ne	CP grade	40

In the field it may not be possible to flood the area under scrutiny with a specific gas, and in those environments which could provide a gas tight atmosphere, the amount of gas could be reduced by targeting the gas at the surfaces. Hurst et al. [58] in their experiments using protons to excite gases, found that it was preferable for the gas to flow through the gas cell they used rather than having a static gas atmosphere, as the

former increased the amount of light intensity. The effects of various gases on alpha-induced fluorescence have been investigated [18, 59 - 63]. However, to address the suitability for field operations and in light of Hurst et al.'s findings, a flow of gas over the source was tested. As the alpha particles travel in the order of 50 mm, the immediate surrounding area may prove to be more important in generating fluorescence photons than flooding the entire surroundings.

Following each experiment, the lid was removed, and the gas vented via the fume hood extractor system. The supply pipe was flushed with the new gas. The lid was then replaced, and the flow allowed to stabilise before the count was initiated.

4.3.6 Verification of Signal Source

In order to verify that the signal being received by the detector was indeed air fluorescence and not due to other emissions from the source, a number of checks were carried out. The set-up was as detailed above in Figure 4-1, with the source inside the gas flow box and the detector in close proximity to the fused silica window. An optical black-out cloth was placed between the source and detector. The observed CPS immediately reduced to zero, returning to its former value when the cloth was removed. A piece of ordinary white paper was then placed between the source and detector, which also reduced the count to zero. Again, this returned to the former value once the paper was removed.

A sheet of fused silica glass of the same specification as the gas flow box window was placed between the source and the detector. This resulted in a small drop in CPS of approximately 0.6%. This is broadly in line with the manufacturer's specification, but not statistically significant due to counting uncertainties of ~2%.

As the signal was transmitted through the fused silica windows, but not through the paper or black-out cloth, a verification was made that the detector was detecting UVC photons from the alpha source and not X/ γ / β radiation.

4.4 Results

4.4.1 Background Count

The UVTRON detector and associated equipment was set up as per Figure 4-1. The lighting in the lab remained on for the duration of the experiment. Lighting in the lab consisted solely of strip (fluorescent) lighting as generally found in commercial buildings.

The background count was taken for a duration of approximately 75 min. Over this period a total of 10 pulses were recorded by the Arduino from the UVTRON driver. This gives an average pulse rate of $2.224 \times 10^{-3} \pm 0.7034 \times 10^{-3}$ CPS. The pulses were randomly spread out over the time period and did not show any pattern.

The UVTRON is subject to an extremely low background count and this had negligible effect on measurements taken using the alpha source, accounting for less than 1% of the detected signal for all gas environments investigated.

Several background counts have been made in different indoor locations and gave a range of results from $1.5 \times 10^{-3} \pm 0.3 \times 10^{-3}$ to $3.6 \times 10^{-3} \pm 0.72 \times 10^{-3}$ CPS. All counts were carried out indoors. When in close proximity to a double-glazed window, the exterior lighting affected the count. As standard glazing attenuates UVC, it is likely that background counts outdoors will be higher.

For normal operation as a flame detector this value is negligible. For the detection of UVC from an alpha source, where the signal is far less intense than from a flame, this will be a limiting factor to the minimum sensitivity of the detector.

4.4.2 Air Atmosphere Results

Using the detector and associated equipment set-up as in Figure 4-1, the ^{210}Po source was placed inside the gas flow box in close proximity to the fused silica window. The UVTRON detector was placed outside the box close to the fused silica window (see Figure 4-2). There was an approximate distance between the source and detector of 20 mm. With the lab lighting remaining on for the duration of the experiment, the output pulses of the UVTRON driver circuit were counted by the Arduino.

Over the 16 hours of the experiment, 18,890 pulses were counted, giving an average of 0.3280 CPS. This average varied over the duration of the experiment, with average hourly CPS measured between 0.3097 and 0.3503. Figure 4-5 shows the hourly average CPS, compared with the overall average. This variation may have been due to changes in the environment over the 16-hour period, for example pressure in the lab (which varied between 1015 and 1010 mbar), humidity, temperature, etc., which may have affected UVC absorption or detector response. The variability of the CPS will also be a limiting factor in the minimum sensitivity of the UVTRON.

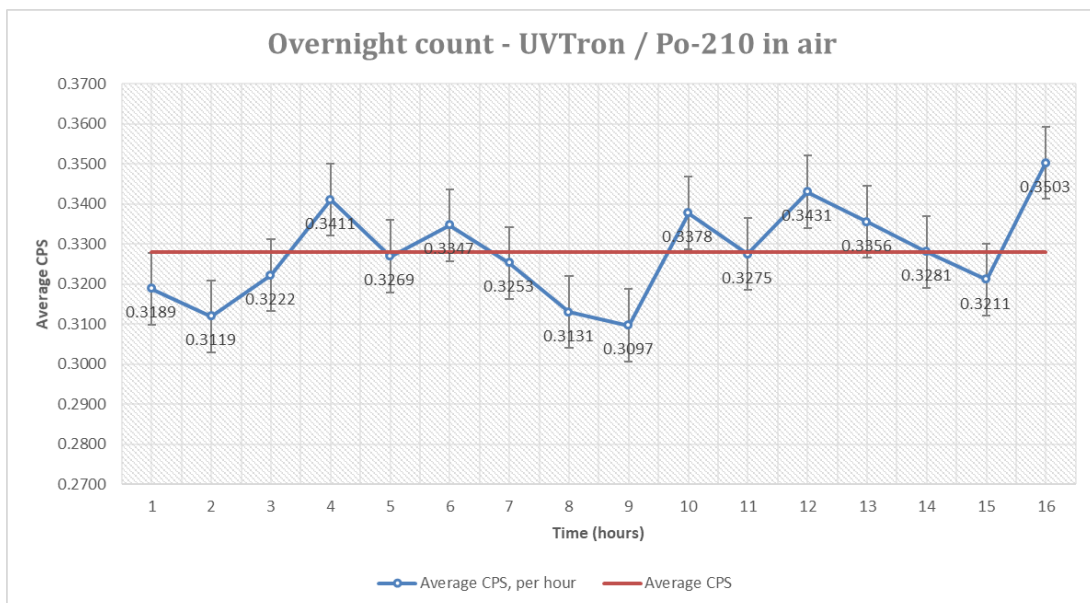


Figure 4-5: Average counts per second (CPS) per hour - ^{210}Po source in air.

4.4.3 Gas Flow Results

Five different gases were flowed over the source and the fluorescence measured was compared to an air atmosphere. These were selected following research into gases which were both likely to ionise at suitable energies and to emit photons of the required wavelength [59 - 66]. Although several of the studies used focus on ionisation of gases [64 - 66], this leads to secondary electrons which are believed to generate the fluorescence photons [59]. Saito et al. [63] identified Krypton, Xenon, and Argon as fluorescing in the UVC wavelength range. Using the evidence from Saito and the other literature, Nitrogen, Argon, Xenon, Krypton, and Neon were selected for testing. Argon was not available at the time of the experiment, however, there was an available supply of P-10 which was included in the testing due to its ionising properties.

The gas was flowed over the source from a distance of approximately 30 mm. The gases and flow rates are detailed in Section 4.3.5, Table 4-1. Each experiment was carried out for a duration of no less than one hour to provide a counting uncertainty below 3%. The results are shown in Figure 4-6 and in Table 4-2.

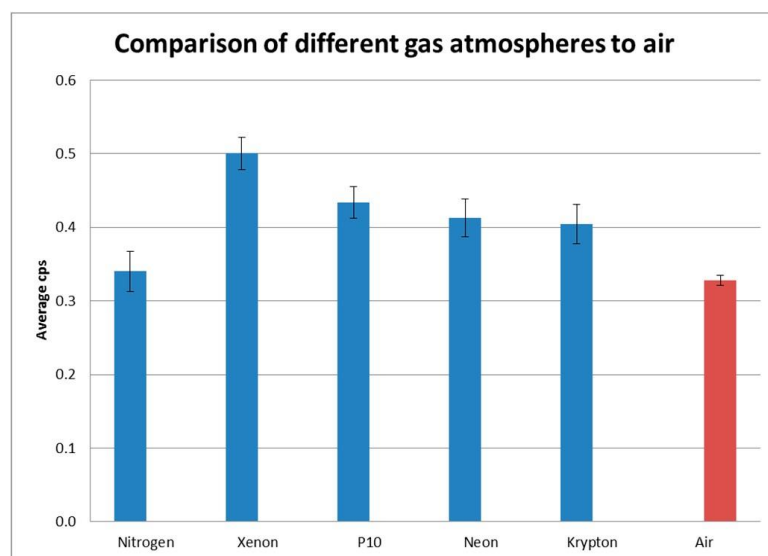


Figure 4-6: Comparison of average CPS in different gas atmospheres.

Table 4-2: Variation in average counts per second (CPS) by gas in comparison to air.

	Air	Nitrogen	Xenon	P10 CH4 10%; Ar 90%	Neon	Krypton
Duration of experiment (s)	57,600	3888	4203	5073	3721	3550
Total counts	18,890	1322	2103	2201	1537	1436
Average CPS	0.3280	0.3400	0.5004	0.4339	0.4131	0.4045
Counting Uncertainty	0.7%	2.8%	2.2%	2.1%	2.6%	2.6%
Average CPS difference to air	-	0.012	0.1724	0.1057	0.0851	0.0765
Percentage increase from air	-	3.6%	52%	32%	26%	23%

As can be seen from Table 4-2, there was an increase in the average CPS for all gases compared to the air atmosphere. Xenon provided the greatest effect, with a 52% increase in the average CPS compared to air. This finding is most significant as an increase in the signal will make detection easier, and the ability to replicate this in the field could greatly enhance detection possibilities.

P10 (10% Methane, 90% Argon) is used in gas-filled ionising radiation detectors due to its ionising properties, and was tested to determine if these properties would be beneficial in this application. It increased the CPS by 32% compared to the air atmosphere. Neon and Krypton also showed a significant increase in the CPS recorded, 26% and 23% respectively.

Nitrogen showed only a small increase, which could be accounted for within the uncertainty and therefore may not be an actual observed increase. As this is the primary constituent of air and it is known to enhance fluorescence in the 300–400 nm wavelength range [1, 5, 13, 15, 30, 35] this result was unexpected. Sand et al. [18] found an increase in fluorescence in the deep UV (around 260 nm) using a Nitrogen purge. As Brett et al. [60] found there was a lack of fluorescence in the 230–290 nm wavelength range in air as compared to a pure Nitrogen atmosphere, which they attributed to Oxygen quenching. In this instance, using a flow of gas as opposed to a fully purged gas atmosphere would appear to have a great effect on fluorescence. For field operations the possible effect of Oxygen quenching on the gases which showed a

marked increase in fluorescence in these tests may merit further investigation, and that a repeat of the experiments to determine replication possibilities in the field be carried out.

4.4.4 Pulse Shape

The oscilloscope was used to record the pulse shape from each of the experiments in order that any differences could be observed and the pulse could be compared to pulse shapes from other UVC emitting sources, such as a UVC-emitting bulb, flame, or from a different gas atmosphere. Although the design of the detector rather than the source is most likely to determine the output pulse, differences would provide a valuable avenue for determining the source of the UVC photons and therefore increase the potential of a detector in the field. A minimum of 50 pulses were recorded for each experiment for comparison.

For each of the experiments carried out with the ^{210}Po source, the pulse shape showed no distinguishable difference between different gas atmospheres. Figure 4-7 shows a comparison of the shapes of a single pulse recorded during each of the gas experiments. From this it can be seen that it is not possible to differentiate one gas from the other in terms of the pulse shape. Therefore, it can be concluded that different gas atmospheres do not affect the characteristics of the pulse outputted by the UVTRON.

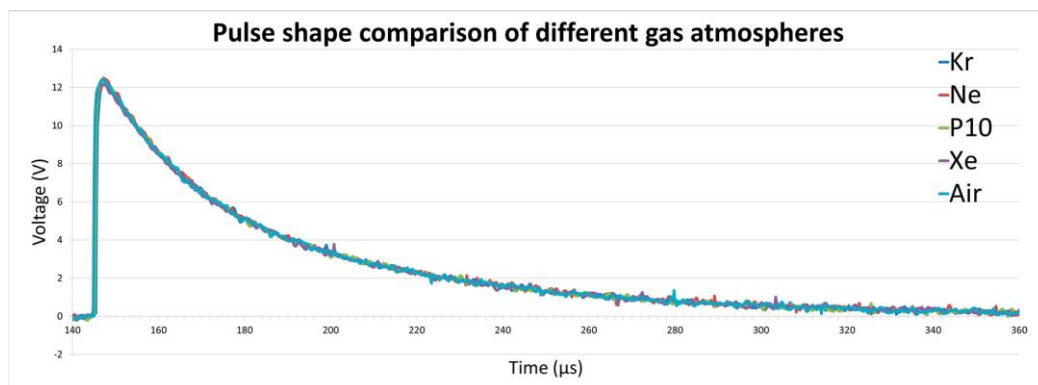


Figure 4-7: Pulse shape comparison of different gas atmospheres.

4.5 Conclusions

These experiments show that it is possible to detect alpha-induced air fluorescence using the UVTRON flame detector in normal lighting conditions.

Assuming a standard $1/r^2$ relationship for the drop off in signal with distance (r) between the source and detector, the limit of detectability, based on the signal being above the level of background, is approximately 240 mm, as shown in Figure 4-8. This data is for the 6.95 MBq source with the R9533 UVTRON sensor. This may be the potential limit of this particular configuration, however it is much greater than the distance of alpha particle travel and indicates that this method has potential for stand-off detection through further work.

It is also possible to estimate the minimum detectable activity for this sensor. Assuming a source of equal properties to the ^{210}Po source of 6.95 MBq, excepting a reduced activity level, the minimum activity level which would provide a count of greater than the background count is $47.1 \text{ kBq} \pm 14.9 \text{ kBq}$. The margin for error is calculated from the error for the background count as this is much greater than that for the CPS with the source in air. As the activity levels of alpha contamination which would be encountered in the field would be of a wide range of values, from Bq to GBq, this sensor shows the potential for stand-off detection in a number, but possibly not all, potential situations. However, other sensors in the UVTRON range are available, and these experiments were carried out with the off-the-shelf set up without optimisation or alteration for the specific use.

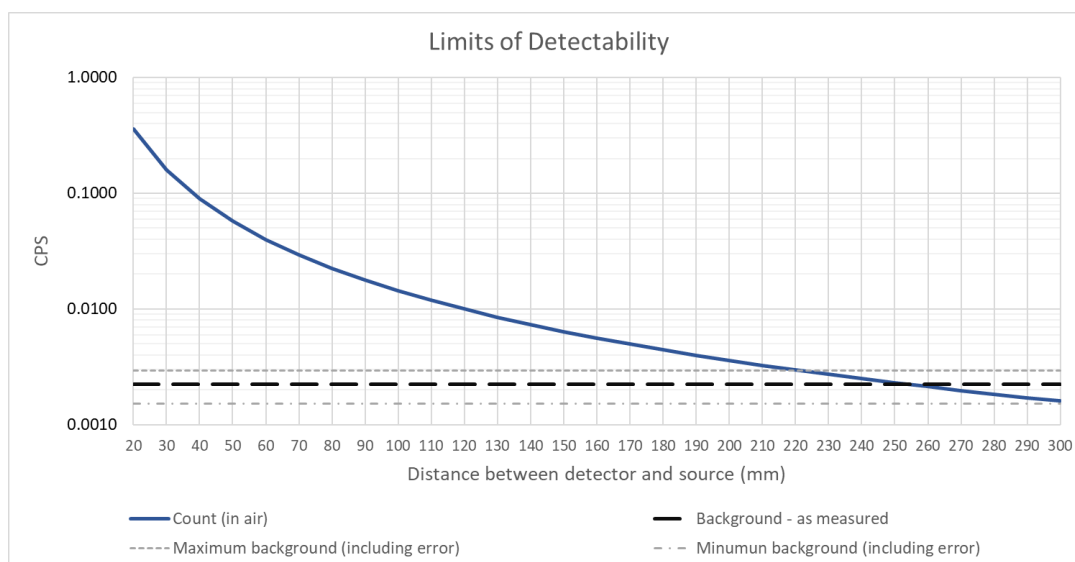


Figure 4-8: Limits of detectability showing the drop off in signal due to increased distance between sensor and source. The recorded background count \pm the calculated error is shown.

As the UVTRON is similarly unresponsive to ambient light when in a room illuminated by either or both commercial lighting and natural light, the UVTRON has little issue from interference from other lighting sources when used indoors. Although the background count is negligible in such conditions, it will provide a limiting factor in the sensitivity of the UVTRON for alpha detection applications when counts approach background levels due to a decrease in signal either from a less active source or increased distance between source and detector. This may be relevant in applications with a low source activity, but will be less so in decommissioning where activity levels may be significantly high.

In combination, the background count in different lighting conditions, the effect of distance, the activity level of the source, and the variation of count frequency over time will determine the minimum sensitivity of the detector in any given field condition.

It has also been shown that a flow of gas over an alpha source, which may be more easily deployed in the field, can increase the fluorescence detected. Xenon resulted in an increase of 52%, with P-10 (32%), Neon (26%), and Krypton (23%), also enhancing

fluorescence. Nitrogen did not provide a significant increase. Further gas flow tests, including the verification of results by repetition of the experiments carried out to date are planned.

Chapter 5

Gas Flow to Enhance the Detection of Alpha-Induced Air Radioluminescence Based on a UVTRON Flame Sensor

Anita J. Crompton , Kelum A. A. Gamage, Steven Bell, Andrew P. Wilson, Alex W. Jenkins and Divyesh Trivedi

Reprinted from Sensors, 18(6), 1842; June 2018, with permission from Sensors.

5.1 Abstract

In many field applications where alpha-induced radioluminescence (or so-called UV fluorescence) could potentially be used for stand-off detection of alpha-emitting materials, it may not be possible to create a fully purged gas atmosphere. Hence, an alternative gas delivery method to utilise the radioluminescence enhancing properties of gases has been investigated, with the novel results from this presented herewithin. A solar blind ultraviolet C (UVC) sensor (UVTRON R9533, Hamamatsu, Japan) has been used to detect changes in the signal in the UVC wavelength range (180–280 nm), where

gases of Ar, Xe, Ne, N₂, Kr, and P-10 were flowed over a 6.95 MBq ²¹⁰Po source using a narrow diameter pipe close to the source. In comparison with an air atmosphere, there was an increase in signal in all instances, the greatest being the flow of Xe, which in one instance greater than doubled the average CPS. This increase in signal could prove beneficial in the design of a stand-off alpha detector to detect the very small UVC radioluminescence signals from alpha-emitting materials found in nuclear decommissioning environments.

5.2 Introduction

Due to the short range of alpha particles in air (approximately 5 cm depending on energy), detectors which require direct interaction to detect alpha radiation are required to be operated in very close proximity to any surface under examination. This means that detection of alpha-emitting contamination is time-consuming and places personnel in close proximity to potentially hazardous materials, including the possibility of exposure to a mixed radiation field as is found in many real world nuclear environments.

As alpha particles travel, they transfer energy to and ionise the air. The relaxation from this excited state causes the emission of optical photons. These photons have a much greater MFP than the original alpha particle and hence provide a possible opportunity for stand-off alpha detection. This radioluminescence is mainly in the 300–400 nm wavelength range [1, 29]. However, in this range, there is much interference from background light, either from the sun or from indoor lighting, making the detection of this radioluminescence problematic. Stand-off detectors trialled to date have usually operated in darkness or special lighting conditions [1, 12, 13, 16, 17, 18, 26, 30, 44].

Other work has looked at the emissions in the UVC (ultra violet C) wavelength range (180–280 nm), which although lesser in intensity has much lower background levels with which to contend. UVC from the sun is mainly stopped in the atmosphere, meaning little reaches the surface of the earth, and UVC is generally not emitted by indoor lighting as it can be hazardous to eyes and has no practical benefit as it is well outside of the visible light spectrum [37]. This has meant that stand-off alpha detection in the UVC wavelength range has been investigated with some positive results for detection in daylight conditions [43,33].

In light of the low signal intensity of UV, and especially UVC photon emissions even from a relatively active alpha source, a means to enhance the signal could reduce the burden on any detector system in terms of how sensitive it would be required to be to detect alpha-induced radioluminescence in field operation. This would provide a better chance of detecting a low activity source or in bright daylight conditions, and to this end, research has been carried out into the effect of a gas atmosphere on the level of radioluminescence, including in the UVC wavelength range. Section 5.3 looks at previous research to date, with the remainder of sections detailing the results of recent experiments using a flow of gas.

5.3 Gas Atmosphere Influence on Radioluminescence Spectrum and Yield

Nitrogen makes up approximately 78% of the composition of air and is the main cause of radioluminescence in a dry air atmosphere. The other main constituent of air, Oxygen at approximately 21%, has been shown to quench radioluminescence [60, 67]. The remainder comprises small proportions of other gases (approximately 1% Argon, 0.04% Carbon Dioxide, and fractional quantities of Neon, Helium, Methane, and other gases).

To determine if changes in the atmosphere surrounding an alpha source have an effect on the radioluminescence yield, experiments using a purged gas atmosphere have been carried out.

Some researchers have compared the alpha-induced radioluminescence readings of two PMTs in an N₂ atmosphere, one sensitive in the 160–650 nm wavelength range, the other 300–650 nm, and found little difference between the two [67]. From this they concluded that N₂ radioluminescence occurs mainly in wavelengths of above 300 nm. This held true for N₂, dry air, O₂, Carbon Dioxide (CO₂) and Methane (CH₄) atmospheres. O₂, CO₂, and CH₄ produced significantly less radioluminescence than N₂ and dry air and quench radioluminescence when mixed with N₂ due to the excited states of these gases not decaying through the emittance of photons. The amount of quenching depends on the composition of the secondary gas and the percentage of that gas, as can be seen by decreases in the radioluminescence yield in an N₂/O₂ atmosphere when the percentage of O₂ is increased. In an N₂ atmosphere, there is however less Oxygen quenching on the NO lines, which are in the UVC wavelength range [60].

Although this increase in radioluminescence due to N₂ takes place mainly in the ultra violet A and ultra violet B (UVA and UVB) regions (300–400 nm), other gases have the potential to fluoresce in the UVC wavelength range, and these may prove beneficial in detecting alpha particles through UVC photon emissions. There are difficulties in examining luminescence of rare gases due to them fluorescing in the Vacuum Ultraviolet (VUV, 10–200 nm) wavelength region [63]. However, several of these gases also fluoresce in the UVC wavelength region, albeit not as strongly.

Argon has been shown to luminesce in the VUV and UVC wavelength region, in three distinct wavelength bands, with maxima at 130, 180, and 220 nm [62]. The 220

nm peak can be seen in Figure 5-1, which also shows the peaks in the UVA and UVB wavelength ranges.

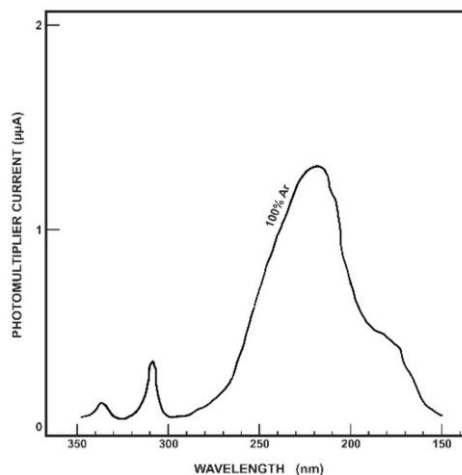


Figure 5-1: Radioluminescence spectrum of 100% Argon. Figure reproduced from [62].

The highest intensity of these maxima was found to be 220 nm, with 180 nm the lowest, although the 180 nm band was less easily quenched, and the intensity of radioluminescence was less dependent on pressure. The 220 nm Ar peak value of 45 (in arbitrary units) is greater than the 236 nm peak produced by N₂, which reached only 32 (in arbitrary units). Increasing the pressure of an Ar atmosphere (between 0.07 and 2.63 atm) leads to an increase in radioluminescence in the 170–280 nm wavelength range, with this being more rapid between 200 and 280 nm.

However, others found an Ar atmosphere fluoresced with a distinct peak at 127 nm, with no other peaks in the 115–300 nm range, but a small, gradual rise between 200 and 270 nm [63], although this has been seen to peak at approximately 250 nm before starting to decline [60]. They identified the VUV peak as due to the recombination of ions with electrons, which in their later work they determined produced one VUV photon per recombination [68]. They suggest that in the 200–270 nm region radioluminescence is due to the third continuum, and that the mechanism of

this has as yet no satisfactory explanation. They also found peaks of 150 nm for Kr and 175 nm for Xe, just outside the UVC range, with a Gaussian distribution of width 13 nm and 15 nm (FWHM) respectively. The Ar 127 nm peak also had a Gaussian distribution with a width of 11 nm (FWHM). They also examined the travel of an alpha particle in different gases and calculated the range of alpha particles is approximately 48 mm in Ar, 34 mm in Kr and 25.2 mm in Xe [63]. They also discovered that increased pressure led to an increase in recombination radioluminescence, and that this was greater in Xe than in Ar or Kr.

In alpha-induced ionisation within gases, the average energy per ion pair was found to be due to the stopping power of the gas and independent of alpha particle energy for Hydrogen, Helium, N₂, Ar, and Nitrous Oxide [69, 70]. Others found that the average energy value per ion pair in Ar for alpha particles of different energies was consistent for particles over 5 MeV [65]. This would suggest that the gas medium rather than alpha energy is more important in determining radioluminescence wavelength and therefore is relevant in potentially increasing radioluminescence intensity in the UVC wavelength range.

Kerst et al. [32] investigated the effect of N₂ on radioluminescence in the UVC wavelength range. They tested a ²¹⁰Po source in an N₂ purged atmosphere and found increased radioluminescence in the sub 300 nm wavelength range due to an increase in nitric oxide (NO) luminescence. Alpha emitters in air produce electronically excited nitric oxide molecules, and the presence of N₂ enhances this radioluminescence to detectable levels [32].

Although Ar is readily available at nuclear facilities and certainly fluoresces in the UVC wavelength region, it may be more beneficial to consider an alternative which produces a significant peak in a wavelength more suited to existing UVC detectors—

for example the UVTRON which has a wavelength detection range of 185–260 nm. Xe peaks at a higher wavelength than Ar and may be more suited to UVC detection enhancement.

5.4 Materials and Methods

Based on the prior research laid out in Section 5.3, an experiment was devised which would test the effect of different gases on alpha-induced radioluminescence in a method which could potentially be used in the field. As a flow over the source does not depend on a purged gas atmosphere, it may be more suited to a wider application in the field, where the contamination could be in a large space or spaces containing personnel. A flow of gas within a purged atmosphere when researching the use of protons to excite gases has been found to be preferable to a static atmosphere as it increases the intensity of the radioluminescence [61]; hence, the use of a flow is not unprecedented for research in this area.

Five noble gases were selected for the tests; N₂, Xe, Ne, Kr, and Ar. These were selected as the most likely to fluoresce in the UVC wavelength range. The results can also be compared to previous research which was carried out with several of the gases. P-10 (90% Ar, 10% Methane) was also tested as this gas mixture is utilised for its ionising properties.

Experiments were carried out at the National Physical Laboratory in Teddington, Middlesex. The set up for the experiments was as follows (see Figure 5-2).

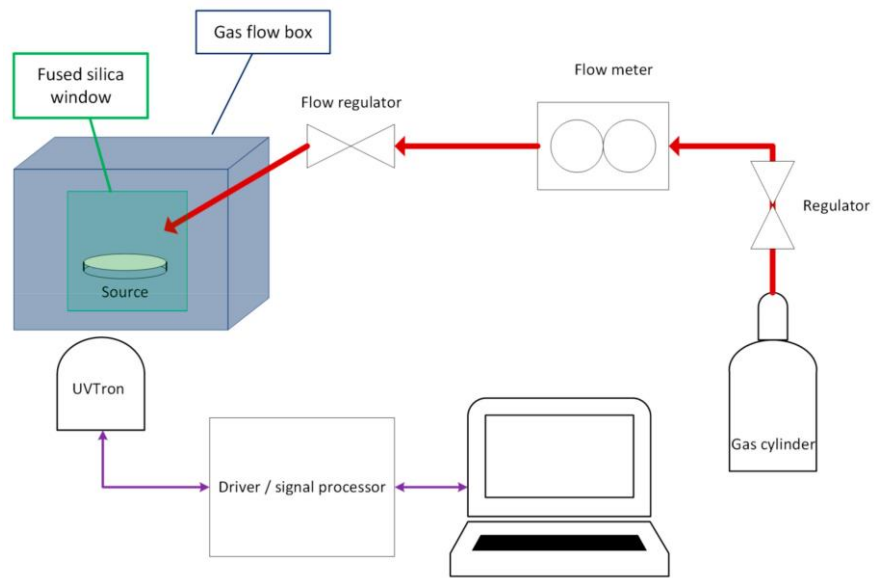


Figure 5-2: Schematic of equipment set up.

A sealed ^{210}Po source with activity of 6.95 MBq (at time of experiment, 29 August 2017) was placed inside a black Perspex box of dimensions $260 \times 234 \times 230$ mm (see Figure 5-3). ^{210}Po was selected for the experiments as it decays through alpha emission only and therefore produces negligible other emissions to affect the sensor reading. The box has a 75×75 mm window of 2 mm thick synthetic fused silica (Spectrosil©). Fused silica is preferable to ordinary glass as it allows UVC to pass with minimal attenuation (less than 10%) [58]. This window also prevented alpha particles being directly incident on the sensor. A lid was placed on top of the box at the commencement of and throughout each experiment to prevent the fume hood extractor system from removing the gas before it reached the source. The chamber was not gas tight, and some loss/exchange of gas would have occurred.

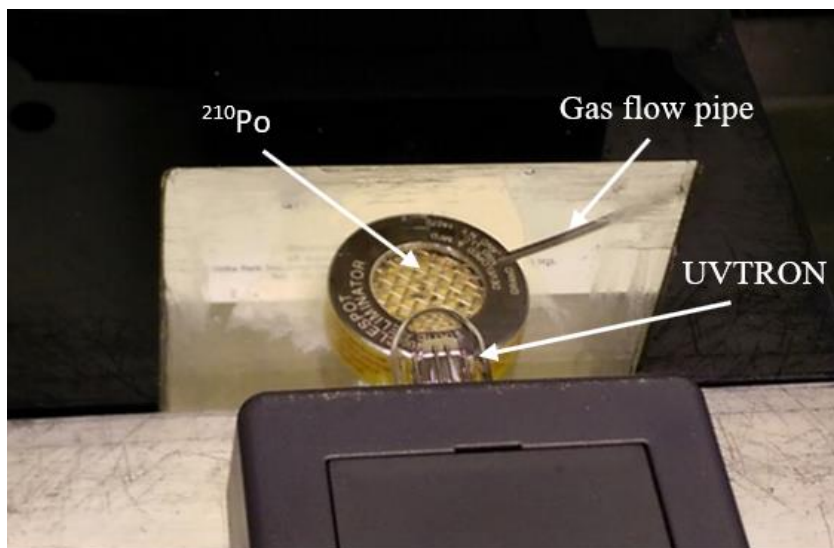


Figure 5-3: Photograph showing the ^{210}Po source inside the gas flow box (silver disk with mesh surface and yellow edge), with the gas flow pipe above and to the left. The UVTRON (small glass bulb) is external to the box and is attached to the grey box in the foreground which houses the detector electronics

The UVTRON sensor was placed outside of the box approximately 20 mm from the source (see Figure 5-3). The UVTRON (R9533, Hamamatsu Photonics, Hamamatsu, Japan) is sensitive in the 185–260 nm range. It is designed to detect flames or corona discharge but has been verified in its use as a sensor to detect alpha-induced air radioluminescence and has a very low background count in laboratory lighting conditions [33]. The UVTRON was used with the off-the-shelf driver circuit (C10807, Hamamatsu Photonics, Hamamatsu, Japan) which both powers the UVTRON and conditions the output signal. An Arduino Uno was used to count the pulse outputs from the driver and relay this to the laptop. The driver outputs one pulse per incident photon, up to a maximum of 40 CPS. This is sufficiently fast for alpha radioluminescence counting for this source activity and separation distance, where less than 10 photons per second are incident on the detector within the wavelength range [33]. The sensor has a peak sensitivity at approximately 210 nm, with an equal increase and decrease in sensitivity on either side of this wavelength between 185 and 260 nm, which are the

limits of the wavelength range of the UVTRON and therefore at which the sensitivity is 0.

The UVTRON was used in these experiments for several reasons. It is solar blind and has a very low background count and so can be used in normal laboratory lighting without the need for filtering or other light-attenuating technology. It is a relatively low-cost, robust, off-the-shelf sensor suited to inclusion in a field operable detector and fitting with the experimental main aim of testing a system which may be more suited for field operations.

Gas was flowed over the source from close proximity in an air atmosphere using a small flexible pipe of 1 mm bore diameter (see Figure 5-3). At the end of the experiment, the lid was removed from the gas flow box and the fume hood extractor system was switched on to extract the gas. Following this, the pipes were purged with the new gas, and the flow was regulated, with a steady flow reading established before the next experiment was undertaken. The gases and flows are listed in Table 5-1 below.

Table 5-1: Table of gases showing flow rates and experiment groups.

Gas	Symbol	Purity	Approximate Flow Rate mL/min		
			Group 1 [13]	Group 2	Group 3
Nitrogen	N ₂	N5.0	65	65	65
Xenon	Xe	N5.0	50	65	65
P10	10% CH ₄ /90% Ar	±5%	60	-	65
Krypton	Kr	N5.0	55	65	65
Neon	Ne	CP grade	40	-	65
Argon	Ar	N5.0	-	-	65

Group 1 experiments consist of those carried out and already reported on by Crompton et al. [33].

5.5 Results

5.5.1 Background

In order to allow for any effect from background lighting, for each of the experimental sessions, a background count was taken. The experiment was set up as detailed in the above section but without the presence of the source. The background had been shown to be very low, with average CPS of $2.2 \times 10^{-3} \pm 0.7 \times 10^{-3}$ for group 1 [33]. For groups 2 and 3, the background was $1.48 \times 10^{-3} \pm 0.53 \times 10^{-3}$. The experiments were carried out in the same laboratory with standard commercial strip (fluorescent) lighting which remained on for the duration of all experiments. The experiments were conducted a number of weeks apart, and therefore differences such as location of the equipment, temperature, humidity etc. in the laboratory between the two dates is most likely the cause of the difference in the background recorded for groups 2 and 3 compared to those for group 1 [33].

5.5.2 Air Atmosphere Results

The experiment was first carried out with the source in place in an air atmosphere to provide a baseline to compare the results of different gas flows. The gas flow experiments were carried out in three groups, and at the commencement of each, the count in air was taken for comparison. This was done to ensure that any changes in the position or orientation of the equipment could be allowed for in the comparison between the air and gas results. The counts in air were average CPS of 0.3282 ± 0.0032 for group 1 [33], 0.4106 ± 0.0107 for group 2, and 0.4503 ± 0.0028 for group 3.

5.5.3 Gas Flow Results

The results of the gas flow experiments carried out on this occasion in comparison with those already reported [33] are shown in Figure 5-4 and Figure 5-5, and Table 5-2. Figure 5-4 shows the average CPS for each of the gases for each of the three groups of experiments (note, not all gases were tested in all groups due to practical issues). Figure 5-5 shows the increases for the different gases as compared to the air atmosphere, which are shown as a percentage increase from the average air CPS. Table 5-2 lists the data for further clarity.

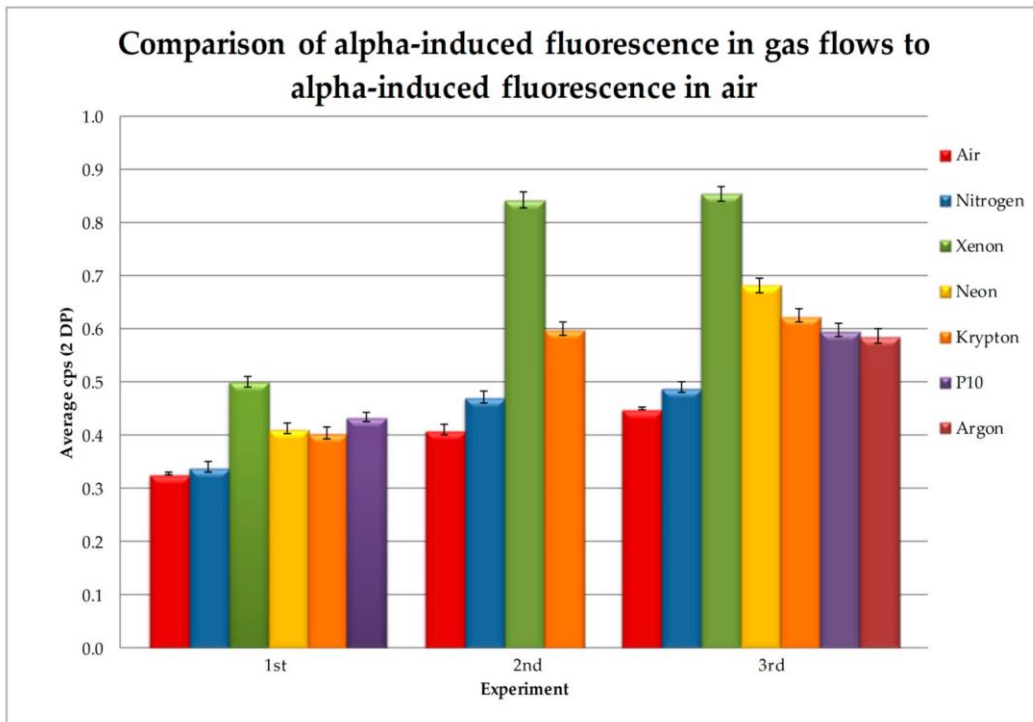


Figure 5-4: Showing the CPS for each of the gas flows in each of the three experiment groups (note: not all gases were tested in the second group due to time constraints) comparing the results of those in the first group reported by Crompton et al. [33] with two following groups.

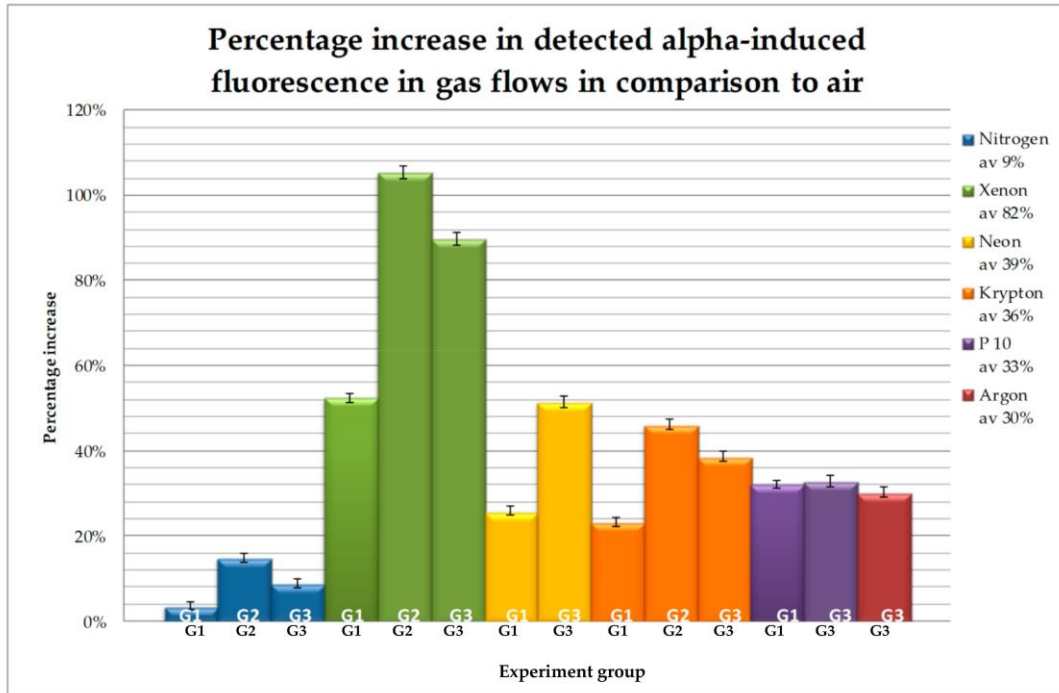


Figure 5-5: Showing the increase in CPS for the different gas flows as a percentage of the air atmosphere results.

Table 5-2: Table of gas flow results.

Gas	Group 1 CPS [33] (% incr)	Group 2 CPS (% incr)	Group 3 CPS (% incr)	Average % Increase
N ₂	0.34 (3.61)	0.4716 (14.86)	0.4898 (8.79)	(9.09)
Xe	0.5004 (52.47)	0.8431 (105.32)	0.8541 (89.71)	(82.5)
Ne	0.4131 (25.87)	-	0.6812 (51.51)	(38.69)
Kr	0.4045 (23.26)	0.6003 (46.21)	0.6247 (38.77)	(36.08)
P10	0.4339 (32.21)	-	0.5983 (32.9)	(32.55)
Ar	-	-	0.5865 (30.27)	(30.27)

As can be seen from Table 5-2, the greatest increase was seen with a flow of Xe, which increased the radioluminescence between 52% and 105%, with an average over the three experiments of an 82.5% increase. Ne provided the next greatest increase, with an average of 39% over the two experiments, which was close to the average increase of Kr of 36%. P-10 gave the next greatest increase, averaging 33% over the two experiments, with Ar slightly lower than this at an average of 30%. P-10 gave the more stable result over the two experiments, with a difference of less than 0.7% between the two readings, giving it the second highest average in the group 1 readings.

Group 1 has the lowest increase across all gases in comparison to groups 2 and 3. This is most likely due to slight differences in the set-up—for example, the position of the gas flow pipe in relation to the source which may have affected the make-up of the atmosphere within the MFP of the alpha particles emitted from the source, for example by increasing quenching by Oxygen.

5.6 Discussion and Conclusions

From these results it can be seen that all the gases increased the radioluminescence detected to some degree. This is most likely due to the replacement of O₂, which quenches radioluminescence, in the scintillation zone of the alpha particles.

The increase in the CPS produced by a Xe atmosphere, especially as the detection rate may be as much as doubled, does indicate that the use of a flow of this gas could be useful in the development of an alpha detection system. As the alpha signal is low in the UVC wavelength range, but in light of this range having the least background interference, the enhancement of the signal could reduce the level of sensitivity required in a detection system. This may make more likely the development a stand-off alpha detector using UVC radioluminescence to indicate the presence of

alpha contamination. It would require the engineering of a solution, which could be stand alone or utilise gas environments already found in some field conditions and could be part of a package of detection solutions, including such elements as lenses and bespoke, optimised electronics, which would make up the final detection system.

The increase in signal using a flow of Xe, which in all three groups of experiments increased the signal intensity by more than 50%, shows a much greater change than in any of the other gases. Saito et al. [63] found a peak at a wavelength of 175 nm which is just under the 185 nm sensitivity range of the UVTRON, but as the peak has a full width half maximum (FWHM) of 15 nm there may be sufficient overlap into the UVTRON detectable range. The shorter travel of alpha particles in Xe (25.2 mm at atmospheric pressure) [63] suggests that alpha deposits its energy closer to the alpha source. The main fluorescing area has been found to be within 10 mm of the alpha source [13]. Hence, this shorter MFP may be instrumental in increasing the signal intensity close to the source and therefore aid location of the source by the UVTRON.

Over the duration of the experiments, which were carried out for no less than and approximately for one hour, there was little variation in the measured CPS despite a likely accumulation of the flowed gas inside the box. This indicates that the flow method may potentially be as useful for increasing radioluminescence as a purged atmosphere. As the area around the source which produces the most radioluminescence is within 10 mm of the source itself [13], hence it is the atmosphere in this area which most affects radioluminescence, which could conceivably be greatly modified by a flow of gas in the vicinity of the source, as these results would suggest.

Slight alteration in the set up due to removal and replacement of the equipment between experiment groups will account for some of the differences seen between the measurements for each of the gases, and hence an average percentage increase is

included in Table 5-2. This variation is likely due to minor differences in distance between or the angle of the sensor relative to the source, indicating that this set up is sensitive to small variations which would need to be addressed in any field operative detector system.

The relatively small increase seen in an N₂ gas flow may seem in conflict with N₂ purged atmosphere results where there is seen an increase in radioluminescence. This likely due to the UVC wavelength range and a possible lack of NO which has been shown to cause radioluminescence in the UVC wavelength range in an N₂ purged atmosphere [32]. The lack of NO produced by a flow as in comparison to a purge may be due to the lack of excited NO molecules being generated by the alpha particles in this circumstance.

Using Hurtgen et al.'s [71] method of calculation, the limit of detection (L_d) was determined. This method was used as it is specifically designed for detectors with a low or zero background count, which the UVTRON has in normal lab lighting conditions. The limit of detection is independent of the signal count, depending only on the background level, and is determined with a confidence level of 95.45% (as advised by ISO, 1993) through the equation;

$$q \text{ at } L_d, s_{net} = 2.86 + 4.78 (b + 1.36) \quad (5.1)$$

where L_d = the limit of detection, s_{net} is the net signal (gross signal minus background), and b is the background count. For laboratory conditions, the limit of detection for these experiments was 17.4 net counts for the first set of experiment, and 15.3 net counts for the second and third sets of experiments for a count time of one hour (3600 s). The difference is due to small changes in background conditions, where the background

counts averaged 7.9 and 5.4 counts, respectively, in 3600 s. As can be seen, the very low background count of the UVTRON leads to a very low limit of detection in laboratory conditions. In comparison, the net counts with a source present ranged from 1223 counts in Nitrogen to 3045 counts in Xenon in one hour (3600 s). Based on the low detection limit, the system could easily be configured to alert for the presence of an alpha emitter based on a count rate above a set threshold, which is likely to be very low. As an example of the sensitivity of this sensor and off-the-shelf electronics, Hurtgen et al.'s [71] method was used to calculate the lowest activity which could have been detected here. In air, the minimum activity at this distance is between 89 and 149 kBq, which is similar to Nitrogen at between 82 and 144 kBq. Xenon as expected has the lowest limit of detection at an activity of 47 kBq in the second and third set of experiments. Although certain applications would find this limit alone beneficial, with the aforementioned use of optics, optimised electronics, collimation, and other elements of a detector system based on this sensor, this limit could be extended significantly. Therefore, the experiments carried out to date would suggest that gas flows could be useful in field conditions to increase the signal and make detection easier.

Through further experimentation, it may be possible to determine the mechanism for luminescence in the UVC region, the third continuum, which may throw light on which gases are more likely to provide a suitable radioluminescence yield in this region and possibly lead to a predictive model of which gases are likely to fluoresce in this region for further testing.

Chapter 6

The Effect of Gamma and Beta Radiation on a UVTRON Flame Sensor: Assessment of the Impact on Implementation in a Mixed Radiation Field

Anita J. Crompton , Kelum A. A. Gamage , Divyesh Trivedi and Alex Jenkins

Reprinted from Sensors, 18(12), 4394; December 2018, with permission from Sensors.

6.1 Abstract

Due to the short path length of alpha particles in air, a detector that can be used at a distance from any potential radiological contamination reduces the time and hazard that traditional alpha detection methods incur. This would reduce costs and protect personnel in nuclear power generation and decommissioning activities, where alpha detection is crucial to full characterisation and contamination detection. Stand-off alpha detection could potentially be achieved by the detection of alpha-induced

radioluminescence, especially in the ultraviolet C (UVC) wavelength range (180–280 nm) where natural and artificial background lighting is less likely to interfere with detection. However, such a detector would also have to be effective in the field, potentially in the presence of other radiation sources that could mask the UVC signal. This work exposed a UVC sensor, the UVTRON (Hamamatsu, Japan) and associated electronics (driver circuit, microprocessor) to sources of beta and gamma radiation in order to assess its response to both of these types of radiation, as may be found in the field where a mixed radiation environment is likely. It has been found that the UVTRON is affected by both gamma and beta radiation of a magnitude that would mask any UVC signal being detected. ^{152}Eu generated 0.01 pulses per second per Bq through beta and gamma interactions, compared to ^{210}Po , which generates 4.72×10^{-8} CPS per Bq from UVC radioluminescence, at 20 mm separation. This work showed that UVTRON itself is more susceptible to this radiation than the associated electronics. The results of this work have implications for the use of the UVTRON as a sensor in a stand-off detection system, highlighting the necessity for shielding from both potential gamma and beta radiation in any detector design.

6.2 Introduction

The short travel of alpha particles in air creates difficulties in the detection of alpha-emitting materials due to the requirement for any directly interacting detector to be around 10 mm from the surface being scanned [5]. In the case of a large surface area or complex geometry, this is time consuming. Where there is a mixed radiation field, this can also pose a potential hazard to detector operators, and may require PPE and limited exposure times. Hence, a stand-off detector is preferable to reduce costs, reduce time and limit any hazard to personnel. As they travel from the emitting source, alpha

particles ionise the air, which generates radioluminescence photons, mainly in the ultraviolet wavelength range. These photons travel in the order of kilometres, much further than the alpha particles themselves, which are limited to approximately 50 mm, depending on their energy. This radioluminescence therefore presents an opportunity for stand-off alpha detection for nuclear operation, decommissioning and security applications. Several previous studies have been made of the radioluminescence phenomenon, and possible detector configurations have been put forward [72]. These have mainly focused on the UVA and UVB wavelength ranges, 300–400 nm, where most of the radioluminescence is generated. However, there is great deal of background interference within this wavelength range, due to sunlight and emissions from artificial lighting.

The UVTRON flame sensor made by Hamamatsu is designed to detect UVC emissions from flames as part of fire warning systems [73]. It uses this wavelength range as sunlight in this range is stopped by the atmosphere, making the UVTRON what is termed ‘solar-blind’. Artificial lighting also does not emit UVC, as it is harmful to human eyes, and is a waste of energy to generate as it does not aid vision [37]. Therefore, there is little or no background light in this wavelength range to interfere with detection of the flame emissions, especially indoors. When UVC photons are detected by the UVTRON, it outputs a pulse which can be detected directly, or more usually can be processed by a specially designed driver circuit (C10807, Hamamatsu, Japan), also available COTS from Hamamatsu, and a 5 V square wave is emitted, which is transmitted to some configuration of warning device to alert people to the presence of a flame.

In previous work, the ability of the UVTRON to detect the UVC wavelength portion of the UV emission from an alpha emitter, ^{210}Po , was established [33]. This

introduced the potential of the UVTRON as the sensing element in a stand-off alpha detector. However, as Po is a pure alpha emitter, this work did not establish the effect of other types of radiation, as may be found in the field, on the UVTRON. Further work has been undertaken to assess the reaction of this sensor to the presence of different gases [74] with a view to determining its potential for use in a stand-off alpha detection system. The work detailed in this paper was carried out to determine the effect of beta and gamma radiation on the UVTRON and its associated electronics in order that the design of a detector system using the UVTRON could take into account and minimise or eradicate the effect of this on the determination of the UVC emissions.

6.3 Materials and Methods

Initial experiments were carried out at the National Nuclear Laboratory (NNL), Cumbria, UK, and subsequent experiments were carried out at Lancaster University, Lancashire, UK. The initial experiments were used to inform the planning of the second set; however, some have been included here where relevant.

The UVTRON is a solar-blind flame sensor available COTS from Hamamatsu. It has a very low background count, which was measured at 2.2×10^{-3} CPS in laboratory lighting conditions at the National Physical Laboratory (NPL) in Teddington, UK [33]. The UVTRON responds to the incidence of photons within the 185–260 nm wavelength range on its Ni cathode. See Figure 6-1.

Using the photoelectric effect, the sensor's Ni cathode, a material which is only sensitive to light in the 185–260 nm wavelength range [54], emits an electron when such a photon is incident upon it. This electron is accelerated through a high-potential field towards the anode. During its transit, through the gas multiplication effect, gas within the UVTRON glass enclosure is ionised by the electron, causing the emission of further electrons, creating a cascade effect at the anode. This generates a current pulse

which is emitted by the UVTRON. This can be detected directly using an oscilloscope or it can be processed by a COTS available optimised driving circuit (C10807, Hamamatsu, Japan), which both provides the high voltage required by the UVTRON and processes the output from the UVTRON into a 5 V square pulse. Figure 6-2 shows the direct and processed 5 V square pulse shapes from the UVTRON during normal operation.

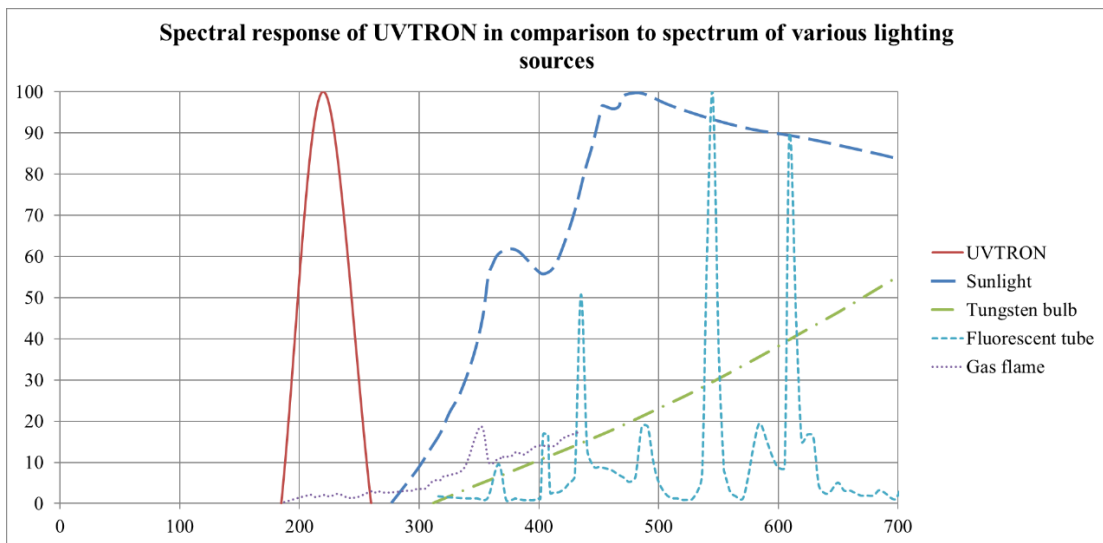


Figure 6-1: Spectral response of the R9533 UVTRON. Derived from data from Hamamatsu [54] and OSRAM [75].

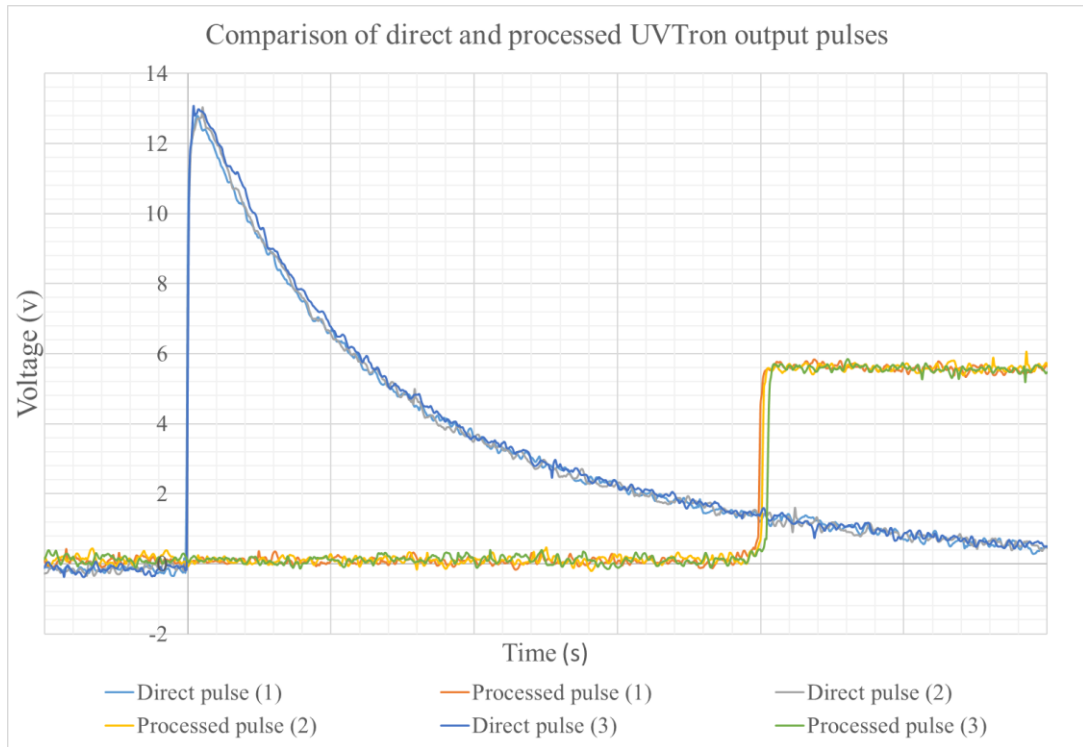


Figure 6-2: Comparison of the pulse recorded directly from the UVTRON and the processed pulse generated by the driver circuit (C10807, Hamamatsu) during normal UVC detection operation. The two pulses generated for three separate photon events (1, 2, 3) are shown.

In these experiments, the driver circuit was connected to an Arduino Uno, which counted the output pulses in each second and transmitted this to a laptop. Figure 6-3 shows a block diagram schematic of the set up.

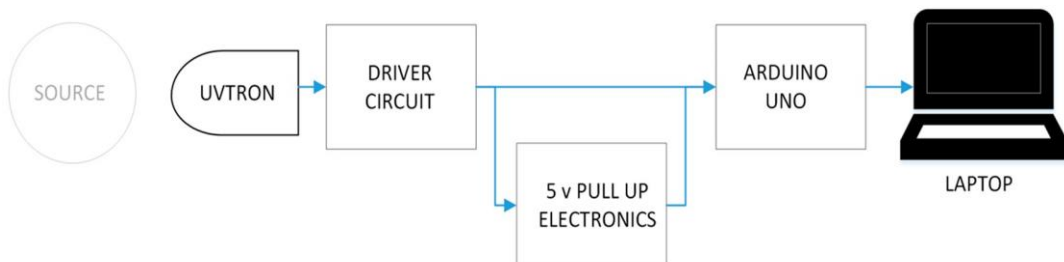


Figure 6-3: Block diagram of the set up used in these experiments.

This configuration of UVTRON and the driver circuit can produce a pulse approximately every 25 ms due to the quenching time of the optimised driver circuit

supplied by Hamamatsu (C10807) [76]. It can therefore generate a theoretical maximum pulse rate of 40 pulses per second. In practice, the UVTRON saturates at between 35 and 37 CPS. Hamamatsu also supply a schematic of their suggested driver circuit as an alternative to their optimised, ready-made driver circuits. Used with this, the UVTRON has a minimum quenching time of 1 ms, depending on the values of the resistor and capacitor used, following the formula

$$tq \approx 0.5 \times C_1 \cdot R_1 \quad (6.1)$$

where C_1 is the value of the capacitor, R_1 is the value of the resistor. Over the duration of these experiments, the UVTRON was working well below saturation levels.

The sources used at NNL were especially prepared samples of varying activity ^{241}Am (100, 200, 500, 750 kBq, and 1 MBq) and a 1 MBq mixed Pu isotope replicating what may be found in the field. A sample of ^{90}Sr with an activity of approximately 11.5 kBq was also available. The sources used at Lancaster University were all sealed sources of various beta-, gamma- and alpha-emitting radionuclides with differing activities, in order that a range of emission effects could be investigated. Five different radionuclides were used in the experiments, see Table 6-1. Due to the low activity of the primary beta emitter, five point sources were used together to give a better level of statistical uncertainty.

Table 6-1: List and properties of radionuclides used.

Isotope	Activity Bq	Type of Source	Emission Type
^{210}Pb	645	Point	Gamma, beta (alpha < 1%)
^{241}Am	44,110	Point	Alpha, gamma
^{36}Cl	50	Point	Beta
^{137}Cs	16,252	Point	Beta, gamma
^{152}Eu	49,830	Point	Gamma, beta
$5 \times ^{36}\text{Cl}$	$5 \times 50 = 250$	$5 \times$ point: area 52 mm ² approx.	Beta

For the duration of the experiments carried out at NNL, each sample was placed within a fume cupboard, and was a set distance of 170 mm from the UVTRON sensor. The UVTRON sensor and associated electronics were placed outside of the fume cupboard, but the door remained open for the duration of the experiments, see Figure 6-4.

The background count was taken, and comparisons were made between the different lighting options available, including the main lighting and the fume cupboard lighting. As there was no difference between any of the lighting conditions, the lights in the laboratory remained on for the duration of all experiments. Foil was inserted between the sensor and source for some of the experiments to assess the impact on the sensor count.

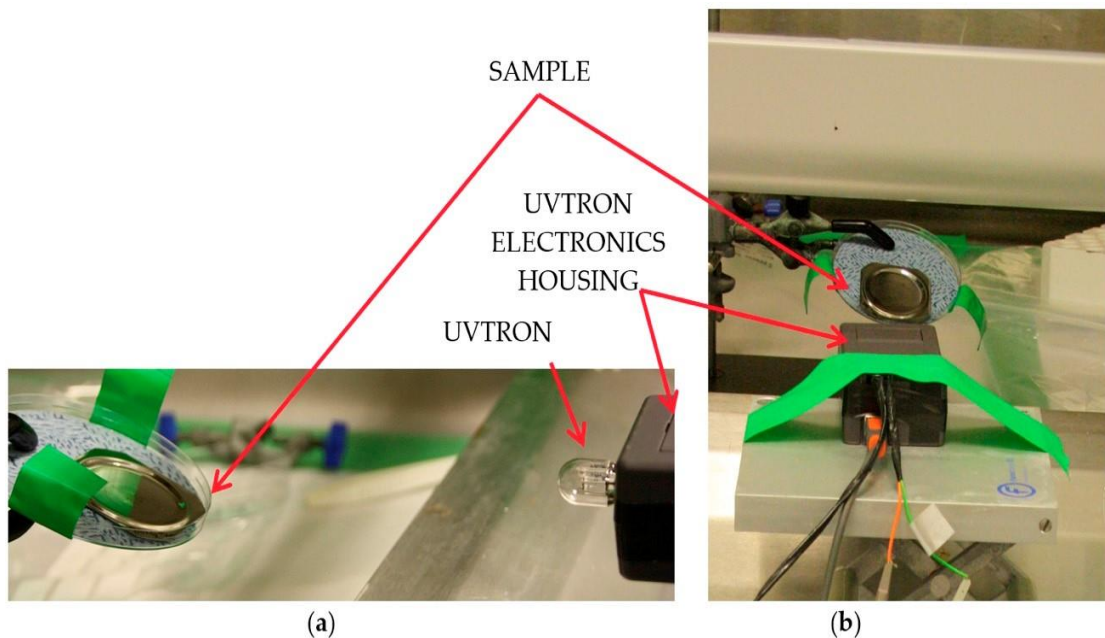


Figure 6-4: Showing the set up at the National Nuclear Laboratory (a) view from the side showing the vertical alignment of the UVTRON and source, and (b) showing the horizontal alignment of the UVTRON to the source.

For the experiments carried out at Lancaster University, the source was placed at a measured distance (between 20 and 100 mm) from the cathode of the UVTRON. To gain insight into the cause of any effect on the UVTRON, several materials were inserted between the source and sensor for some of the experiments, including paper, Aluminium foil, Aluminium sheet of thickness 6.92 mm and Lead blocks of thickness 25 mm. These were placed in close proximity to the UVTRON, see Figure 6-5. The number of output pulses from the UVTRON driver circuit for each second of each experiment were counted using the Arduino Uno and recorded on a laptop. These were then used to provide a gross average CPS. The background response of the UVTRON in situ without the presence of any source was recorded, and this was subtracted from the count to provide a net average CPS for each radionuclide, distance or inserted material. The background with the presence of the inserted materials was also recorded to determine if their presence affected the background reading; however, these were not significantly different.

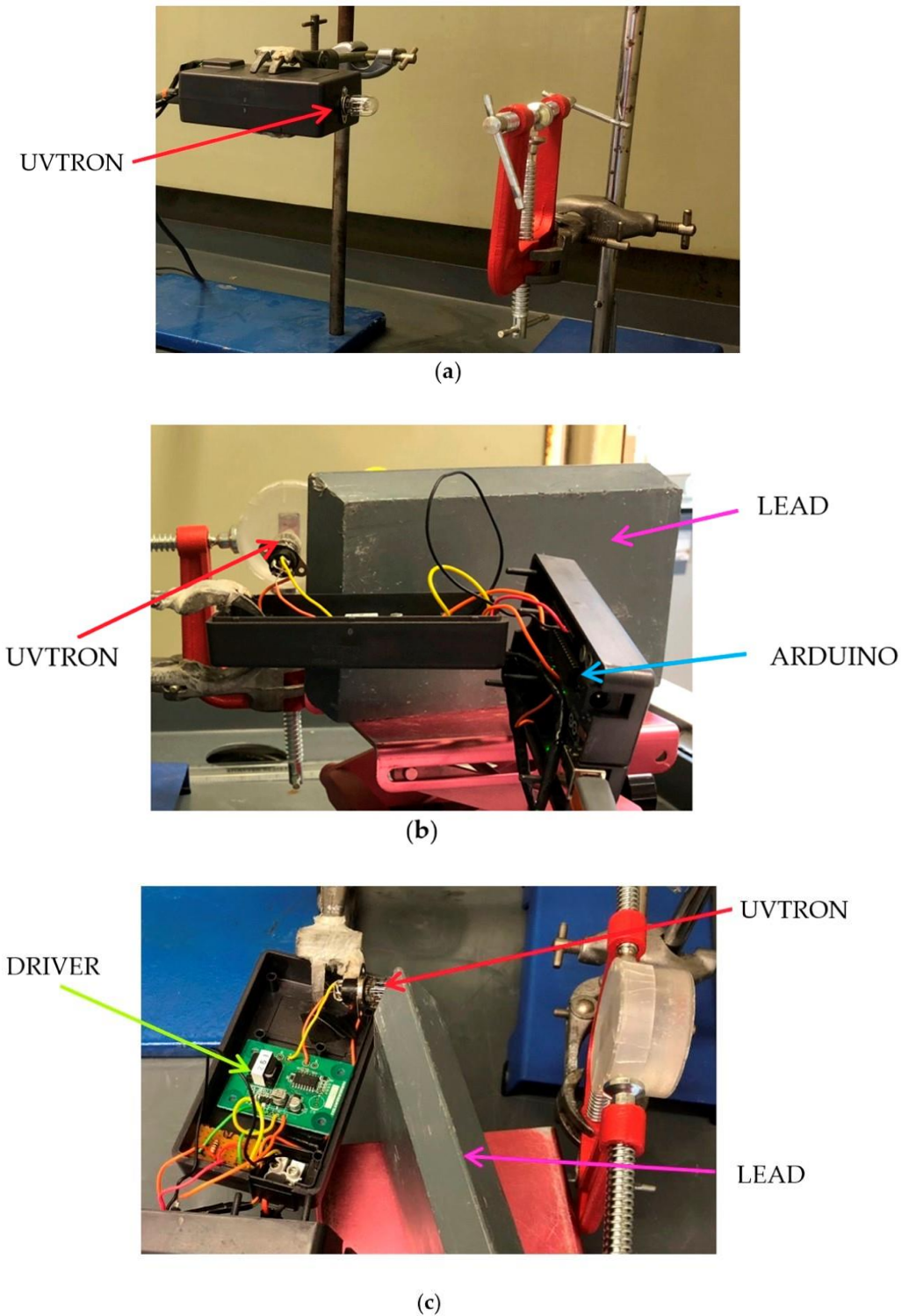


Figure 6-5: The set up at Lancaster University. (a) UVTRON connected to the (closed) electronics housing containing the driver circuit and Arduino microprocessor, and the clamp used to support the source. (b) The UVTRON is exposed to the source with Lead shielding of the electronic driver circuit and Arduino microprocessor, which can just be seen in the lid of the electronics housing. (c) Top view of the shielded electronics and exposed UVTRON, showing the driver circuit (green), which can be seen in the base of the electronics housing.

6.4 Results

Where possible, the results reported here are above the critical limit as devised by Hurtgen et al. [71] for detectors with low background counts. The majority of the results are also above the limit of detection, including all ^{241}Am results, with a 95.45% confidence level. Where the results differ from this, it is stated in the text. Due to the low count values, experiment durations were necessarily long, between one and three hours depending on the sample and distance, and in some instances it was necessary to rely on exceeding the critical limit to show a signal was present, though the exact magnitude of the signal could not be statistically verified.

The background was used to provide a net signal and also to identify the difference between backgrounds of different locations. The background already established at the National Physical Laboratory in previous UVTRON experiments [33] was compared with backgrounds taken at NNL and Lancaster University, see Table 6-2. The Lancaster University background reading is in line with the readings taken at NPL. The NNL readings were taken with the sensor facing into the fume cupboard and facing away. The background is much higher when facing the fume cupboard, which suggests that the samples housed in the fume cupboard were causing the UVTRON to respond. That this value dropped so significantly when the sensor unit was turned away would suggest that it was UVC, beta or low-energy gamma rays that could not reach or penetrate the electronics housing that was causing a reaction from the UVTRON. The background readings in both sets of experiments were taken into account in calculating a net response.

Table 6-2: Background reading comparisons.

Location	Value Av. CPS	Uncertainty CPS
NPL—first visit [33]	2.2×10^{-3}	0.7×10^{-3}
NNL—sensor turned towards fume cupboard	23.2×10^{-3}	2.0×10^{-3}
NNL—sensor turned away from fume cupboard	3.2×10^{-3}	0.7×10^{-3}
Lancaster University	2.3×10^{-3}	0.09×10^{-3}

Results from the NNL experiments indicated that the UVTRON was susceptible to both gamma and beta radiation, though this could not be quantified at that time due to the high background readings. Hence, further experiments were planned and carried out at Lancaster University to verify the NNL findings. Figure 6-6 shows the average CPS of each of the experiments. Table 6-3 shows the results in tabulated form;

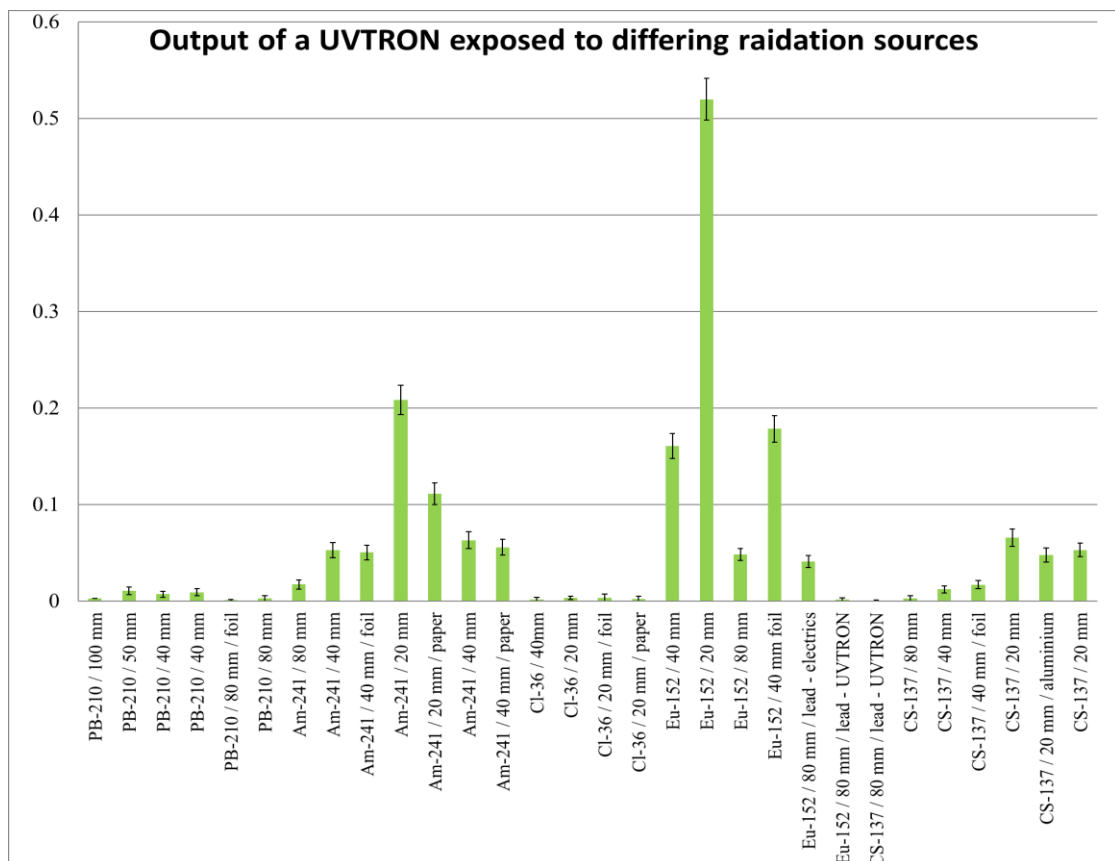


Figure 6-6: Results of the experiments carried out at Lancaster University. The error bars shown are the confidence interval as included in Table 3. Where no error bar is shown, this is due to the count being below the threshold to calculate the confidence interval, i.e., less than the limit of detection as laid out by Hurtgen et al [71]

Table 6-3: Results of experiments carried out at Lancaster University.

Istotope	Activity Bq	Distance mm	Shielding	Counts per Second (Snet)	Confidence interval *
²¹⁰ Pb	645	100		0.0030	<L _d , >L _c
		50		0.0110	± 0.0039
		40		0.0073	± 0.0033
		40		0.0093	± 0.0036
		80	Foil	0.0011	<L _d , <L _c
		80		0.0029	<L _d , >L _c
²⁴¹ Am	44,110	80		0.0175	± 0.0048
		40		0.0530	± 0.0079
		40	Foil	0.0507	± 0.0076
		20		0.2083	± 0.0152
		20	Paper	0.1114	± 0.0112
		40		0.0634	± 0.0085
		40	Paper	0.0560	± 0.0080
5 x ³⁶ Cl	5 x 50 = 250	40		0.0019	<L _d , >L _c
		20		0.0034	± 0.0018
		20	Foil	0.0037	<L _d , >L _c
		20	Paper	0.0027	<L _d , >L _c
¹³⁷ Cs	16,252	80	Lead - UVTRON	0.0007	<L _d , <L _c
		80		0.0028	<L _d , >L _c
		40		0.0124	± 0.0037
		40	Foil	0.0172	± 0.0042
		20		0.0660	± 0.0091
		20	Aluminium	0.0481	± 0.0074
		20		0.0531	± 0.0069
¹⁵² Eu	49,830	40		0.1610	± 0.0128
		20		0.5200	± 0.0217
		80		0.0483	± 0.0062
		40	Foil	0.1786	± 0.0136
		80	Lead – electronics	0.0412	± 0.0061
		80	Lead -UVTRON	0.0020	<L _d , >L _c

* L_d = limit of detection, L_c = critical limit, S_{net}—calculated using Hurtgen et al. [71].

Of the five radioisotopes tested at Lancaster University, when adjusted for the different activity levels, ^{36}Cl showed the greatest count rate, with ^{210}Pb second highest, ^{152}Eu third, ^{241}Am fourth, and ^{137}Cs gave the lowest count. Assuming an isotropic distribution with a $1/r^2$ drop off, all isotopes had a count rate of less than 2% of the anticipated number of impacts onto the sensor cathode. The anticipated number of impacts was calculated using the activity of the source, the distance to the detector and the cathode size by

$$S_1 = S_0 A_d / 4\pi r^2, \quad (6.2)$$

where S_1 is the anticipated number of impacts on the sensor cathode per second, S_0 is the activity of the source in Bq, A_d is the area of the sensor cathode in mm^2 , and r is the distance between the sensor and the source in mm.

The percentage of actual count relative to anticipated impacts (S_1) was found to decline by isotope in approximately the same order as the count rate per Bq declines. ^{210}Pb and ^{36}Cl showed both the most counts relative to activity and the greatest percentage of expected counts due to likely impacts. ^{137}Cs exhibiting the lowest count per Bq and the lowest percentage actual count relative to anticipated impacts.

When a double thickness sheet of domestic Aluminium foil (thickness approx. 0.016 mm per sheet) was placed between the sensor and source, the net count for ^{36}Cl , ^{241}Am and ^{210}Pb dropped slightly. A drop was also recorded at NNL for the ^{241}Am and Pu samples. The net count for ^{152}Eu and ^{137}Cs increased slightly. Using Hurtgen et al's [71] method for determining uncertainty, there is still some overlap in the reporting ranges within which the true value of the count lies. This overlap is small, and may be due to the limited duration of each of the experiments which determines the spread of the confidence interval.

When a sheet of ordinary printer paper was placed between the sensor and source the count rate for ^{36}Cl and ^{241}Am decreased, with no overlap in the confidence intervals for either isotope. These were the only two isotopes where paper was used to test if UVC from alpha or beta emissions were being detected. For ^{36}Cl the count with paper between the source and detector was less than the count with foil between the detector and source. The drop in signal from the ^{241}Am may have been due to some UVC detection, as the alpha emissions would cause radioluminescence and therefore UVC photo emission.

When a 6.92 mm thickness Aluminium sheet was placed between the sensor and source the count rate for ^{152}Eu and ^{137}Cs dropped. The Aluminium sheet was used to block beta while the higher activity gamma would be able to penetrate. These two isotopes had the highest gamma energy of those tested. There was no overlap in the confidence intervals for ^{152}Eu , and a very small overlap for ^{137}Cs .

Lead blocks were used to attenuate the gamma and beta incident on the sensor and electronics (see Figure 6-5). The UVTRON was removed from its housing and placed behind a shield, and the driver circuit and Arduino were exposed to the source. This was repeated with the electronics behind the Lead shield and the UVTRON exposed to the source. The Lead blocks were then used to shield the entire sensor and electronics set up. When all of the sensor and electronics were shielded the signal dropped to approximately 9% of the CPS without the shielding. When the UVTRON only was shielded, the signal dropped to 4% of the CPS without shielding. When the electronics were shielded and the UVTRON exposed to the source, the signal was approximately 85% of the CPS without shielding. Due to the large decrease seen in signal, the limit of detection was not reached for the shielded electronics, but the critical limit was. The time to reach the limit of detection for this due to the low signal was

impractical. However, the large difference in signal, although not fully quantifiable, clearly demonstrates the difference made by the location of the shielding.

6.5 Conclusions and Discussion

The results of these experiments show two disadvantages to the UVTRON as an alpha-induced radioluminescence sensor, firstly the low and variable count and secondly the susceptibility to radiation. However, now identified, the second can be overcome with correct implementation and the first taken into account in the deployment of any system using a UVTRON for alpha detection.

Due to the low count rate for relatively long durations, resulting in fractions of average CPS, coupled with the sensitivity of the UVTRON to small changes in set up, for example, in orientation and distance, there can be significant variations on average CPS. In addition to relatively long durations to exceed the limit of detection, and overlapping confidence intervals, it is not possible to determine absolute figures for the response of the UVTRON to radiological stimuli. However, the suggested implementation of this sensor is in an alpha detection system, where a positive or negative response to the presence of alpha radiation is required. It has been shown that this can be achieved, and nothing in these results would preclude the ability of the UVTRON to detect and locate a source if implemented correctly. As the UVTRON is designed to give an on/off response to flames, and is a sensor rather than a meter, this is also sufficient for the purpose of alpha-induced radioluminescence detection.

The UVTRON has proven to be sensitive to gamma at least in the range 47 to 344 keV and beta from 63 to 710 keV, the ranges of the main emission types and energies of the radioisotopes used in this work [77]. ^{36}Cl gave the highest count per Bq, showing that the UVTRON is strongly affected by beta, which verified findings from a

brief exposure to ^{90}Sr at NNL. The results of using Aluminium shielding indicates that gamma also affects the UVTRON as this would block beta radiation. This can also be verified by the results from the ^{241}Am , which gave a significant reading with paper between the source and sensor, which would prevent any alpha and UVC photons from reaching the UVTRON, but not gamma.

So it can be seen that both gamma and beta, when incident on the UVTRON, cause an output pulse. As the Ni electrodes are not likely to be affected by the gamma or beta radiation, it may be the direct ionisation of the gas within the sensor that leads to the output pulse. Both beta and gamma would be expected to pass through the outer UV glass casing of the sensor and into the ionising gas inside, and as both are types of ionising radiation, this may initiate the cascade of electrons necessary for an output pulse from the UVTRON.

The use of Lead shielding has shown that it is the UVTRON itself, rather than the associated electronics, that are primarily affected by gamma and beta radiation. This is important in any detector design using the UVTRON as the sensor element as it will need to be shielded from gamma and beta radiation, as will the electronics though not to the same degree. This lack of radiation tolerance is an issue, but one that has been seen and overcome in other electronic systems when designed for use in a nuclear environment. The use of shielding will be required if the UVTRON is to be used in an alpha detection system suitable for use in the field.

This work and the preceding work, [33, 74], show that the UVTRON could be used to identify that a source is present and locate it using alpha-induced radioluminescence, but only if adequate shielding was provided to prevent both gamma and beta radiation impacting on the UVTRON. Some idea of the magnitude of the source activity could be inferred from the count rate, but the type of radionuclide could

not be identified from the UVTRON readings alone. As with its use as a flame detector, the UVTRON primarily has the potential to be used as an on/off stand-off alpha detector, with the low background and the ability to use the UVTRON in daylight conditions giving it an advantage over other radioluminescence detectors of this type. In applications like the long-term storage of radioactive waste, the low-cost continual monitoring of storage facilities to ensure no leakage of radioactive materials would be one example of the benefits of a detector system based on the UVTRON, as may the continual monitoring of nuclear facilities where radioactive material contamination could be a potential occurrence.

Chapter 7

Performance characteristics of a Tungsten collimator and UVTRON flame sensor for the detection of alpha-induced radioluminescence; Impact of UVC reflecting mirror and the effect of beta and gamma radiation sources.

*Anita J. Crompton, Kelum A. A. Gamage, Alex Jenkins, Steven Bell, and Divyesh Trivedi
Submitted to Sensors journal.*

7.1 Abstract

It has been established that the UVTRON flame sensor (Hamamatsu) can detect alpha-induced radioluminescence, but that the presence of gamma and beta radiation both interfere with this detection. A UVTRON was placed inside a Tungsten collimator and exposed to a range of radioisotopes, ^{210}Po , ^{241}Am , ^{137}Cs , ^{90}Sr and ^{60}Co , to investigate the effect of shielding the UVTRON. The collimator is a cylinder with a hole in the curved wall to allow light and particles to access the interior, without providing a direct shine path to the UVTRON sensor. Ultraviolet C (wavelength 180-280 nm) radioluminescence is reflected onto the UVTRON sensor using a UVC reflecting

Chapter 7 : Performance characteristics of a Tungsten collimator and UVTRON flame sensor for the detection of alpha-induced radioluminescence; Impact of UVC reflecting mirror and the effect of beta and gamma radiation sources.

mirror. It was found that the collimator does not affect the low background count of the UVTRON, but that it does greatly reduce the UVC signal reaching the UVTRON from an alpha source. Beta particles entering the collimator, although not directly impacting on the UVTRON, do increase the count, likely due to bremsstrahlung radiation. The collimator attenuates gamma radiation dependent on the gamma energy, but as expected, does not block it. When using more than one source, the count is cumulative and therefore it may be possible to determine the presence of UVC radioluminescence through subtraction of the gamma and beta element of the signal. The results and findings of the experiments carried out are presented herewithin.

7.2 Background

The detection of alpha radiation is difficult and time consuming due to the short travel of alpha particles, around 50 mm in air depending on their energy. This means that detectors which require the direct impact of the alpha particle on a probe or sensor window must be within approximately 10 mm of the surface to ensure direct interaction [5]. This is time consuming for large areas or complex geometries, for example where pipes or equipment are present. It may also present a hazard to operators, both from accidental alpha contamination and from other radiation sources which may be present. Hence a stand-off alpha detector has long been sought.

As alpha particles travel they ionise the air, causing the production of ultraviolet (UV) photons, known as radioluminescence. These photons travel in the order of kilometres and so provide a potential means to detect alpha radiation from a distance. The majority of the UV is produced in the UVA and UVB wavelength ranges (280 – 400 nm). However, there is a significant background of natural and artificial light in this wavelength range, making identification of the radioluminescence difficult. The

Chapter 7 : Performance characteristics of a Tungsten collimator and UVTRON flame sensor for the detection of alpha-induced radioluminescence; Impact of UVC reflecting mirror and the effect of beta and gamma radiation sources.

emissions in the UVC wavelength range (180-280 nm) are much fewer in number, but there is no competition from other lighting sources. The UVC in sunlight is absorbed by the ozone layer, and bulbs used for general artificial lighting do not routinely emit UVC. Although special UVC emitting bulbs are available they are not used for indoor lighting as the human eye cannot see in the UVC wavelength range and it can be damaging to the eye.

A solar-blind flame detector, the UVTRON (Hamamatsu, Japan) has proven capable of detecting the UVC emission from a ^{210}Po source [33]. It is designed to detect the UVC from flames in fire detection systems and has excellent background light rejection capabilities. However, it is susceptible to interference from beta and gamma sources [78]. Hence a collimator has been designed to attenuate gamma and to block any shine path to the UVTRON. A UVC mirror is used to reflect the UVC onto the UVTRON within the body of the collimator.

A set of experiments were carried out at the National Physical Laboratory (NPL) in Teddington, UK, to assess the efficacy of the collimated system prior to field trials. The results of these experiments, conclusions and recommendations are laid out in this document.

7.3 Experimental set up

7.3.1 UVTRON

The UVTRON (Hamamatsu, Japan) is a UVC detector designed to detect UVC from flames for commercial applications. The R9533 model selected for this application is sensitive to light in the 180 – 260 nm wavelength range. It uses the photoelectric effect and gas multiplier effect to generate an output pulse when a UVC photon is incident on its Ni cathode. This pulse can be channeled into a bespoke driving circuit (C10805,

Chapter 7 : Performance characteristics of a Tungsten collimator and UVTRON flame sensor for the detection of alpha-induced radioluminescence; Impact of UVC reflecting mirror and the effect of beta and gamma radiation sources.

Hamamatsu, Japan) which processes the signal and outputs a 5 V square wave. In the configuration used within the collimator, this signal is outputted to an Arduino Uno which counts the pulses for each second and outputs this value to a computer. Due to the 25 ms quenching time of the driver circuit the UVTRON's maximum output is a theoretical 40 CPS. However, in practice the value reaches no greater than 38 CPS.

7.3.2 Collimator

The collimator is a bespoke design for this application. It is made of a Tungsten alloy (Wolfmet HA190) which has good radiation shielding properties due to the density of the material. It is 90% Tungsten with a nickel and copper binder [79]. It provides a 15 mm shield wall around the UVTRON and associated electronics. Its geometry is cylindrical, enclosed at both ends, with a 15 mm diameter hole in the side wall through which the UVC enters the collimator (see Figure 7-1). The UVTRON is mounted vertically inside the cylinder. A UVC reflecting mirror is located at 45° to the hole and to the UVTRON, positioned to reflect any UVC entering the collimator onto the cathode of the UVTRON (see Figure 7-1 a & b). Modelling of the effect of the mirror angle showed that this is the optimum angle (see Figure 7-2) as well as being convenient for limiting the space required inside the collimator. The UVTRON is positioned to prevent a shine path from the hole to the sensor, ensuring that no particle entering the hole can impact directly on the UVTRON.

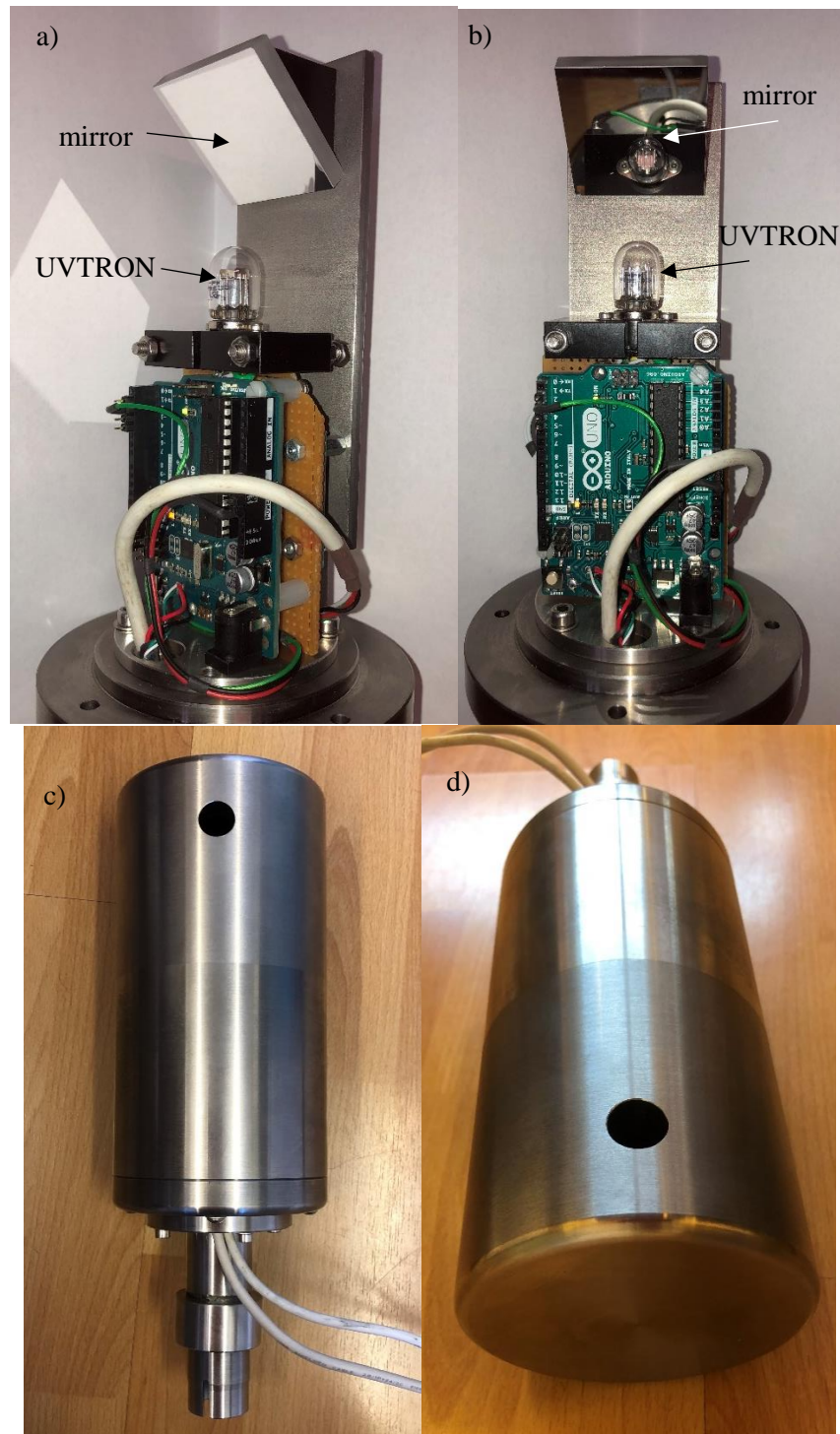


Figure 7-1: Tungsten collimator: a) & b) internal electronics showing placement of UVC reflecting mirror, c) external geometry (front view), d) external geometry (top view)

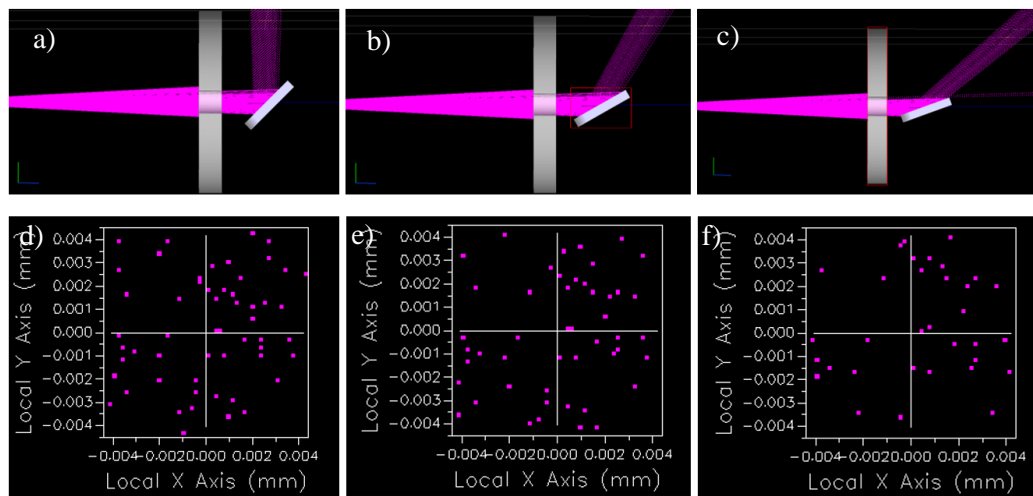


Figure 7-2: Modelling of different mirror angles (45° , 60° and 70°) using FRED32 raytracing software [80]; a), b) and c) show the rays passing through the collimator hole and reflecting from the mirror onto the UVTRON cathode; d), e) and f), show the rays incident on the UVTRON cathode. Using a limited number of rays, it is possible to see the decrease in incident rays with increase in angle, from 55 at 45° , to 48 at 60° , to 32 at 70° . At 70° not all rays impact on the mirror.

The collimator system was tested as a ‘black-box’ with the output to stimuli recorded without reference to any internal processes. The performance of the system as a whole is presented in this document, with some discussion of the cause of certain results and suggestion for further work.

7.3.3 Sources

Five sources were used for the experiments. A table is provided of the sources and their relevant characteristics. These are included in Table 7-1.

Table 7-1: Sources

Source	Activity MBq	Main emissions, energies and percentage [77]	Notes
²¹⁰ Po	180	Alpha 5304 keV (100%)	Disc source with thin window allowing alpha emission
²⁴¹ Am	73	Gamma 60 (36%), 18 (18%) & 14 (13%) keV	Sealed source with no alpha emission
¹³⁷ Cs	4.5	Beta 512 keV (95%) Gamma 662 keV (85%)	Sealed source with beta and gamma emissions
⁹⁰ Sr	32	Beta 546 (199%) & 2284 (100%) keV	Sealed source with beta emissions
⁶⁰ Co	8.1	Beta 318 keV (100%) Gamma 1173 (100%) & 1333 (100%) keV	Sealed source with beta and gamma emissions

The sources were used in isolation or in combination as required, as stated in the results section.

7.3.4 Set up

The collimated UVTRON was placed at a horizontal separation from the source, as can be seen in Figure 7-3. The uncollimated UVTRON was placed directly above the source.

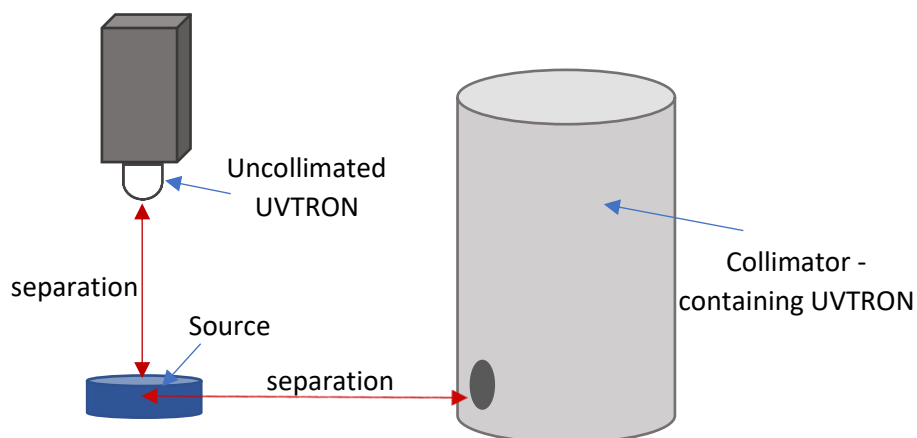


Figure 7-3: set up of the collimator, uncollimated UVTRON and source - showing the separation distances

7.4 Results

7.4.1 Background

A background count was taken in the laboratory under normal lighting conditions without the presence of a source. CPS were recorded over a period of approximately 17 hours. The collimated UVTRON recorded 92 counts in 62,591 seconds, giving an average CPS of $1.47 \times 10^{-3} \pm 0.153 \times 10^{-3}$. The uncollimated UVTRON recorded 88 counts in 62,542 seconds, giving an average CPS of $1.41 \times 10^{-3} \pm 0.150 \times 10^{-3}$. These are in line with earlier background counts taken in the same laboratory at NPL [33, 74]. The overlap in confidence intervals for the collimated and uncollimated results indicate that the background count is unaffected by the collimator. This supports the assertion that the background count is not related to ambient light, but is a function of the UVTRON system itself.

Comparisons to background in this document utilise the recorded background count relevant to the UVTRON system used for that particular set of results (collimated or uncollimated).

7.4.2 UVC / alpha response

When the 180 MBq ^{210}Po source was placed before the sensor, the count increased to 56 times background at a separation of 25 mm, 88 times at a separation of 60 mm, and 84 times at a separation of 120 mm, see Table 7-2. When a black-out cloth was placed over the collimator to attenuate radioluminescence, the signal reduced from 56 to 1.5 times the background signal. In line with earlier research [33, 74] this confirms the collimated UVTRON was detecting UVC from the ^{210}Po source. It has already been shown through earlier experimentation that the UVTRON can detect UVC from ^{210}Po

Chapter 7 : Performance characteristics of a Tungsten collimator and UVTRON flame sensor for the detection of alpha-induced radioluminescence; Impact of UVC reflecting mirror and the effect of beta and gamma radiation sources.

[33, 74]. However, this is the first time that collimated UVC, reflected onto the UVTRON using a UVC mirror has been detected. It confirms that the collimator design will admit and reflect UVC onto the UVTRON sensor.

By taking measurements with an uncollimated UVTRON at the same distances, the effect of the collimator was investigated. The collimator reduced the signal by 94 % at 60 mm, and 78 % at 120 mm, see Table 7-2. The signals were still far greater than background, 88 and 84 times background respectively. The untypical signal drop off, discussed in the following paragraph, may account for the large difference in collimator effect between the 60 mm and 120 mm results.

Table 7-2: Comparison between the signal between the collimated and uncollimated UVTRON when exposed to ^{210}Po , and the recorded background

	60 mm separation	120 mm separation
Collimated - CPS	0.125	0.118
Collimated - Times background	88	84
Uncollimated - CPS	2.013	0.543
Uncollimated – times background	1340	369
Collimated/ uncollimated	0.06	0.22

Using a UVC bulb to represent the source, the effect of the collimator was further investigated. The body of the collimator was removed to provide the uncollimated result for comparison (see Figures 7-1 a & b). At 15 cm separation, the uncollimated UVTRON saturated (38 CPS) at all angles (up to 90° was tested) and so the UVTRON itself was shielded, with the mirror reflecting UVC onto the UVTRON sensor. It was found that at 15 cm separation and a 0° angle, the UVTRON saturated both with and without the collimator cylinder in place (see Figure 7-1). However, the drop off in signal was much greater when the collimator was turned at an angle to the source with the

body in place (collimated) than without (uncollimated) (see Figure 7-4). At 15 cm separation the collimated signal reduced by half over each 5 ° s turned between 5° and 20°. The uncollimated signal remained saturated until 30° was reached, and then reduced by just under a half over the next 10°. With the light source at 2 m the collimator had a greater effect on the drop in signal caused by angle, with a drop to 72 % in the first 5°, but a drop to less than 3% of the 0° count at 10°. Without the collimator, the signal dropped by only 10% in the first 20°. It can therefore be seen that the reduction in signal produced by the collimator during the experiments with the radioactive sources is due to the reduced field of view caused by the entrance hole diameter. There is also a reduction caused by the reflection of the signal in the UVC mirror, which reflects 85% of UVC, as was demonstrated by the saturation at all angles when the UVTRON was directly exposed to the UVC bulb at 15 cm. The length of travel inside the collimator is also likely to cause a reduction in signal due to the widening of the collimated light over distance (see Figure 7-2). Modification to the geometry of the collimator and the addition of optics could increase the UVC reaching the UVTRON.

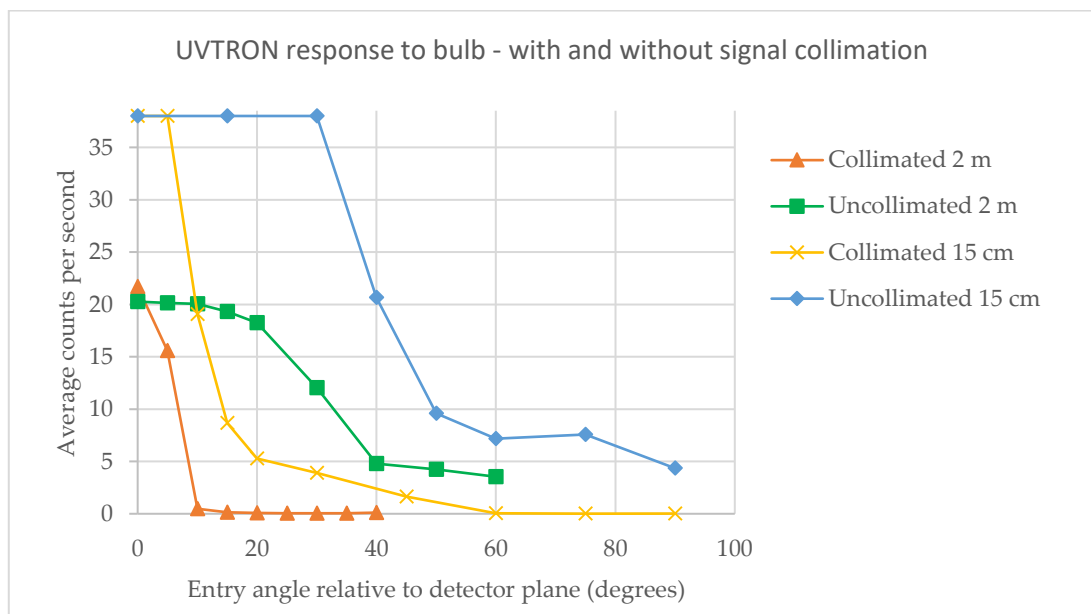


Figure 7-4: Response of UVTRON within collimator and with collimator body removed, at a separation between the bulb and collimator of 2 m and 15 cm.

The increase in signal from 25 mm to 60 mm separation, when a reduction would be expected, is likely due to two factors; the collimator being within range of the alpha particles and the geometry of the collimator. An estimate of the average distance of travel of the alpha particles emitted by the ^{210}Po can be calculated using the empirical equation;

$$R_{air} = (0.005E + 0.285)E^{1.5} \quad (7.1)$$

where R_{air} is the travel of the alpha particle in cm, and E is the energy of the alpha particle in MeV. The alpha particles emitted by the ^{210}Po , which are of energy 5.304 MeV, would travel approximately 38 mm. Therefore, some of the particles would impact on the collimator at 25 mm, reducing the path length along which the radioluminescence photons are produced. As the Bragg peak shows, the main energy loss of alpha particles is close to the end of their travel path and so impact on the collimator wall would reduce the total radioluminescence caused by alpha ionisation of the air. The collimator was tested as a 'black-box', but the internal geometry extends the travel path of the radioluminescence photons and the mirror attenuates the signal, meaning that the $1/r^2$ drop off in signal which would be expected may be affected by the collimator design.

The uncollimated UVTRON showed a more expected response to distance, with the signal varying less than 10% from the expected signal at 60 mm and 120 mm separation distances. To determine the expected CPS at each distance, equation 7.2 was used to calculate the $1/r^2$ relationship in the drop off in signal;

$$S_2 = S_1 \left(\frac{R_1^2}{R_2^2} \right) \quad (7.2)$$

where S_2 is the expected signal, S_1 is the recorded signal, R_2 is the separation at which S_2 is expected, and R_1 is the separation at which S_1 was recorded. This was applied to the data and the results for both the collimated and uncollimated UVTRONs are shown in Table 7-3. The table shows the actual CPS at each separation, and the expected CPS at different separations. Assuming the actual CPS is the true value and the $1/r^2$ relationship will be observed, the expected CPS is the counts that would be measured at a different separation. For example, at 25 mm the reading was 0.0784 CPS. The expected CPS at 60 mm would therefore be 0.0136 (using equation 7.2). As the actual count at 60 mm was 0.1245 this is 9.14 x the expected count.

Table 7-3: Showing the expected and actual results of exposure to ^{210}Po

If CPS at this separation is true		these are the expected CPS at the other separation (difference to expected in brackets)		
Collimated	Actual CPS	Expected at 25 mm	Expected at 60 mm	Expected at 120 mm
25 mm	0.0784		0.0136 (9.14 x)	0.0034 (34.7 x)
60 mm	0.1245	0.7170 (0.11 x)		0.0311 (3.80 x)
120 mm	0.1182	2.7227 (0.03 x)	0.4727 (0.26 x)	
Uncollimated	Actual CPS	Expected at 95 mm	Expected at 60 mm	Expected at 120 mm
60 mm	2.0132	0.8041 (0.71 x)		0.5040 (1.08 x)
95 mm	0.5721		1.4843 (1.41 x)	1.2634 (0.42 x)
120 mm	0.5425	0.8656 (0.66 x)	2.1699 (0.93 x)	

It can be seen from the table that the actual signal was 93 % of the expected signal at 60 mm and 108 % at 120 mm for the uncollimated UVTRON, meaning the actual and expected values are a close match, whereas for the collimated UVTRON, it was 26 % at 60 mm and 380 % at 120 mm, which shows a marked variation from what

Chapter 7 : Performance characteristics of a Tungsten collimator and UVTRON flame sensor for the detection of alpha-induced radioluminescence; Impact of UVC reflecting mirror and the effect of beta and gamma radiation sources.

would be the expected count. This is likely due to the collimator internal design which will affect the distance of travel of the UVC photons.

When the result at 25 mm is considered as S_1 , the count at 60 mm was 914 % of expected and 3472 % at 120 mm. This is likely due to the close proximity of the source to the collimator, within the alpha travel for the R_1 value. As noted earlier, this is likely due to the alpha particles impacting on the collimator before reaching their maximum energy transfer point, and the source being a sphere of radioluminescence with radius equal to the travel of the alpha particles and not a point source.

7.4.3 Beta response

It has already been shown that the UVTRON is susceptible to interference from beta radiation and gamma radiation [78], which the collimator seeks to reduce or remove. The collimated UVTRON was exposed to the ^{90}Sr source with the following results (see Table 7-4);

Table 7-4: Results of exposure of collimated and uncollimated UVTRONs to ^{90}Sr source

Separation mm	Av CPS	Comparison to background (times)	Uncollimated (150/300/450mm)	^{210}Po (25/120mm)
35	1.803	1281.23		0.0784
140	0.105	74.8	2.131	0.1182
240	0.047	33.64	0.8003	
600	0.007	4.88		

It can be seen from the results shown in Table 7-4 that up to at least 600 mm separation the signal generated by the beta emissions can be distinguished from background by the collimated UVTRON system. Comparisons of recorded CPS with the anticipated CPS at different distances shows that the drop off in signal follows an approximate $1/r^2$ reduction.

In comparison with uncollimated results at similar distances, the collimator greatly attenuates the beta signal, by up to 94 %. However, at a similar distance the collimated beta signal and alpha signal recorded are of a similar magnitude, 0.105 and 0.1182 CPS respectively, though the alpha source has a much greater activity level. The pulse shape is the same for any stimulus which causes the UVTRON to emit a pulse, as verified using an oscilloscope connected directly to the UVTRON. Therefore, it is not possible to distinguish with this collimated system between an unknown beta and an unknown alpha source. The results of exposing the collimated UVTRON to mixed sources are presented in section *7.4.5 Mixed radiation response*.

When a sheet of fused silica, thickness 2 mm, was placed over the entrance to the collimator, the signal reduced from 0.1053 to 0.008 CPS, a reduction of 93% of the signal without the fused silica. As it requires 5 mm of glass to fully attenuate beta particles emitted by ^{90}Sr , some ingress of beta particles to the collimator is to be expected, and the CPS with the fused silica was found to be five times background which would support this. When the collimator entrance was turned to 90° relative to the source, the signal dropped from 1.8028 to 0.005 CPS, a more than 99 % reduction, indicating that it is the ingress of beta particles to the collimator which is generating the signal.

Although the geometry of the collimator prevents beta particles impacting directly on the UVTRON, it is possible that bremsstrahlung radiation is being created within the collimator, affecting the UVTRON and causing the response. The collimator was tested as a 'black-box' in these experiments and any internal processes were not investigated at this stage. However, as the fused silica glass used in these experiments has a transmittance of over 90 % at up to 10 mm thickness, it is likely that the inclusion

Chapter 7 : Performance characteristics of a Tungsten collimator and UVTRON flame sensor for the detection of alpha-induced radioluminescence; Impact of UVC reflecting mirror and the effect of beta and gamma radiation sources.

of a fused silica window in excess of 5 mm thickness would have negated the collimated UVTRON response to beta radiation from the ^{90}Sr source.

The distance travelled by beta particles from ^{90}Sr is approximately 10 m in air. However, assuming a $1/r^2$ reduction the signal would be equal to background in approximately 1.3 m for this source. In the field where the activity of any source is likely to be unknown, although the isotope in question and therefore energy of beta particles may be known, it is unlikely that the distance calculation can be made. Hence the travel of the beta particles will determine the minimum separation required to ensure the prevention of beta particles entering the collimator. This further supports the necessity for a fused silica window if beta particle interference is to be eliminated from any alpha detection count.

The collimated UVTRON was also exposed to a ^{60}Co source, with and without the fused silica window being present. The thickness of the fused silica window (2 mm) is sufficient to block the low energy beta particles from the ^{60}Co , which are stopped by as little as 0.4 mm of glass. The gamma radiation emitted from ^{60}Co requires 46 mm of Lead to reduce the signal by 1/10 and is unlikely to be attenuated by the fused silica to any discernible amount in this instance. By a comparison with and without the fused silica it was determined that approximately 5% of the signal could be attributed to beta radiation at 35 mm distance. This was supported by the results when the collimator was turned through 180° where a 4% difference was found between comparisons with and without the fused silica window (see Table 7-5).

7.4.4 Gamma response

The collimated UVTRON was also exposed to sources of gamma radiation, ^{241}Am , ^{60}Co and ^{137}Cs . The ^{241}Am was a sealed source which prevented the emission of alpha

Chapter 7 : Performance characteristics of a Tungsten collimator and UVTRON flame sensor for the detection of alpha-induced radioluminescence; Impact of UVC reflecting mirror and the effect of beta and gamma radiation sources.

particles. ^{60}Co and ^{137}Cs also emit beta radiation, though of a low energy which is easily shielded. The results are presented in Table 7-5.

Table 7-5: Results of exposure of collimated UVTRON to gamma sources

Source	Separation mm	Shielding / angle	Average CPS	Times background
^{60}Co	35		1.601	1138
	35	Fused silica	1.528	1086
	35	180°	1.423	1011
	60	180° & 50 mm Lead	0.059	41.8
^{214}Am	60		0.027	19.5
	80		0.025	17.8
	140		0.012	8.7
^{137}Cs	35		0.105	74.4
	35	Fused silica	0.076	53.9
	140		0.029	20.8
	600		0.005	3.5

The beta element of the ^{60}Co signal is approximately 5% (see section 7.4.3 *Beta response*). When the collimator was orientated at 180° to the source (i.e. the collimator entrance was turned away from the source), the signal reduced to 89% of the unshielded signal and 93% of the signal measured whilst the fused silica was in place. This suggested that the gamma radiation is attenuated, but not blocked by the collimator. To verify that the signal was caused by gamma entering the collimator interior through the walls, the distance between the source and collimator was increased to 60 mm to allow a 50 mm thickness of Lead block be inserted between the two. The collimator entrance remained at 180° to the source. In this configuration the signal dropped significantly, to only 4% of the signal without the Lead. This is still 42 times background as some of the gamma may still pass through the Lead and the collimator wall. The drop upon turning the collimator indicates that only a small

Chapter 7 : Performance characteristics of a Tungsten collimator and UVTRON flame sensor for the detection of alpha-induced radioluminescence; Impact of UVC reflecting mirror and the effect of beta and gamma radiation sources.

percentage of the signal, up to 7%, is due to gamma entering through the hole. The largest part must be entering through the collimator wall.

The gamma radiation from ^{241}Am is attenuated to 1/10 of the signal by less than 1 mm of Lead, compared to 46 mm for ^{60}Co . The collimated average CPS both at 60 mm and 120 mm were approximately 200 times smaller than the uncollimated results at those distances, showing that the collimator was able to greatly attenuate the gamma from the ^{241}Am source. The average CPS from the ^{210}Po source were 4.5 and 9.7 times that from the ^{241}Am , indicating that it may be possible to distinguish between the two, see section 7.4.5 *Mixed radiation response*.

7.4.5 Mixed radiation response

The collimator was exposed to combinations of alpha, beta and gamma radiation using ^{210}Po , ^{241}Am and ^{137}Cs sources. The results are presented in Table 7 - 6. The individual CPS for each of the sources at 60 mm and 120 mm separation were recorded. Due to the geometry of the sources, the ^{241}Am and ^{137}Cs were at an approximately 20 mm greater separation than the ^{210}Po when the sources were tested in combination.

Table 7-6: Results of mixed radiation field

Separation	60 mm	120 mm
Recorded average CPS		
^{210}Po	0.1245	0.1182
^{241}Am	0.0250	0.0122
^{137}Cs		0.0292
(^{210}Po & ^{241}Am)	0.2202	0.1293
(^{210}Po & ^{241}Am & ^{137}Cs)		0.1501
Addition of CPS	<i>(percentage of recorded average CPS)</i>	
$^{210}\text{Po} + ^{241}\text{Am}$	0.1495 (68%)	0.1304 (100.8%)
(^{210}Po & ^{241}Am) + ^{137}Cs		0.1585 (105.6%)
$^{210}\text{Po} + ^{241}\text{Am} + ^{137}\text{Cs}$		0.1596 (106.3%)

It can be seen from the percentage of recorded average CPS that at 120 mm the combination of sources resulted in a very similar result to the addition of the individual measurements, being only around 6 % greater. At 60 mm the addition of individual results was much less than the combined sources.

7.5 Conclusions and discussion

It can be seen from the results of the experiments, that the collimator provides protection for the UVTRON from beta and gamma radiation to some extent, whilst still allowing for the detection of alpha radiation through UVC radioluminescence. The internal configuration shields the UVTRON from the direct path of beta particles and gamma rays, with the UVC mirror successfully reflecting the UVC onto the UVTRON cathode. However, the collimator also greatly reduces the UVC signal, by approximately 80%, compared to the uncollimated UVTRON, although this is dependent on the distance from and the angle to the source as shown by the UVC bulb experiments. Further work on the configuration of a collimator, possibly with the inclusion of optics, may increase the field of view of the UVTRON without compromising the shielding. As the portion of alpha-induced radioluminescence is small in the UVC wavelength range, an increase in the field of view would be beneficial to increase the sensitivity of the system. It would also improve the signal to noise ratio by increasing the signal strength. It may also be beneficial in further work to investigate the drop off in signal with distance, as the effect of the collimator may change with distance and this should be characterised.

The collimator highly attenuates the low energy gamma emissions from ^{241}Am , but is insufficient to block higher energy gamma radiation, for example from ^{60}Co .

Although the half thickness of the Tungsten used is 7.5 mm, a 15 mm thickness was unable to sufficiently attenuate the ^{60}Co in this instance. Dependent on the specific radionuclides which the collimated UVTRON will encounter in field conditions, further shielding may be required to remove the interference from gamma radiation when attempting to detect alpha radiation. It may be useful to determine if there is direct impact on the UVTRON or a secondary phenomenon, such as Compton scattering or x-ray production, is causing the signal. This would determine the type of shielding required.

As the addition of the signals caused by different radioisotopes is in line with exposure to a combination of the sources, it may be possible to subtract the gamma part of the signal from the overall signal by shielding against UVC and beta ingress to the collimator. This would require further investigation, but the results of this work suggest that this may be a possible route to using the collimator in a mixed radiation field. Some modification to the collimator would be required to implement a UVC and beta shield in the field.

Although not directly incident on the UVTRON, beta particles which enter the collimator do cause a signal, likely through bremsstrahlung radiation. The collimator provides sufficient shielding against beta, which is only able to enter through the hole. A sheet of fused silica of sufficient thickness across the entrance hole should prevent any interference from beta radiation.

The effectiveness of this collimated UVTRON system in the field will depend on the radioisotopes to which it is exposed. Activity levels and energy levels of any source will impact on the response of the system. In an environment high in alpha particles with low energy gamma emissions it may be possible in its current

Chapter 7 : Performance characteristics of a Tungsten collimator and UVTRON flame sensor for the detection of alpha-induced radioluminescence; Impact of UVC reflecting mirror and the effect of beta and gamma radiation sources.
configuration to detect alpha-induced radioluminescence. Field trials and further experimentation are warranted based on the results of this work.

Additional to the testing of the collimator, the research has also determined that the background count is a function of the system and not reliant on ambient lighting conditions. Measurement of the output pulse directly from the UVTRON using an oscilloscope has shown that the pulse characteristics do not vary depending on the stimulus. The pulse shape, amplitude and duration remained the same for all pulses observed from the UVTRON. It is therefore not possible to determine the source from the output pulse.

Chapter 8

Discussion and conclusion

8.1 Summary

Along with a better understanding of how stand-off alpha detection may be achieved, in this thesis a novel alpha-induced radioluminescence detector has been designed and developed. This is from the initial research which led to the concept, through sensor characterisation, to the construction of a prototype for field trials. This novel detector is not only capable of detecting alpha radiation from further than the MFP of alpha particles, but it can do this in normal lighting conditions, setting it apart from previous alpha-induced radioluminescence detecting prototypes.

Through the repurposing of an existing flame sensor for use in a novel application, the detector not only addresses the issue of stand-off alpha detection and overcomes the issue of daylight interference, but also provides it in a cost-effective manner using tried and tested technology. In the nuclear sector, the development of new technology represents a risk when deployed in a hostile radioactive environment. Failure of equipment can result in expensive remediation activities or be hazardous to personnel and the environment. Hence the nuclear industry has been necessarily cautious in terms

of the adoption of new technology. By repurposing technology in this application, it is possible to remove some of the uncertainty by using components which are tried and tested with decades of use in commercial applications.

The initial step in producing this prototype detector was to undertake research into alpha-induced radioluminescence and to review existing prototypes in this field (see Chapter 2: *Alpha particle detection using alpha-induced air radioluminescence: A review and future prospects for preliminary radiological characterisation for nuclear facilities decommissioning*) [72]. It became clear that there was one major stumbling block to detectors using this phenomenon; background light. Although some prototypes could detect alpha radiation from a distance, those which did this in the peak radioluminescence wavelength range, 300 – 400 nm, all required to be operated in darkness or special lighting conditions [1, 13, 15, 17, 18]. Without the capability to work in normal lighting conditions, this meant they were severely limited in their application in the field. However, there was some promising work using the UVC wavelength range [43] where there is no background from normal lighting conditions and daylight, and this was adopted as the method to be investigated in this work. By removing the problem of background light, the focus could be turned to detecting the radioluminescence.

A UVC sensor suitable for use in a detector system which could be used in the field was first identified (see Chapter 3: *Experimental approach and set up*). Equipment designed to measure the amount of UVC present, for example MFPs and CCD cameras, had issues with high background counts and the need for cooling to reduce this [15]. As the amount of UVC is small in comparison to UVA and UVB, even a reduced background could mask the signal, and the requirement for cooling reduced their ease of use in the field. Hence, an alternative UVC sensor was sought from other

applications. The UVTRON from Hamamatsu is used in fire alarm systems. It detects the UVC in flames and emits an output pulse. It has a very low background count and is solar blind, making it a reliable system in normal commercial lighting conditions. It is small, robust and readily available [76].

Initial experiments were carried out to test the potential of the UVTRON using a UVC bulb in place of an alpha source. It was shown that the UVTRON could detect a small UVC light source from a significant distance away, over 27 m. It was also capable of being used in a scanning platform to locate a source (see Chapter 3: *Experimental approach and set up*). Following these successful initial tests, experiments were carried out with live sources to determine if the UVTRON could detect alpha-induced radioluminescence in the UVC wavelength range. It was discovered that the UVTRON could detect alpha radiation from a distance further than the travel of the alpha particles themselves, and in normal lighting conditions (see Chapter 4: *First results of using a UVTRON flame sensor to detect alpha-induced air fluorescence in the UVC wavelength range*) [33].

As the UVC element of the radioluminescence is very small, a method to enhance the signal was sought. Previous experiments in the UVA and UVB range had shown that a N₂ atmosphere increased the radioluminescence in this wavelength range, and that a dynamic atmosphere increased this further [32, 59]. Combining these two findings, and results from research into gases likely to radioluminesce in the UVC wavelength range, it was found that a flow of gas over the source, especially Xe, increased the UVC signal (see Chapter 5: *Gas flow to enhance the detection of alpha-induced air radioluminescence based on a UVTRON flame sensor*) [74]. The use of a flow would make implementation in the field easier than a purged atmosphere.

As any alpha detector system will likely be used in a mixed radiation field, the effects of gamma and beta radiation on the UVTRON were tested. It was found that it is sensitive to both (see Chapter 6: *The effect of gamma and beta radiation on a UVTRON flame sensor: assessment of the impact on implementation in a mixed radiation field*) [78]. Therefore, a collimator was designed to shield the UVTRON from these radiation types, which was tested in the laboratory (see Chapter 7: *Performance characteristics of a Tungsten collimator and UVTRON flame sensor for the detection of alpha-induced radioluminescence; Impact of UVC reflecting mirror and the effect of beta and gamma radiation sources*). The collimator geometry was designed to protect the UVC from any shine path from the collimator entrance, with a UVC mirror reflecting the radioluminescence onto the UVTRON cathode. It was found that beta particles upon entering the collimator caused a signal, although they were not directly incident on the UVTRON. This is likely due to bremsstrahlung radiation inside the collimator. Fused silica was shown to attenuate the number of beta particles entering the collimator whilst allowing UVC to enter. Some gamma radiation from high energy sources was able to penetrate the 15 mm Tungsten alloy shielding and impact on the UVTRON despite the lack of a shine path. It was found, however, that the count from a combination of alpha, beta and gamma sources was very close to the count from the same sources when recorded individually. It may be possible to take a count in the field from a mixed radiation environment, followed by a count where the UVC is blocked from entering the collimator, and the one subtracted from the other to show the presence of UVC, indicating the presence of alpha-induced radioluminescence.

8.2 Outlook

Current alpha detectors require direct interaction with alpha particles to operate. Stand-off alpha detectors which use the radioluminescence phenomenon in the 300-400 nm wavelength range required darkness or special lighting conditions to operate. The detector developed in this work presents a potential avenue for detecting alpha-induced radioluminescence in the field, without the need for special lighting conditions. Depending on the isotopes to be detected and the environmental conditions, the UVTRON system could be configured for use in a number of different applications as required.

Due to the low cost, small size and proven reliability, it could be used in real-time monitoring systems over the whole of an active plant area, much as the UVTRON is currently used in large-area, fast-response fire alarm systems, but with the modifications identified in this work for the radioactive environments. It could carry out this task without interfering with site operations.

It may also be deployed in areas with limited access, making it ideal for decommissioning projects or waste monitoring. The UVTRON itself is only 36 mm long and 15 mm in diameter (see Figure 3-3). This is especially useful on nuclear sites where there is often limited access to areas for shielding purposes. The prevention of radiation emission is paramount and access ports are limited in size for this reason. Or there may be complex geometries, for example pipe work or ducting as is required on a working commercial site, which limit access.

UVTRONS could be combined into an array to give a greater field of view, reducing detection time for larger areas. They may be used in concert with scanning platforms for automated scans of large areas or over long timescales for greater sensitivity, as has been shown during the preliminary work (see Chapter 3:

Experimental approach and set up). The longer the detector is pointed at an area, the greater the certainty that a signal has been detected, using established principles of uncertainty based on a low background detector system [71]. The automation of the scanning process would allow operators to be located elsewhere whilst the scan was being performed, removing them from potentially harmful environments, or freeing them up for less laborious tasks.

It is possible to imagine with further development, that UVTRON based systems could potentially be deployed on remote access vehicles, such as UAV, drones and robots, to provide even greater access to potentially contaminated areas, if the requirements of mixed radiation field operation can be satisfied in a way which retains the small and light nature of the sensor system.

It may also prove of national importance through being beneficial in nuclear security applications, detecting illicit alpha emitting materials, where its small size could also provide discreet monitoring equipment. The use of Po in the assassination of Alexander Litvinenko in 2006 and the work required to detect the trail of the Po across London [81], has led the security forces to look to stand-off alpha detection for security purposes. As Po does not emit radiation other than alpha, existing gamma and beta monitoring devices are unable to detect its presence. This UVTRON based detector could be used as a tool for national security with further development, potentially providing discrete, real time monitoring for SNM (special nuclear materials) at ports and airports as required.

8.3 Future work

This thesis has proven this stand-off alpha detection technology has good potential for commercial use, but for the above applications to be realised further development work

is required. The field-test ready prototype has shown promising results, however, there are a number of improvements which could be made, both in the design and in the understanding of the radioluminescence phenomenon, which would benefit future iterations of the prototype.

8.3.1 Changes to the instrument design

Having completed laboratory trials, the UVTRON system has been shown to respond to radiation sources other than alpha particles in a mixed radiation field. In order to focus specifically on alpha-induced radioluminescence detection, enhancing the radiation shielding of the prototype would be beneficial.

The inclusion of a 10 mm fused silica window over the entrance to the collimator in any future iteration would prevent the ingress of beta particles, making the detector insensitive to beta radiation. Using available data on the thickness of glass able to block beta particles and the transmission of UVC through fused silica, a 10 mm thickness of window would provide suitable beta protection with a minimal UVC attenuation [58, 77]. This would depend on the beta isotope present and could be modified in terms of thickness if required using the same data as used to recommend the 10 mm thickness.

Improved shielding of gamma radiation will require a solution which increases the attenuation without increasing weight. The current collimator is 16 kg, a relatively substantial weight for an item of equipment for mobile deployment and the maximum recommended safe lifting weight for women. It is however, the first iteration of the design and tests have shown it has successful elements, including the use of Tungsten, the lack of shine path, and the UVC mirror. A modification to the shape of the collimator could be implemented based on the results of the experiments carried out to date, with a change in geometry and layout which provides targeted areas of increased shielding.

The strategic placing of shielding, the use of further UVC mirrors, and removing the electronics from the collimator to reduce the overall size will all contribute to increasing shielding whilst limiting the weight and size to make a manageable mobile detector.

It may also be possible through the addition of a UVC-blocking cover which can be deployed over the collimator window, to separate the UVC and gamma parts of the count. Having shown that the count is approximately cumulative (see Chapter 7.4.5 *Mixed radiation response*), a gamma only count could be subtracted from a gamma plus UVC count to give a UVC only result and a gamma only result. This would allow for the detection of alpha-induced radioluminescence in a gamma field using the UVTRON without the need for alternative shielding, as long as saturation was not reached by the gamma-only signal. The combination of more targeted gamma attenuation and the count separation technique could be used in tandem to provide a lighter, smaller and more effective further iteration of the collimator design.

8.3.2 UVC sensor technology

The UVTRON used for these experiments was selected as it met the criteria for the sensor required for this application and has other benefits as well. It is truly solar blind and has a very low background count. It is easily implemented, relatively cheap and generally available. It is robust and is a tried and tested technology that has proven itself reliable in commercial applications for decades. It is also small for easy deployment.

Should the absence of a response by the sensor to beta or gamma radiation be required, it may be desirable to find an alternative UVC sensor. However, this would still require the properties of the UVTRON in terms of being truly solar blind, with a low background count, robust, easily available and easy to implement. Sensing area would need to be maintained, either in a single unit or by use of an array. Although no

preferable alternative was identified during the initial stages of this work, it may be possible to find something with less features, but with better radiation tolerance that could provide a suitable trade-off.

It may also be possible to modify the existing UVTRON design to include radiation tolerance into the sensor in a new configuration. The benefits of a tried and tested, easily available sensor may be retained by the new configuration, depending on the changes desired. But even should significant changes be required, and a new bespoke sensor be the result, the benefits may well outweigh any loss of COTS availability.

8.3.3 Beta detection

In some instances, for example storage monitoring, detecting the presence of beta radiation as well as alpha radiation may be desirable. Where a background of gamma radiation is expected due to its penetrating nature, the presence of alpha or beta may indicate that there has been a leak or that there is contamination from some other source. In this case, removing any beta radiation shielding, for example the 10 mm fused silica window as suggested be implemented in *8.3.1 Changes to the instrument design*, may assist in detecting contamination by turning the detector into an alpha/beta detector. The collimator design is not optimised for this purpose and changes in geometry could be investigated to enhance the scope of the detector to include an alpha/beta detector option.

8.3.4 Electronics

The driving circuit used in this work is supplied by Hamamatsu and is optimised for use with the UVTRON. However, it is possible to take the pulse directly from the UVTRON

and it may be possible to design an alternative circuit design which would use this direct pulse. As the direct pulse shape has been measured for all sources and the UVC bulb with no difference seen, it is unlikely that the pulse can be used to discriminate as to the nature of the source of the UVC. The saturation level of 40 pulses per second may be increased through alternative electronics. Further investigation of this may provide avenues for the improvement of output pulse processing.

8.3.5 Research

It was not possible within the scope of this work to determine the number of UVC photons per alpha particle, or the specific wavelength. There have been attempts to quantify this and efforts are continuing, but as yet there is no published value for the UVC part of the radioluminescence spectrum. The quantification of the UVC will require a truly solar blind system that can count the UVC in the presence of background light, or it will require sufficient blacking out of any background light to allow a partially solar blind detector to work. Cooling or other background reduction measures will be required to detect the small quantity of UVC photons generated by radioluminescence against any background to maintain a good signal to noise ratio. A quantification of the UVC radioluminescence would be beneficial in calculating minimum detection levels for the sensor, which as yet have been deduced empirically.

An understanding of the exact mechanism through which the UVC photons are generated would also be beneficial. This is beyond the scope of this work being more relevant to a study of physics than engineering, but it would be advantageous to understand the UVC radioluminescence physics in order to progress such work as the enhancements using gas flows as found in this work.

8.3.6 Optics

The inclusion of lenses or reflectors may be beneficial to increase the sensitivity of the detector system. The use of a UVC reflective mirror and fused silica window during these experiments has shown that these materials can be used successfully in a UVC detector system. Ordinary glass will attenuate UVC, hence the need to use specialist UVC transmitting materials. There are many COTS optical parts for UVC applications already available, and many optics manufacturers can produce bespoke optical components as required. The optimum mirror angle was established in this work. It may be beneficial to also find a more effective mirror geometry that may enhance the sensitivity of the detector in a future iteration.

Lenses could also be used to increase the field of view of the detector system. Modelling of potential lenses has shown that a two lens system would be beneficial in collecting and collimating radioluminescence photons, increasing the field of view (see Figure 8-1). Lenses would need to be made of a UVC transmitting material, such as fused silica.

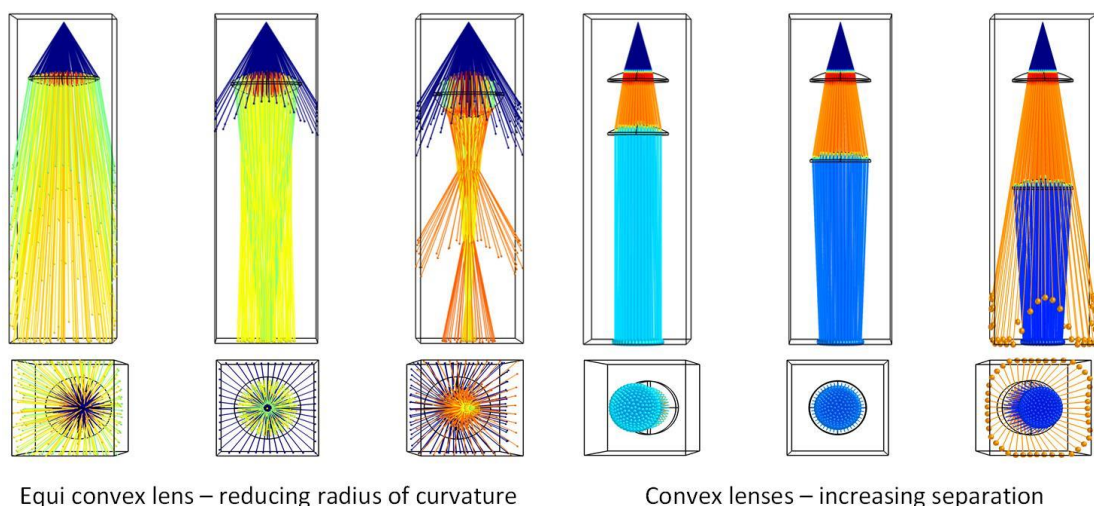


Figure 8-1: COMSOL lens simulations - showing the effect of a single or dual lens system on the focus and collimation of light from a point source

8.3.7 Arrays and scanning platforms

In this work a collimated scanning platform was used in the initial experiments to determine the potential of the UVTRON for a scanning-based detection system. It was modelled using CAD and produced using an additive manufacture process. The scanning platform was used with the UVC bulb during the initial testing phase. It was not possible to run scans with active sources in the timescales where the resources were available due to the lengthy count times required for the confidence intervals desired. In order to scan at 10° intervals over an area of -50° to 50° in both the vertical and horizontal directions would have required at least 121 hours, or 5 days, per scan. Limits to resources in this instance made this unattainable. However, it would be interesting to see the results of this in future work. The ability to run an automated scan where count times is not essential is one of the benefits of the stand-off detector where in the field the overall scan time is not as limited as in the laboratory.

The system was found to be sensitive to small changes in set-up, for example orientation to or distance from the source, and a deployment platform would be beneficial in ensuring a consistent application of the detector. This could be a stand-alone system or integrated into the scanning platform.

A single UVTRON sensor was used for each of the experiments in order to simplify the analysis of the results. Moving from the sensor characterisation phase further into the deployment phase, the combination of signals from more than one UVTRON in the form of an array would increase the detection area. As the UVTRON gives out UVC whilst in operation, shielding between each UVTRON would be required for them not to sense each other. An increase in detection area would increase the sensitivity of the detector. The low cost and ease of availability make the UVTRON ideal for implementation in an array.

Appendix A



15th International Conference on Environmental Science and Technology

Rhodes, Greece, 31 August to 2 September 2017

UVC Detection as a Potential for Alpha Particle Induced Air Fluorescence Localisation

CROMPTON A.J. *, GAMAGE K.A.A.

Department of Engineering, Lancaster University, Lancaster LA1 4YW, UK.

*corresponding author:

e-mail: a.crompton1@lancaster.ac.uk

Abstract: As part of the decommissioning process, Plutonium-Contaminated Material (PCM) has to be identified, so it can be disposed of appropriately. Most conventional alpha detectors are only effective at relatively short range. This puts personnel in close proximity to the radiation exposure from this and other types of radiation. Alpha particles cause ionisation in air resulting in the emission of ultraviolet (UV) photons. These have a considerably longer mean free path than alpha particles, providing an avenue to detect alpha contamination from a distance. However, the intensity of this UV light is exceedingly small in comparison to natural daylight, making detection difficult in the field. Although the majority of emitted photons are in the 300 to 400 nm wavelength range, it may be possible to detect those in the UVC range (180 – 280 nm) as natural UVC is blocked by Earth's atmosphere. UVC detection is already used in the detection of fires and corona discharge. A group of such detectors have undergone a series of tests to determine their suitability for detecting UVC emissions from alpha particle induced air fluorescence. Results to date have shown that long range UVC detection and location is possible with these detectors.

Keywords: UVC detection, Alpha-induced air fluorescence, UVTRON detector, Nuclear

decommissioning, Plutonium-contaminated material

1. Introduction

Due to the limited range of alpha particles in air and the well documented difficulties this presents in the detection of alpha contamination in the field [A1-A3], a stand-off detection system using a secondary effect of alpha emission will provide benefits in terms of safety and cost savings to the nuclear industry. Alpha-induced air-fluorescence is such a secondary effect and is due to the ionisation of the air by the alpha particles. Research is underway to develop a detector system which will detect the fluorescence photons at a distance from the source.

Alpha particles ionise the air along their trajectory following emission during the radiation process. As they are positively charged they interact with the air molecules, transferring kinetic energy. This elevates the air atoms into an excited state. These then emit UV photons to return to their ground state. The exact mechanism for this has been described by other researchers [A4, A5].

The main alpha-induced fluorescence intensity peaks in air are in the 300 to 400 nm wavelength range due to the excitation of Nitrogen, the main

constituent of atmospheric air. Therefore much of the work on detection has been centred in this range [A1, A6-A8]. This has led to several successful stand-off alpha detectors [A1, A9, A10]. However, due to the interference of natural and man-made light in normal daytime conditions, these detectors require to be operated in darkness or under special lighting conditions. By using a solar blind CCD camera designed for the detection of corona discharge and arcing from high voltage power lines [A11] Ivanov et al [A12] were able to image alpha-induced air-fluorescence in daylight conditions. This use of the UVC wavelength range means detectors do not require darkness or special lighting conditions as sunlight in the UVC range is blocked by the atmosphere. Although the intensity of fluorescence in the UVC wavelength range is significantly smaller than in the 300 – 400 nm range, the lack of interference from daylight means that this could provide an avenue for detection in the field.

By specifically concentrating on detection in the UVC wavelength range, 180 – 280 nm, it is necessary to select equipment which result in a system which is sensitive only in this range, so called 'solar blind'. Due to the reduced intensity of fluorescence at this wavelength (95% is in the 300 – 400 nm wavelength range), the equipment must also be sufficiently sensitive to detect low intensity signals, and have low noise and a high signal noise ratio. It is also important that any optical elements have a high transmittance at the required wavelength to reduce attenuation of the signal.

The UVTRON from Hamamatsu is such a solar blind detector and this paper presents initial tests with this detector, using UVC source lamp, to determine if it could be used for alpha-fluorescence detection.

2. UVTRON Detector

2.1. Uses of UVTRON

The detection of UVC light is one method used in the detection of flames in fire alarm systems or to detect corona discharge from high voltage power lines as UVC is emitted by both these phenomena. Commercial off-the-shelf (COTS) equipment for this purpose is available from several suppliers, for example Hamamatsu, UVIRCO and Ofil. These detect the presence of electromagnetic radiation in the UVC range (180 to 280 nm wavelength). They can therefore be

used in daylight conditions as the atmosphere blocks natural UVC light from the sun. They are also designed to be used at a distance of several metres from the source of the UV light, depending on the application. As this proven technology is used to detect UVC for these phenomena, it may provide a route for detecting alpha induced fluorescence in daylight conditions.

The UVTRON range of detectors has been selected for these experiments for several reasons. They are easily available and provide a number of options in terms of their sensitivity, wavelength range and other properties. They are available with pre-assembled drive circuits if required which have been optimised for these detectors. They can be used with a simple driving circuit allowing a bespoke circuit to be designed to test the response to variations in the circuit specification. The R9533 is vibration and shockproof making it more robust for possible future detectors. Due to the relatively low cost, these detectors could be used in an array to give a wider angle of view. This will reduce the scanning time of the detector system, whilst improving the ability to identify the location of the source. A UVC source lamp for checking the operation of these detectors is available, allowing set up to be carried out without the need to use an active alpha source, reducing potential experiment hazard. The aim of the experiments are to determine if the UVTRON may be viable as a stand-off alpha detector by research into its response to a UVC emitting bulb under different condition.

2.2. Principle of Operation

The UVTRON detectors utilise the photoelectric effect and gas multiplication to generate an output pulse when a photon is incident on the photocathode. The UVTRONS used in this research have a Ni cathode which is insensitive to photons with a wavelength of greater than 260 nm. This makes them effectively solar blind (see Figure A 1: Spectral Response of UVTRON in comparison to sunlight, Tungsten light and gas flame). Photons within the 180 – 260 nm range, when incident on the photocathode of the UVTRON cause an electron to be emitted through the photoelectric effect. An electric field generated by a voltage differential between the cathode and the anode causes this free electron to be accelerated through the gas contained within the UVTRON. As the negatively charged electron passes

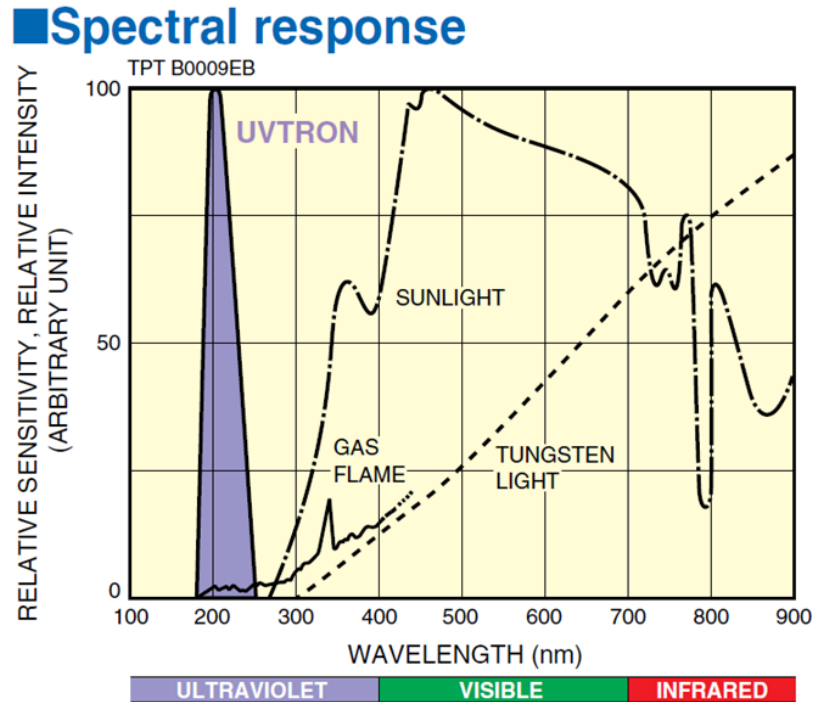


Figure A 1: Spectral Response of UVTRON in comparison to sunlight, Tungsten light and gas flame [A13].

through the gas it interacts with the gas molecules and transfers energy, causing ionisation and creating ion pairs. Noble gasses do not readily absorb free electrons, unlike Oxygen which does and therefore quenches the process, and it is likely a noble gas, possibly Argon or similar, is used in the UVTRON to enhance the ionisation process. The created positive ions are attracted to the cathode, whilst the negative free electrons are attracted to the anode. As each free electron generates further free electrons there is an avalanche reaction which causes an exponential increase in the number of free electrons incident on the anode. This generates a signal which is interpreted by the driver circuit and a pulse is outputted by the driver circuit when this avalanche phenomenon occurs.

3. Experimental Method

The experimental system comprises of; one or two UVTRON detectors with their associated driver circuits, UVC light source, an optional oscilloscope to confirm output, a microprocessor to detect and count the pulses (in this instance an Arduino Uno), and a PC to collect the count from the Arduino and to process the results. Schematic of the experimental set up is show in

Figure A 2. The UVTRONs may be collimated. A second detector may be used to detect any variation in background lighting, electronic noise etc. which can be eliminated from the results. For example one of the UVTRONs is collimated and mounted on a pan and tilt device for scanning, the other is not collimated and remains static to act as a control. The driver circuit provides the high voltage power supply and converts the output signal from the detector to a pulse. The UV light intensity input signal and output from UVTRON and driver circuit are approximately proportional, with an increase in light intensity generating an increase in pulse frequency.

These experiments use a checker lamp for the UVTRON (Hamamatsu L9657-03) in place of an alpha source in order to test the response of the UVTRON detector and to provide a robust experimental method which can be applied to experiments using active alpha sources. It has a spectral distribution of 185 to 400 nm. There are two advantages to using the lamp at this stage. The first is that it does not cause radiation which could affect the detector system electronics. The second is that it will emit a far greater number of photons than an alpha source suitable for use in a laboratory experiment. Once the experimental

set up has been verified and the UVTRON characterised, the checker lamp will be replaced by an alpha source in the laboratory and if successful here, thence in the field.

Experiments were carried out indoors in close proximity to a double glazed external window. Internal lighting was provided by modern strip lights. No attempt was made to attenuate the room or natural lighting, and experiments were carried out during the day. The background count level was measured in these conditions over a 20 minute period. The location of the detectors was varied, including pointing at the window in close proximity and pointing directly at internal

4. Results

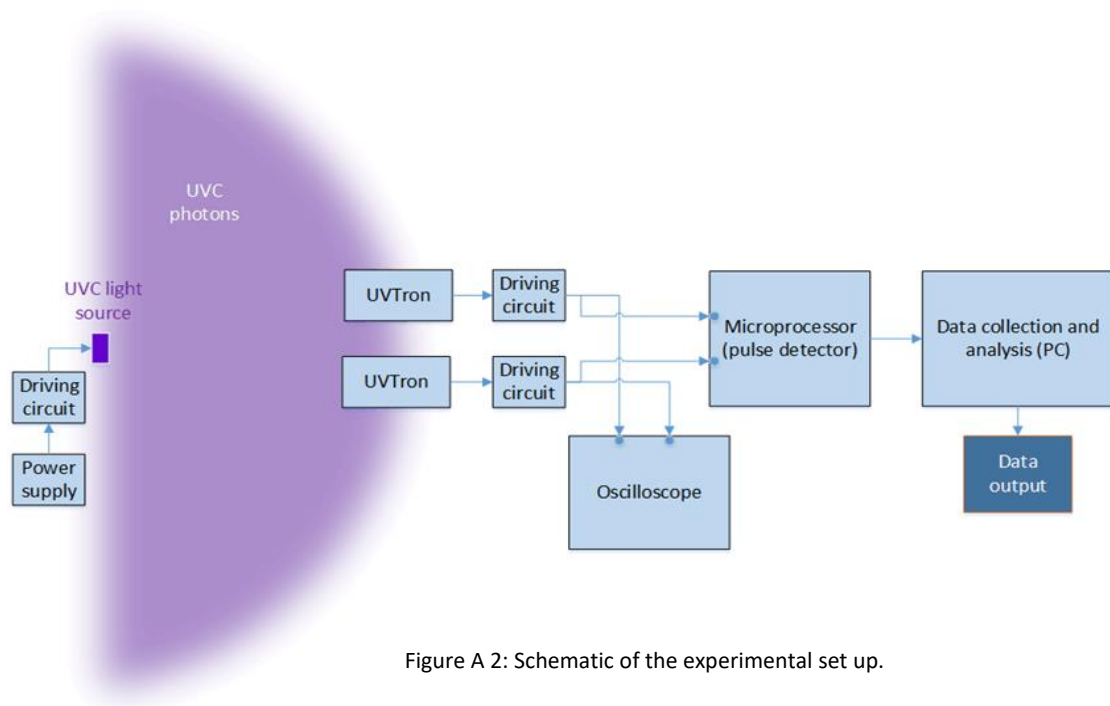


Figure A 2: Schematic of the experimental set up.

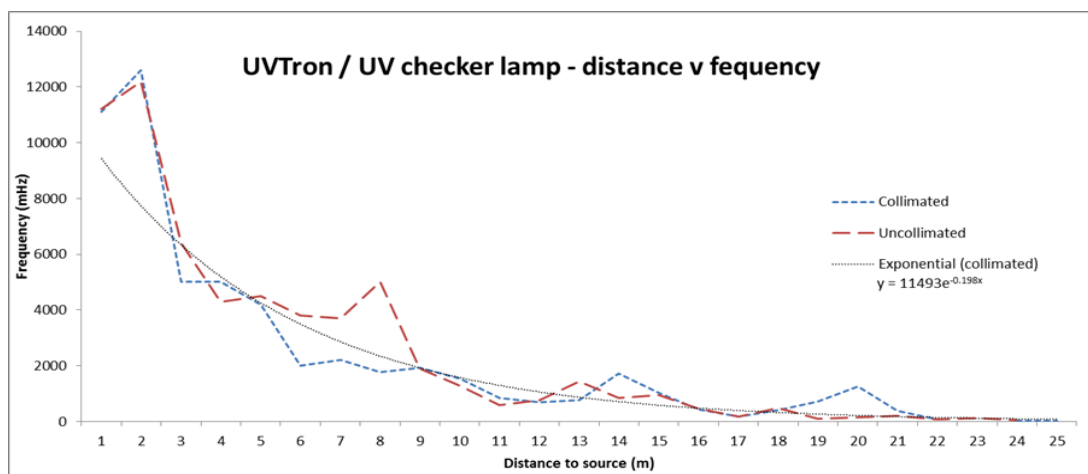


Figure A 3: Frequency variations with respect to distance to source from the detector.

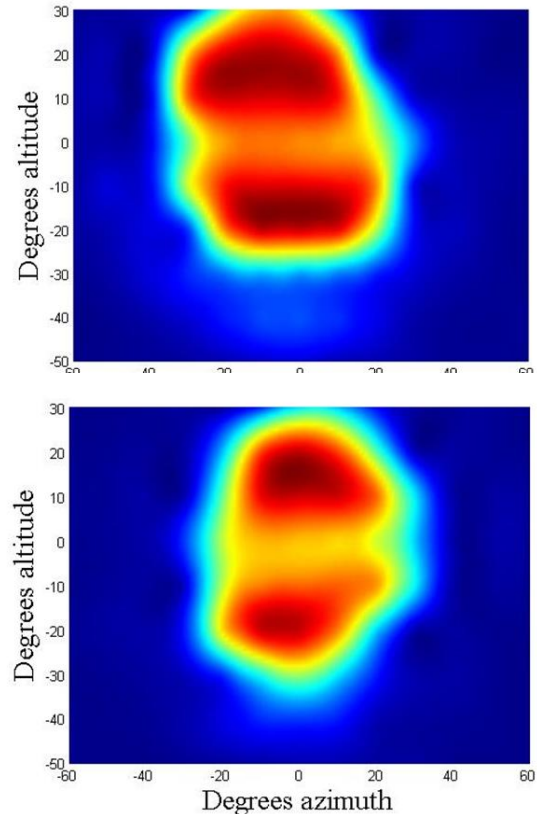
lighting. Whilst the UV checker bulb was not within the field of view of the detector, the driver circuit did not emit any pulses. There was therefore, no background count.

The first experiment carried out was to determine the furthest distance over which the UVTRON could detect the checker lamp. The driver circuit output was connected to an oscilloscope, which was manually read at each distance. An approximate average of the output over 15 seconds was recorded. The aim of this experiment was not to provide a detailed count at each distance, but to simply determine the furthest distance over which the UVTRON would detect the UV photons from the UVC lamp. The results are shown in figure A3. As can be seen there is an overall drop in frequency of pulses as the distance between detector and lamp is increased.

During the experiment a cover was placed at random intervals between one of the detectors and the source. This led to a cessation of the output signal pulse from that detector driver circuit, verifying that the pulses were due to the detection of UV photons. At 27 m, which is the maximum space available for the experiment, pulses from the driver circuits were still clearly visible on the oscilloscope screen, showing that the UVTRON detectors were still detecting the photons at this distance. Although these pulses were sporadic and infrequent, it indicates that the detector will work over significant distances.

In decommissioning it will be important that alpha contamination be not only detected, but that the location be determined. To test the suitability of the UVTRON for this purpose a pan and tilt device was devised which included the collimation of the detector it housed. A pair of stepper motors were used to

provide the motion, with the Arduino controlling the motors and carrying out the count of the pulses. The detector was placed directly in front of the source, at (0,0) degrees position, and scans were carried out with a step of 10 degrees, from -90 to 90 degrees azimuth and -30 to 30 degrees altitude. At each location data collected for 10 second and results for two cases are shown in Figures A 4. The counts per second (CPS) at each of the point of the scan has been allocated a colour, where dark red show the area of greatest signal intensity as a hotspot. A double hotspot is observed due to



the angular sensitivity of the UVTRON [A13]. It can be

Figure A 4: Localisation of the UVC light source for detector source separation of 1 m (top) and 2 m (bottom).

seen that the maximum intensity area of the hotspot become smaller the further the detector is from the checker lamp. A clear hotspot (or the centre of gravity of the double hotspot) is indicating that the UVTRON could be viable for detecting the location of UVC emissions source.

5. Summary

It can be seen from the above results that the UVTRON does appear to have the potential to detect alpha-induced fluorescence in the field, though there is a great deal of work to do in order to develop this into a robust detection system. The output of the UV checker bulb in the UVTRON sensitivity wavelength range requires quantifying in order that the sensitivity of the UVTRON can be characterised. This should include a spectral analysis so that the different wavelengths within the range can be considered. As alpha-fluorescence photons have different wavelength intensity peaks, being able to map the sensitivity of the

UVTRON against different wavelengths would be useful in designing a detector system.

As distance increased, there appears to be a greater fluctuation in the CPS over time and this should be investigated further to determine if this is a general phenomenon and if so, how this effect is generated in order to characterise the performance of the UVTRON detector. Further scans will be carried out to test and improve the ability of the UVTRON to locate the source of UVC photons. This will include collimation and orientation to take into account the angular sensitivity of the UVTRON to give the best sensitivity and remove the double hotspot effect. This will eventually provide more accurate positioning of the detector and a better resolution.

Results from the two detectors, indicate that there is variation between UVTRON detectors and this requires further investigation. Upon completion of the characterisation of the UVTRON, it will be possible to determine if it is theoretically possible to use the UVTRON to detect alpha-induced air fluorescence.

Acknowledgment

The authors would like to acknowledge the funding support from the Nuclear Decommissioning Authority, UK. We also acknowledge the help and advise of Mr. Alex Jenkins at Sellafield Ltd. and Dr. Divyesh Trivedi at National Nuclear Laboratory, UK.

References

- A1. Baschenko, S.M., *Remote optical detection of alpha particle sources*. Journal of Radiological Protection, 2004. 24(1): p. 75-82.
 - A2. Ihanola, S., et al., *Fluorescence-assisted gamma spectrometry for surface contamination analysis*. IEEE Transactions on Nuclear Science, 2013. 60(1): p. 305-309.
 - A3. Morishita, Y., et al., *Development of a Si-PM based alpha camera for Plutonium detection in nuclear fuel facilities*. Nuclear Instruments and Methods in Physics Research, Section A: Accelerators, Spectrometers, Detectors and Associated Equipment, 2014. 747: p. 81-86.
 - A4. Waldenmeir, T., *Spectral resolved measurement of the Nitrogen fluorescence yield in air induced by electrons*. Astroparticle Physics, 2008. 29: p. 205 – 222'
 - A5. Thompson, C.I., Barritt, E.E., Shenton-Taylor, C. *Predicting the air fluorescence yield of radioactive sources*. Radiation Measurement, 2016. 88: p. 48 - 54
 - A6. Hannuksela, V., J. Toivonen, and H. Tivonen. *Optical remote detection of alpha radiation*, in Third European IRPA Congress. 2010. Helsinki, Finland.
 - A7. Sand, J., et al., *Remote optical detection of alpha radiation*, in Symposium on International Safeguards. 2010: Vienna, Austria.
 - A8. Lamadie, F., et al., *Remote alpha imaging in nuclear installations: new results and prospects*. IEEE Transactions on Nuclear Science, 2005. 52(6): p. 3035 - 3039.
 - A9. Sand, J., et al., *Imaging of alpha emitters in a field environment*. Nuclear Instruments and Methods in Physics Research A, 2015. 782: p. 13-19.
 - A10. Mahe, C. *Characterization and Visualization Technologies in DD&R - Alpha Imaging*, in Practical workshop on characterization and visualization technologies in DD&R. 2011. Marcoule, France: IAEA.
 - A11. Ofil Systems. *Reliable Corona Cameras for Daytime Inspection*. [Webpage] 2013 [cited 2016 07/06/2016]; Information regarding Ofil DayCor cameras]. Available from: <http://www.ofilsystems.com/>.
 - A12. Ivanov, O.P., et al., *Development of method for detection of alpha contamination with using UV-camera "DayCor" by OFIL*, in Nuclear Science Symposium and Medical Imaging Conference (NSS/MIC). 2011, IEEE: Valencia. p. 2192 - 2194.
- Hamamatsu. *Flame Sensor UVTRON*. 2010. Available from: http://www.hamamatsu.com/resources/pdf/etd/uvtron_TPT1021E.pdf

Appendix B

2018 IEEE Nuclear Science Symposium and Medical Imaging Conference
(NSS/MIC) November 2018, DOI: 10.1109/NSSMIC.2018.8824570

Detecting Alpha-induced Radioluminescence in the UVC Wavelength Range Using a UVTRON Flame Sensor, and the Effect of a Gas Flow on Detection Rates as Compared to an Air Atmosphere.

Anita J. Crompton, Kelum A. A. Gamage, Alex Jenkins and Divyesh Trivedi

Abstract – Alpha-induced radioluminescence provides a potential avenue for the detection of alpha-emitting materials from a distance far greater than the travel of alpha-particles themselves. This work details experiments carried out into the detection of this radioluminescence in the ultraviolet C wavelength range (180-280 nm) using an off-the-shelf flame sensor, the UVTRON (Hamamatsu, Japan). There is less interference from natural and artificial background lighting in the ultraviolet C wavelength range than at other ultraviolet wavelengths. A UVTRON flame sensor (R9533, Hamamatsu, Japan), which is sensitive only in the ultraviolet C wavelength range, was used to detect the presence of a 6.95 MBq ^{210}Po source at a distance of approximately 20 mm. The signal (0.3280 counts per second) was over 147 times that of the background, which was very low (2.224×10^{-3} counts per second) under the general laboratory/commercial lighting conditions. The limit of detection, where the signal can be distinguished from background, can be calculated to be approximately 240 mm under these conditions, assuming a standard $1/r^2$, which is much greater than the alpha particle travel. Gas was flowed over the alpha sample to determine if this would enhance the radioluminescence and hence the detection by the UVTRON. Gases of Ar, Xe, Ne, N₂, Kr and P10 were tested, all of which increased the signal detected by the UVTRON sensor. The greatest increase was found to be in a flow of Xe, which greater than doubled the counts per second of the detector in one instance. The ability of the UVTRON to detect the radioluminescence from alpha-emitting materials and the enhancement which may be possible using a flow of gas, indicate the potential of the UVTRON sensor for inclusion in an alpha-emitting materials detection system which could be operated at a

distance in the field, for example for nuclear decommissioning characterisation purposes or nuclear security applications.

I. INTRODUCTION

THE detection of alpha-emitting materials, deposited either through contamination, anticipated nuclear operations, or potential security threats, is essential in nuclear decommissioning, nuclear power generation and nuclear security operations. Many of the radionuclides resulting from nuclear operations, e.g. Uranium, Plutonium, Americium, are primarily alpha emitters and therefore the detection of emitted alpha particles is essential in detection and characterisation of equipment and plant. However, the short travel of alpha particles in air makes their detection time consuming and hazardous. The difficulties in alpha detection has also resulted in slow progress to develop new technologies to overcome these issues, with gamma, beta and neutron detection having more advanced and mature technologies.

The short travel of alpha particles, around 50 mm depending on energy, means detectors and therefore their operators require close proximity to contaminated surfaces to allow the direct interaction of the alpha particles with the detector probe. In areas with complex geometry or where a large surface area requires scanning, it can be time consuming to maintain a 1 cm distance between the detector probe and the surface as is required

Manuscript received Nov 21, 2018. This work was supported in part by the Nuclear Decommissioning Authority and the Nuclear Science Network.

Anita J. Crompton is with Engineering Department, Lancaster University, Lancaster LA1 4YW, UK (e-mail: a.crompton1@lancaster.ac.uk).

Kelum A. A. Gamage is with the School of Engineering, University of Glasgow, Glasgow G12 8QQ, UK (e-mail: kelum.gamage@glasgow.ac.uk).

Alex Jenkins is with the Characterisation, Inspection & Decontamination Group, Sellafield Ltd., Cumbria CA20 1PG, UK (email: alex.jenkins@sellafieldsites.com)

Divyesh Trivedi is with The National Nuclear Laboratory, Warrington WA3 6AE, UK (email: divyesh.trivedi@nnl.co.uk)

with traditional alpha detectors. To speed up the detection process by allowing automated scanning of large areas, and to remove personnel from contaminated areas, which may include a hazardous mixed radiation environment, a stand-off alpha detector has long been sought. Although desirable, there are significant difficulties in achieving such technology. However, the use of radioluminescence in the ultraviolet C (UVC) wavelength range may provide a solution.

II. background

To design a stand-off alpha detector, it is essential to understand what mechanism could be used. As alpha particles travel they transfer energy to the surrounding atmosphere, ionising gases and causing the emission of radioluminescence photons. These travel in the order of km, much greater than the travel of the alpha particles themselves. Hence, these have been investigated for their potential in a stand-off alpha detection system. The main radioluminescence comes from the Nitrogen, which comprises just over 78% of air. This radioluminescence is mainly in the 300 – 400 nm wavelength range, ultraviolet A (UVA) and ultraviolet B (UVB). When trying to detect this radioluminescence, however, there is a great deal of interference from natural and artificial lighting. Fig. 1 shows the overlap between the radioluminescence spectrum of alpha particles in air and the spectrum of daylight.

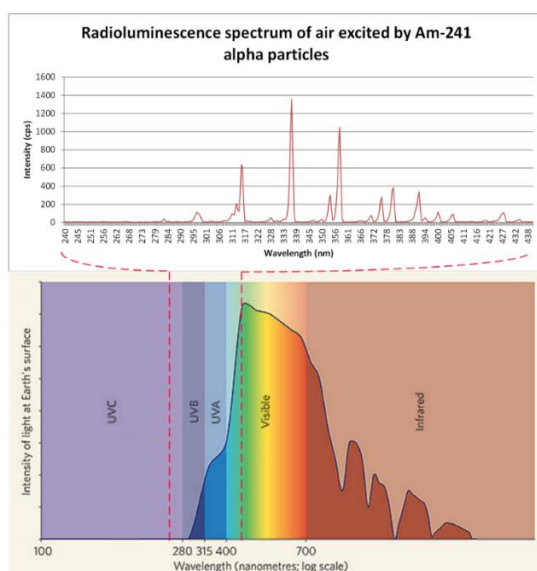


Figure B 1: Showing the overlap between the radioluminescence from ^{214}Am alpha particles [B1] and the wavelength of light at the earth's surface [B2]

It can be seen from Fig. B 1. that there is overlap between the alpha-induced radioluminescence and

light from the sun in the UVA and UVB wavelength ranges. This has led to the development of stand-off detectors which use filtering or background subtraction methods, and which also require operation in darkness or special lighting conditions [B3 - B5].

However, there is a small amount of radioluminescence in the UVC wavelength range, 180 -280 nm. As UVC light from the sun is blocked by the earth's atmosphere there is not the background interference from natural light, as can be seen from Fig. 1. Artificial lights also do not emit UVC, due to it being a waste of energy and potentially harmful to the human eye. Although there has been previous work on the viability of the UVC approach due to the small signal size [B6], there are many implementation scenarios for a stand-off alpha detector and therefore it is worth further exploration from a practical standpoint with empirical research to supplement the purely theoretical.

III. materials and methods

Experiments to determine the ability of a flame sensor to detect radioluminescence photons from an alpha source and the effect of a gas flow on this detection were carried out at the National Nuclear Laboratory, Teddington, Middlesex, UK.

The UVTRON R9533 (Hamamatsu) is a flame sensor which is sensitive to photons in the 185-260 nm wavelength range, as given off by flames and corona discharge. Using the photoelectric effect, when a photon in this wavelength range is incident on the Ni cathode an electron is emitted. Using the gas multiplication effect, this electron is accelerated through a high voltage field, generating more electrons and causing a current at the anode, which is outputted as a pulse. This is detected by the driver circuit (C10807, Hamamatsu) and a 5 V square wave is emitted. In these experiments an Arduino Uno was used to count the pulses from the driver circuit. This was relayed to a laptop where the number of counts for each second was recorded. The total number of counts for each experiment was divided by the duration (in seconds) of each experiment, and an average count per second (CPS) was determined.

A 6.95 MBq ^{210}Po sealed source was placed inside a black Perspex box of dimensions 260 x 234 x 230 mm. The UVTRON was placed at approximately 20 mm from the source. A fused silica window allowed the UVC photons generated by the source's alpha emissions to reach the UVTRON cathode. The fused silica window had a transmittance of greater than 90% in this wavelength range [B7]. It also prevented the alpha particles impacting directly on the UVTRON.

Appendix B: Detecting Alpha-induced Radioluminescence in the UVC Wavelength Range Using a UVTRON Flame Sensor, and the Effect of a Gas Flow on Detection Rates as Compared to an Air Atmosphere.

A small gas pipe of 1 mm diameter was positioned inside the Perspex box order that a flow of gas could be directed over the surface of the source. The set up can be seen in Fig. B 2.

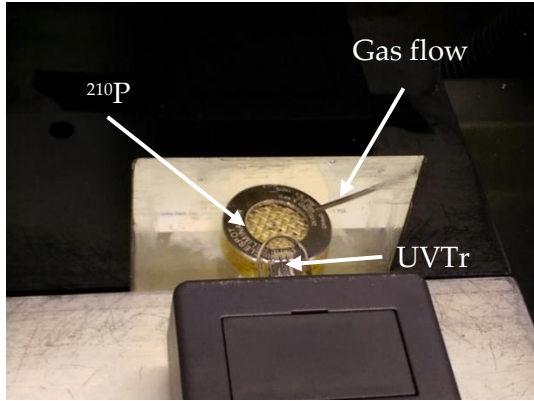


Figure B 2: Showing the UVTRON protruding from the grey box which houses the electronics, and the ^{210}Po source (the yellow and silver disk) inside the Perspex box, behind the fused silica window. The gas flow pipe can be seen angling down from the top right of the fused silica window.

IV. results

A background count was taken prior to placement of the source, with the ordinary laboratory lighting turned on. This was strip (fluorescent) lighting. The count was taken over 75 min and gave an average CPS of $2.224 \times 10^{-2} \pm 0.7034 \times 10^{-3}$. This equates to 10 pulses in the 75 min count, which is very low in comparison to other light detecting equipment, e.g. photomultiplier tubes.

The ^{210}Po source was place inside the Perspex box at approximately 20 mm from the UVTRON sensor. Under the same laboratory lighting conditions, the count increased to 0.3280 CPS, which is significantly above the background count. A second layer of fused silica was inserted between the source and detector to ensure that UVC photons were the cause of the count. The count dropped by approximately the same margin as the attenuation of the silica glass as specified by the manufacturer. A sheet of paper between the source and sensor blocked the signal completely.

Gas was then flowed across the surface of the ^{210}Po to determine the effect of this on the count. Table 1 lists the gases, their flow rates and the average increase in signal in comparison to air over up to three repetitions of the experiment.

TABLE B 1: GAS FLOW INFORMATION AND RESULTS

GAS	PURITY	FLOW RATES (1 ST /2 ND /3 RD RUN)	SIGNAL INCREASE %
NITROGEN	N 5.0	65/65/65	9.09
XENON	N 5.0	50/65/65	82.50
NEON	CP GRADE	60 / - / 65	38.69
KRYPTON	N 5.0	55 / 65 / 55	36.08
P10	$\pm 5\%$	40 / - / 65	32.55
ARGON	N 5.0	- / - / 65	30.27

Each of the gases caused an increase in the count, with Xenon causing the highest increase (see Fig. B 3.). Each of the counts was compared to a baseline count taken in air at the commencement at each set of gas flow measurements. This allowed a determination of the increase in signal achieved in relation to air for each experiment.

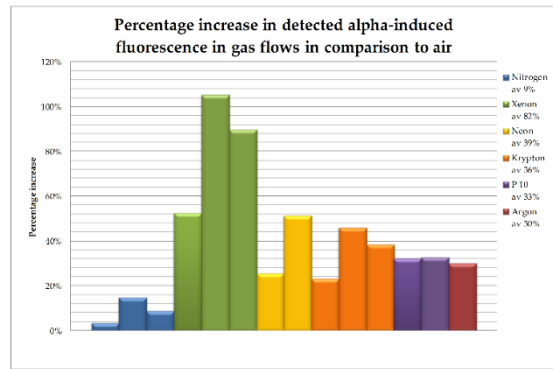


Figure B 3: Showing the percentage increase in the alpha-induced radioluminescence signal when different gases were flowed over the source.

This increase in the signal is likely due to the replacement of O_2 from the area surrounding the source, which is known to quench radioluminescence in the UV range. The different gases also affect the distance travelled by an alpha particle. Xenon for example reduces the travel to 25.2 mm [B8], meaning that the alpha energy is deposited in a smaller area and this may enhance the radioluminescence in the area closest to the source. It has been shown that the area of most radioluminescence is with 10 mm of the source [B3]. This may also be the reason why a flow of gas, as can also be found with a purged atmosphere, can increase the signal, and why over the duration of the experiment where the Perspex box would have been filling with the gas, the count did not increase over time.

v. conclusions

The results show that under normal indoor lighting conditions it is possible to detect UVC radioluminescence using the UVTRON.

The background is low under normal lighting conditions. Using Hurtgen et al's equation [B9], with a confidence level of 95.45% (as advised by ISO, 1993), the limit of detection was determined using the equation;

$$\text{at } L_d, s_{net} = 2.86 + 4.78\sqrt{(b + 1.36)} \quad (\text{B1})$$

where L_d is the limit of detection, s_{net} is the net signal (gross signal minus background), b is the background. This gives a limit of detection of 17.4 counts per hour, which is low in comparison to the counts measured in air and in the different gas flows.

Assuming a $1/r^2$ drop off in signal value as would be expected with an isotropic emission of alpha particles and photons, the limit of detection would be approximately 240 mm between the ^{210}Po source and UVTRON detector, before the signal would reach background levels. Alternatively, at the same distance, approx. 20 mm separation, the minimum detectable activity level would be approximately 47 kBq (± 15 kBq). The sensitivity of any detection system using the UVTRON would depend on the distance separation and the activity level. However, 240 mm is well beyond the travel of alpha particles, and the activity level found in some areas where such a detector could be used in the field are in the GBq range. This therefore is a positive indication that this sensor could be part of a field operational detector system for certain deployment scenarios.

The results of the gas flow experiments show that if this can be introduced, the small UVC signal from alpha emissions could be enhanced. It is not unusual in the nuclear industry for alternative atmospheres to be used for some routine operations, and there is already some infrastructure for the supply of gas to areas of interest.

Acknowledgment

We thank Mr Peter Jones and Mr Andrew Verden from Lancaster University for their technical expertise, and Dr Jordan Tompkins of the National Physical Laboratory for providing the ^{210}Po source.

References

- [B1] A. Khan, "Device physics: A bug-beating diode." *Nature*, 2006, 441(7091), pp. 299-299. DOI: 10.1038/441299a.
- [B2] J. Sand, A. Nicholl, E. Hrnccek, H. Toivonen, J. Toivonen, K. Peräjärvi, "Stand-Off Radioluminescence Mapping of Alpha Emitters Under Bright Lighting." *IEEE Trans. Nuclear Sci.* 2016, 63, pp.1777–1783.
- [B3] J. Sand, S. Ihtola, K. Peräjärvi, A. Nicholl, E. Hrnccek, H. Toivonen, J. Toivonen, "Imaging of alpha emitters in a field environment." *Nuclear Instrum. Methods Phys. Res. A* 2015, 782, pp.13–19.
- [B4] J. Sand, V. Hannuksela, S. Ihtola, K. Perajarvi, H. Toivonen, J. Toivonen, "Remote Optical Detection of Alpha Radiation." IAEA, International Nuclear Information System, 2010 Ref: IAEA-CN-184/23. Available online: http://www.iaea.org/inis/collection/NCLCollectionStore/_Public/42/081/42081464.pdf (accessed on 12 January 2018).
- [B5] D. S. Haslip, T. Cousins, V. Koslowsky, H. Ing, H. R. Andrews, E. T. Clifford, D. Locklin, "Standoff Radiation Imaging Detector." U.S. Patent 7,317,191 B1, 8 January 2008.
- [B6] M. Roberts, "Detection of Ionising Radiation using Solar Blind Air Fluorescence." Australian Government, Department of Defence, Defence Science and Technology Organisation, 2013. Ref: DSTO-TR-2842.
- [B7] UQG Optics, "UV Fused Silica—Spectrosil—Data Sheet". Available online: <http://www.uqgoptics.com/pdf/Fused%20Silica%20-%20Spectrosil1.pdf> (accessed 7 September 2017).
- [B8] K. Saito, H. Tawara, T. Sanami, E. Shibamura, S. Sasaki, "Absolute number of scintillation photons emitted by alpha particles in rare gases." *IEEE Trans. Nuclear Sci.* 2002, 49, pp. 1674–1680, doi:10.1109/TNS.2002.801700.
- [B9] C. Hurtgen, S. Jerome, M. Woods, "Revisiting Currie—How low can you go?" *Appl. Radiat. Isot.* 2000, 53, pp. 45–50.

Appendix C

NuSec Summary Project Report – November 2017

Fluorescence spectra of alpha emitting isotopes for stand-off detector development - Summary Project Report

Anita J. Crompton, Lancaster University and Kelum A.A. Gamage, University of Glasgow.

Summary and outcomes: This project carried out experiments to detect alpha-induced fluorescence using flame detectors, part of a larger body of work which aims to develop a means to detect alpha emitting materials from a distance. It looked at the detection of alpha-induced fluorescence photons in the UVC portion of the light spectrum (180-280 nm). As there is very little background light in this part of the spectrum due to the absorption of UVC by the earth's atmosphere, the potential to use UVC sensors which are insensitive to light above 260 nm could provide an avenue for stand-off alpha detection in normal lighting conditions, eventually leading to a detector suitable for use in the field. As the UVC portion of the emitted photons is small, experiments were carried out to determine if these UVC flame sensors were sensitive enough to detect the UVC emitted by alpha particles.

Three UVTRON flame sensors, R9533, R1753-01 and R259 (Hamamatsu), designed to detect the UVC emissions from flames for fire alarm purposes, were tested in various gas atmospheres with a ^{210}Po alpha source to determine if this could provide an avenue for stand-off alpha detection. The results of these experiments showed that the UVTRONs are capable of detecting UVC photons produced by the alpha emitting material. A very low background count was detected in normal laboratory lighting, indicating that the R1753 could be capable of distinguishing the 6.95 MBq ^{210}Po source from up to 0.5 m distance in those conditions. The R9533 was slightly less sensitive (< 0.4 m), with the R259 proving far less sensitive than the other models in this application.

Differing the gas atmosphere produced an increase in the detector count, with Xenon having the greatest effect with a measured 52% increase in the sensor response, with P-10 (32%), Neon (26%) and Krypton (23%) also enhancing fluorescence. Nitrogen did not provide a significant increase, an important result as air consists mainly of Nitrogen and has been proven to increase fluorescence in other wavelength ranges, indicating that a different mechanism may be responsible for the production of UVC fluorescence photons.

This project has given the first indications that detection of the UVC portion of the wavelength spectrum of alpha induced fluorescence may provide an avenue for a stand-off alpha detection system, and that these flame detectors may be a basis for this technology. Further work can now be undertaken with confidence and underpinning data to develop this technology into an alpha detection system which could be operated at a distance, where it would potentially provide a more cost effective, safer and faster solution to detect and characterise alpha contamination in security and nuclear decommissioning applications.

Executive non-technical summary: Alpha radiation, emitted from such substances as Po, U, Pu, Am, etc. interacts with atoms and molecules in the air/gas in which it travels, both slowing the alpha particle, meaning it travels only approximately 50 mm, and transferring energy. In order to return to their normal energy state the excited gas atoms may emit a photon, called fluorescence or radioluminescence. This emitted light travels much further than the original alpha particle and therefore may provide an avenue for detecting alpha emissions from a distance.

At present traditional detectors need to be in close proximity to any potentially contaminated surface to directly detect alpha particles. This makes alpha detection time consuming, and where other radiation sources may be present, dangerous to personnel. Hence a stand-off detector would reduce scanning time and risk to personnel, whilst also being able to detect alpha emitting materials from a distance, even if the material was obscured behind an object.

The spectrum of fluorescence from alpha particles in air has been researched, and the majority of the photons emitted are primarily 300 – 400 nm which is known as UVA and UVB. A small number are in the UVC wavelength range, 180 – 280 nm. Although outside of our own visual spectrum, there is a significant amount of UV light in normal lighting conditions, making the fluorescence difficult to detect except in darkness or special lighting conditions. As the atmosphere blocks out the vast majority of UVC light from the sun there is less background light to interfere with detecting the fluorescence in this range, but there is a much smaller signal. This project has focused on investigating the possibility of detecting the UVC fluorescence in normal indoor lighting conditions to determine if it would be possible to design a detector suitable for use in field conditions.

Flames also emit UVC as do corona discharge from power lines, and UVC detectors are used to detect both these phenomena. Flame sensors, UVTRON by Hamamatsu, were tested to determine if it is possible to detect the UVC from alpha fluorescence using these sensors. A Po source was placed in front of the detector at a distance of 20 mm. A fused silica window was used to prevent alpha directly hitting the detector. It was established by using a black out cloth that the response of the sensor was due to light and not any other emissions from the source. Once the set-up had been established and verified, a background count was taken over

a 15 hour period to establish a baseline to compare results against. This gave an average counts per second of 0.0015 (less than one count per hour). With the Po source in place, this count increased to 0.4502 CPS, showing that the UVTRON was capable of detecting UVC photons produced from alpha radiation.

Ways to enhance the fluorescence were investigated in terms of determining if a different gas atmosphere would increase the count. Five different gases were tested by flowing the gas over the source. It was found that Xenon increased the average counts per second by 52%, as did P-10 by 32%, Neon by 26% and Krypton by 23%. So it can be seen that gases can be used to enhance the fluorescence. Part of this phenomenon will be due to the removal of Oxygen from around the source, as Oxygen is known to quench fluorescence. However, this will not account for all of the increase and further work will look into identifying why this was the case.

In summary, it has been shown that in normal indoor lighting conditions, a 6.95 MBq alpha only emitting source can be detected from 20 mm away using a UVTRON. As the number of photons hitting the detector will decrease over distance with a proportion of double the distance, four times the reduction in photons, the sensor would be detecting a value indistinguishable from background from up to 0.5 m away, giving the maximum distance for this detector with this activity of source. Flowing Xenon over the source would increase this to 0.6 m. Whilst these sensors may not in their off the shelf form meet the needs of a stand-off detector system, these results do show that there is potential to use this technology in a detector for use in the field.

Background:

The ability to detect alpha emissions from nuclear materials is important in nuclear operations, nuclear decommissioning and nuclear security applications. Due to their relatively large particle size and positive charge, alpha particles travel only a short distance after emission from nuclear materials, typically around 50 mm through air depending on their energy. Therefore detectors which require direct contact with alpha particles need to be in close proximity to any surface or object to determine if alpha contamination is present, at a distance of less than the MFP of the alpha particles. This causes a number of issues as documented by other researchers [C1 – C3]. As objects to be monitored may be in a mixed radiation environment, personnel carrying out detection activities may require PPE and may have limited time in which they can operate safely. Large structures or complex geometries take significant time to monitor in such close proximity. A stand-off detector, where a significant distance between the detector and surface can be achieved, can reduce the time taken for monitoring whilst distancing the operator from the radioactive environment.

As an alpha particle travels it ionises the air, transferring energy to the atoms and molecules in its path, mostly due to its positive charge. These excited atoms may emit a photon to return to a stable state and these photons have a MFP in the order of kilometres [C4, C5]. So in theory they could be detected from a significant distance, much further than direct alpha particle interaction detectors could achieve.

Although there have been experiments and several prototype detectors which have utilised this effect for stand-off alpha detection [C1, C6 - C10], there are significant problems with this approach. The main issue is the interference of light, natural or from lighting equipment, which is typically present in much greater intensity compared with the signal from alpha-induced fluorescence. . Although operating in dark or special lighting conditions alleviates this problem somewhat, it is not possible in the field where a variety of environments provide a variety of lighting conditions with which any viable detector must be able to cope. The variability of lighting levels over short time periods, especially from natural light sources, means that subtracting the background is not yet a viable option, and filtering causes an unwanted attenuation of the signal as well as removing background light. Ivanov et al had some success in using a solar blind CCD camera [C11] which could image UV fluorescence in daylight.

Therefore, this research has focused on a detector which is less affected by natural and artificial light, the UVTRON by Hamamatsu. This detector is designed to detect UVC emissions from flames for use in fire detection systems and to have a negligible background count in normal indoor lighting. Experiments were carried out to determine if the UVTRON was able to detect the UVC fluorescence photons generated by an alpha source, and the effect of different gas atmospheres on this detection.

Materials and Methods:

Experiments were carried out at the National Physical Laboratory in Teddington, Middlesex. The set up for the experiments was as follows (see Figure C 1);

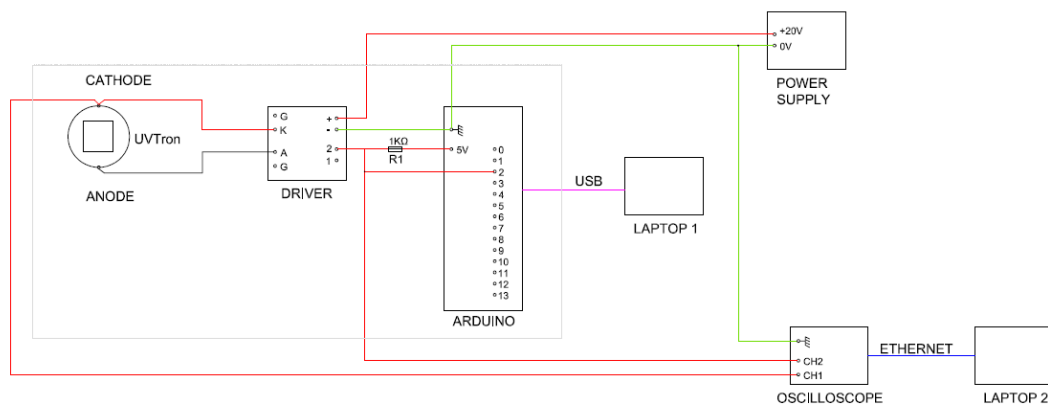


Figure C 1: Schematic of equipment set up

A ^{210}Po source of 6.95 MBq was placed in close proximity to the UVTRON detector (Hamamatsu, R9533, R1753-01 and R259), with an approximate separation of 20 mm between the source and detector. ^{210}Po decays through alpha emission only, with a very low X/ γ emission intensity (see reference 13 for ^{210}Po nuclide table), eliminating the possibility of other radiations generating a response from the UVTRON, either through direct interaction or secondary effects.

Experiments were run with the source inside a gas flow box (see Figure C 2) with a window of 2 mm thick synthetic fused silica (Spectrosil©) which is specifically designed for deep UV (UVC) applications as it allows UVC to pass with little attenuation (<10%). During testing, the gases were flowed over the source using a small flexible pipe of 1 mm bore diameter. As the effect of different gases atmospheres on alpha induced fluorescence have been tested in the past and there is much prior literature, this work tested out a possible field-operable gas delivery method which could be used where a complete gas atmosphere is not possible. Due to the flowed delivery system the gas composition at the source was therefore a mix of air and sample gas, assumed to be dominated by the sample gas in the vicinity of the source. However the exact composition was not directly measured and the chamber was not completely filled so it is not possible to provide accurate composition. Quenching by Oxygen is presumed to be reduced as Oxygen in the vicinity of the source would have been displaced by the sample gas. Again, this was not quantifiably measured.

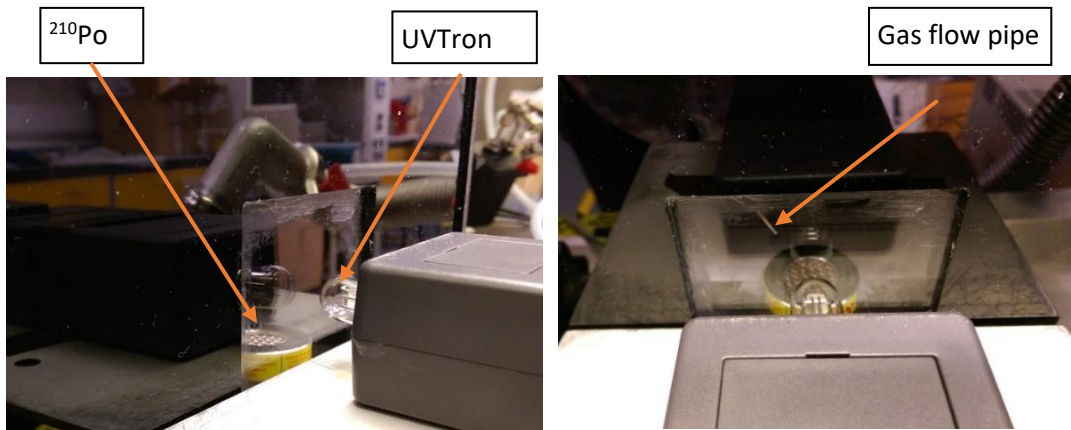


Figure C 2: Photographs a) and b) showing the ^{210}Po source inside the gas flow box (silver disk with mesh surface and yellow edge) and the UVTRON (small glass bulb), attached to the grey box housing the detector electronics. In photograph b) to the left and above the source can be seen the tube through which the gas was flowed over the source.

The lab in which the experiments were carried out had no windows and conventional strip lighting. This lighting remained on for the duration of all experiments. The background count rate was found to be $2.224 \times 10^{-3} \pm 7.034 \times 10^{-4}$ counts per second. This was less than 1% of the count rate of all other experiments.

UVTRON detectors utilise the photoelectric effect and gas multiplication to generate an output pulse when a photon is incident on the photocathode. The UVTRONs used in this research have a Ni cathode which is insensitive to photons with a wavelength of greater than 260 nm. This makes them effectively solar blind (see Figure C 3).

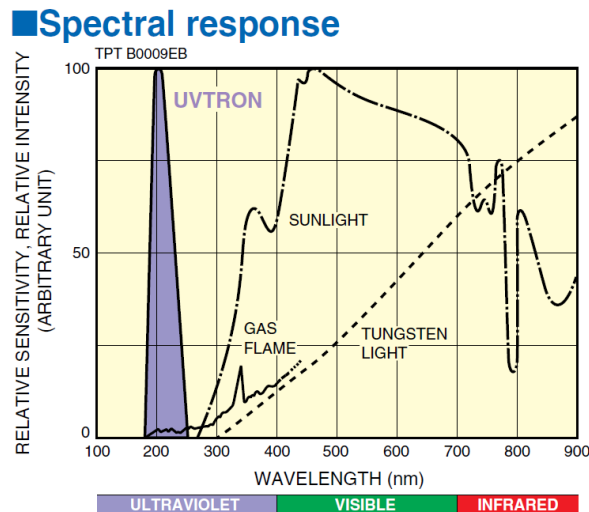


Figure C 3: Spectral response of UVTRON in comparison to sunlight, Tungsten light and gas flame [C12]

In order to verify that the signal being received by the detector was indeed air fluorescence and not due to other emissions from the source, an optical black out cloth, a piece of paper or a sheet of fused silica were placed between the source and detector. With the optical cloth or the paper the observed CPS immediately reduced to zero, returning to its former value when removed. The sheet of fused silica resulted in a negligible drop in counts per second. As the signal was transmitted through the fused silica window, but not through the paper or black out cloth, verification was made that the detector was detecting UVC photons from the alpha source and not $X/\gamma/\beta$ radiation.

Results:

With the equipment and source as detailed above over a period of approximately 16 hours (60,871 s), 19,978 pulses were counted, giving an average of 0.3280 counts per second.

Five different gas environments were compared to air. These were selected following research into gases which were both likely to ionise at suitable energies and to emit photons of the required wavelength. The results are shown in Table C 1.

Table C 1: Variation in average CPS by gas - in comparison to air

	Air	Nitrogen	Xenon	P10	Neon	Krypton
Gas flow rate (ml/min)	-	65	50	60	40	55
Average CPS	3.28	3.40	5.00	4.34	4.13	4.05
uncertainty	±2.32	±9.35	±1.09	±9.25	±1.05	±1.07
% increase from air	-	3.61%	52.47%	32.21%	25.87%	23.26%

There was an increase in the average CPS for all gases compared to the air atmosphere. Xenon provided the greatest effect, with a 52% increase in the average CPS compared to air. This new finding is most significant as it may provide a way to enhance fluorescence detection in the UVC wavelength range.

Nitrogen showed only a small increase, which could be accounted for within the uncertainty and therefore may not be an actual observed increase. As this is the primary constituent of air and is known to enhance fluorescence in the 300-400 nm wavelength range [C1, C2, C5, C6, C8, C9] this result was unexpected. It may be indicative that Nitrogen can be ruled out as the primary source of fluorescence in the UVC wavelength range. There were no indications from the other gases that one of these is the primary source. However the aim of the experiments was to test out the sensor and gas delivery system and not to determine the cause of UVC fluorescence.

For each of the experiments carried out with the ^{210}Po source, the pulse shape of the output from the UVTRONs showed no distinguishable difference. Figure C 4 shows a comparison of the shapes of a single pulse from each of the gas experiments. From this it can be seen that it is not possible to differentiate one gas from the other in terms of the pulse shape.

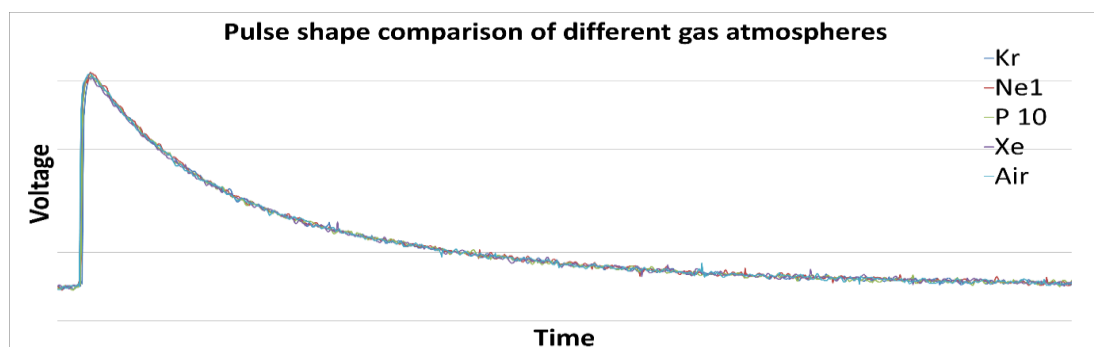


Figure C 4: Pulse shape comparison of different gas atmospheres

Acknowledgements:

The authors would like to acknowledge the following: funding support from the Nuclear Security Science Network (NuSec) and Sellafield Ltd to carry out these experiments, and the Nuclear Decommissioning Authority; the assistance of Steven Bell from NPL and Andrew Wilson with planning and carrying out the experiments; the work of Alex Jenkins (Sellafield Ltd) in providing supervision and facilitating accessing funding; the support and supervision of Divyesh Trivedi (NNL); the assistance and technical expertise of Peter Jones and Andrew Verden from Lancaster University.

References:

- C1. Baschenko, S.M., *Remote optical detection of alpha particle sources*. Journal of Radiological Protection, 2004. 24(1): p. 75-82.
- C2. Ihantola, S., et al., *Fluorescence-assisted gamma spectrometry for surface contamination analysis*. IEEE Transactions on Nuclear Science, 2013. 60(1): p. 305-309.
- C3. Morishita, Y., et al., *Development of a Si-PM based alpha camera for Plutonium detection in nuclear fuel facilities*. Nuclear Instruments and Methods in Physics Research, Section A: Accelerators, Spectrometers, Detectors and Associated Equipment, 2014. 747: p. 81-86.
- C4. Waldenmeir, T., *Spectral resolved measurement of the Nitrogen fluorescence yield in air induced by electrons*. Astroparticle Physics, 2008. 29: p 205 – 222’
- C5. Thompson, C.I., Barritt, E.E., Shenton-Taylor, C. *Predicting the air fluorescence yield of radioactive sources*. Radiation Measurement, 2016. 88: p 48 - 54
- C6. Hannuksela, V., J. Toivonen, and H. Tivonen. *Optical remote detection of alpha radiation*, in Third European IRPA Congress. 2010. Helsinki, Finland.
- C7. Sand, J., et al., *Remote optical detection of alpha radiation*, in Symposium on International Safeguards. 2010: Vienna, Austria.
- C8. Lamadie, F., et al., *Remote alpha imaging in nuclear installations: new results and prospects*. IEEE Transactions on Nuclear Science, 2005. 52(6): p. 3035 - 3039.
- C9. Sand, J., et al., *Imaging of alpha emitters in a field environment*. Nuclear Instruments and Methods in Physics Research A, 2015. 782: p. 13-19.
- C10. Mahe, C. *Characterization and Visualization Technologies in DD&R - Alpha Imaging*, in Practical workshop on characterization and visualization technologies in DD&R. 2011. Marcoule, France: IAEA.

- C11. Ivanov, O.P., et al., *Development of method for detection of alpha contamination with using UV-camera "DayCor" by OFIL*, in Nuclear Science Symposium and Medical Imaging Conference (NSS/MIC). 2011, IEEE: Valencia. p. 2192 - 2194.
- C12. Hamamatsu. *Flame Sensor UVTRON*. 2010. Available from: http://www.hamamatsu.com/resources/pdf/etd/uvtron_TPT1021E.pdf.
- C13. Laboratoire National Henri Bequerel. Recommended Data table for ^{210}Po . Accessed 11/09/17. Available from: http://www.nucleide.org/DDEP_WG/Nuclides/Po-210_tables.pdf

Appendix D

Outdoor experiments data

Conclusions from outdoor readings: The result of readings taken outdoors is inconclusive. There appears to be an increase in count when there is an increase in temperature, in general. However, this can not be quantified or predicted by the results and is observed as a general trend. The weather conditions and therefore light levels appear to have no effect on the background count.

It is therefore tentatively put forward that temperature may affect the UVTRON count, with an increase in the temperature around the UVTRON corresponding to an increase in the count. It is therefore likely that it is not light levels which affect the background count outdoors, but the temperature.

These are both positive results in terms of use of the UVTRON in the field. Light conditions are more difficult to control than the sensor temperature, which could be regulated by consistent monitoring and cooling aides. Further experimentation is required on the effect of temperature on the UVTRON, and to fully confirm that outdoor lighting levels do not affect the count.

Table D 1: Table of outdoor and indoor background readings

	MAX	MIN	Average
Outdoor 1 – UVTRON in shade	3.89×10^{-3}	0.56×10^{-3}	2.04×10^{-3}
Outdoor 2 – UVTRON in direct sun	16.7×10^{-3}	1.1×10^{-3}	8.97×10^{-3}
Outdoor 3 – UVTRON in direct sun	2.48×10^{-3}	27.54×10^{-3}	15.16×10^{-3}
Indoor readings	CPS	±	
NPL	2.224×10^{-3}	0.7034×10^{-3}	
NPL2	1.48×10^{-3}	0.53×10^{-3}	
NPL 3	1.41×10^{-3}	0.150×10^{-3}	
Lancaster university	2.3×10^{-3}	0.09×10^{-3}	

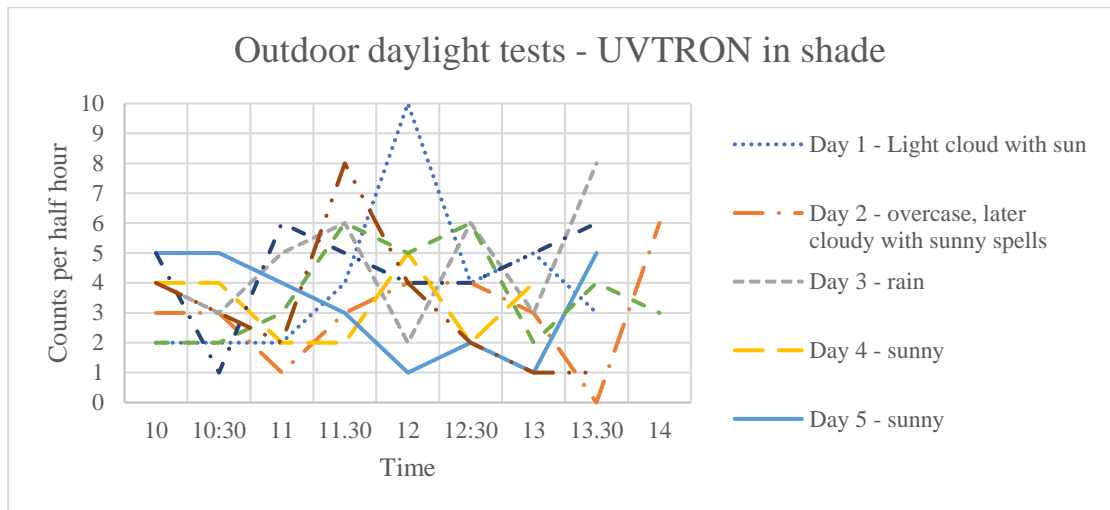


Figure D 1: Graph of outdoor daylight tests of the UVTRON

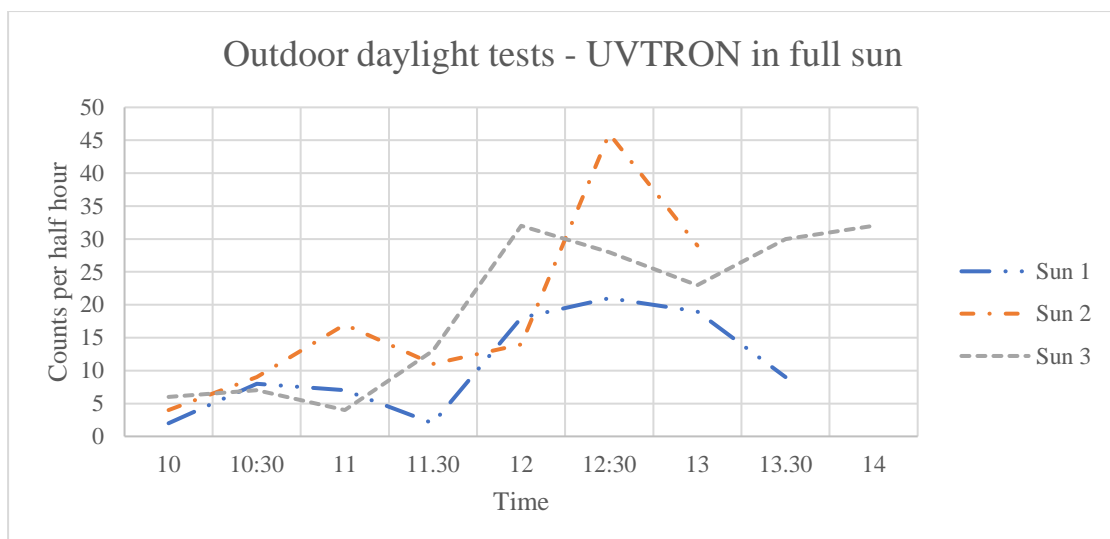


Figure D 2: Graph of outdoor daylight tests in full sun

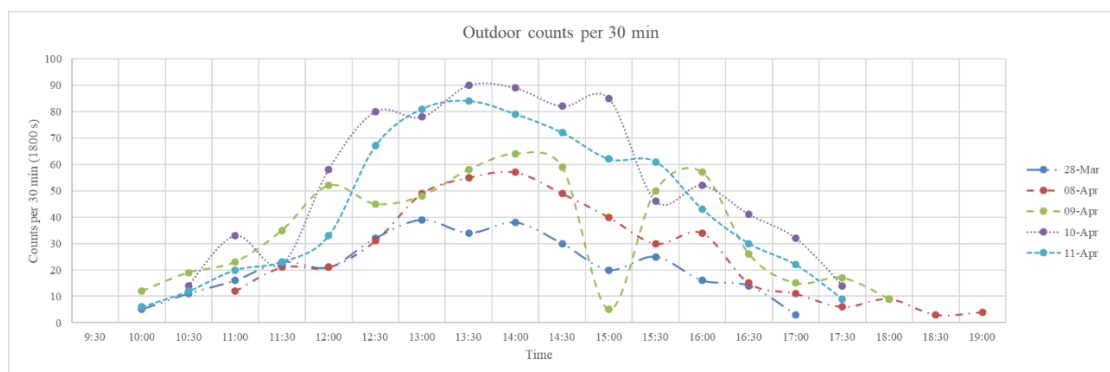


Figure D 3: Graph of results of outdoor count

Appendix D: Outdoor experiments data

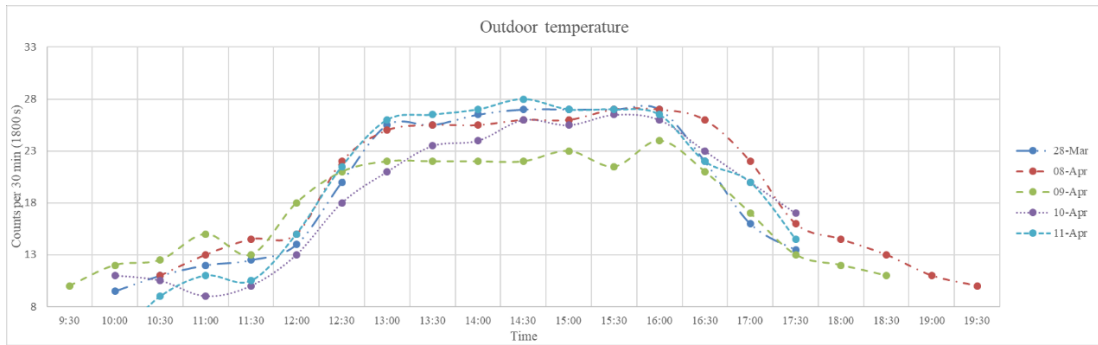


Figure D 4: Graph of temperature readings whilst count was being taken

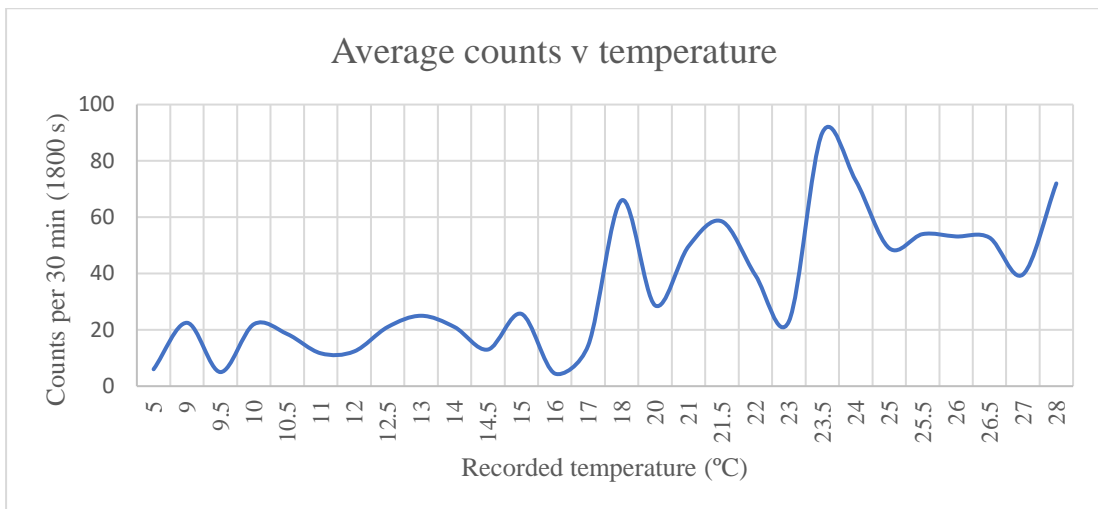


Figure D 5: Graph of number of counts at each recorded temperature

References

1. Baschenko, S.M. Remote optical detection of alpha particle sources. *J. Radiol. Prot.* **2004**, *24*, 75–82.
2. UK Radioactive Waste Inventory. **2016**. Available online: <http://ukinventory.nda.gov.uk/the-2016inventory/2016-uk-data/waste-forecasts/> (accessed on 11 January 2018).
3. Nuclear Decommissioning Authority Strategy effective from April **2016**. Available online: https://assets.publishing.service.gov.uk/government/uploads/system/uploads/attachment_data/file/518669/Nuclear_Decommissioning_Authority_Strategy_effective_from_April_2016.pdf (accessed on 14th February 2019)
4. Roberts, M. Detection of Ionising Radiation using Solar Blind Air Fluorescence; DSTO Defence Science and Technology Organisation: Canberra, Australia, **2013**.
5. Ihanola, S.; Sand, J.; Perajarvi, K.; Toivonen, J.; Toivonen, H. Fluorescence-Assisted Gamma Spectrometry for Surface Contamination Analysis. *IEEE Trans. Nuclear Sci.* **2013**, *60*, 305–309.
6. Alpha Pen Probe. Mirion Technologies. Available online: <https://www.mirion.com/products/alpha-pen-probe-external-multirad-llr-probe> (accessed on 14th February **2019**)
7. Bachelor, P.P., Jordan, D.V., Harper, W.W., Cannon, B.D., Finn, E.C. Self-absorption effects on alpha-induced atmospheric Nitrogen fluorescence yield. *J Radioanal Nucl Chem* **2009** 282:873 – 876.
8. Argyriades, J., Arnold, R., Augier, C., Baker, J., Barabash, A.S., Bongrand, M., Broudin-Bay, G., Brudanin, V.B., Caffrey, A.J., Chapon, A., Chauveau, E., Daraktchieva, Z., Durand, D., Egorov, V.G., Fatemi-Ghomi, N., Flack, R., Freshville, A., Guillon, B., Hubert, Ph., Jullian, S., Kauer, M., King, S., Kochetov, O.I., Konovalov, S.I., Kovalenko, V.E., Lalanne, D., Lang, K., Lemièrre, Y., Lutter, G., Mamedov, F., Marquet, Ch., Martin-Albo, J., Mauger, F., Nachab, A., Nasteva, I., Nemchenok, I.B., Nguyen, C.H., Nova, F., Novella, P., Ohsumi, H., Pahlka, R.B., Perrot, F., Piquemal, F., Reyss, J.L., Ricol, J.S., Saakyan, R., Sarazin, X., Simard, L., Shitov, Yu.A., Smolnikov, A.A., Snow, S., Söldner-Rembold, S., Štekl, I., Sutton, C.S., Szklarz, G., Thomas, J., Timkin, V.V., Tretyak, V.I., Tretyak, V.I., Umatov, V.I., Vála, L., Vanyushin, I.A., Vasiliev, V.A., Vorobel, V., Vylov, Ts. NEMO Collaboration (**2009**). Measurement of the background in the NEMO 3 double

- beta decay experiment. *Nuclear Instruments and Methods in Physics Research Section A Accelerators Spectrometers Detectors and Associated Equipment*. 606. Volume 606, Issue 3, 21 July **2009**, Pages 449-465.
9. Nuclear Power. Bragg Curve and Bragg Peak. Available online: <https://www.nuclear-power.net/nuclear-power/reactor-physics/interaction-radiation-matter/interaction-heavy-charged-particles/bragg-curve-bragg-peak/> (accessed on 27th February **2019**)
 10. Grum, F.; Costa, L.F. Spectral emission of corona discharges. *Appl. Opt.* **1976**, *15*, 76–79.
 11. Newport Corporation. Tutorial: Introduction to solar radiation. Available online: <https://www.newport.com/t/introduction-to-solar-radiation> (accessed 5th March **2019**)
 12. Sand, J.; Perajarvi, K.; Toivonen, H.; Nicholl, A.; Hrnccek, E.; Toivonen, J. EMCCD imaging of strongly ionizing radioactive materials for safety and security. In Proceedings of the 2013 Conference on Lasers & Electro-Optics Europe & International Quantum Electronics Conference CLEO EUROPE/IQEC; Munich, Germany, 12–16 May **2013**, p. 1.
 13. Sand, J.; Ihantola, S.; Peräjärvi, K.; Nicholl, A.; Hrnccek, E.; Toivonen, H.; Toivonen, J. Imaging of alpha emitters in a field environment. *Nuclear Inst. Methods Phys. Res. A* **2015**, *782*, 13–19.
 14. Ihantola, S.; Sand, J.; Peräjärvi, K.; Toivonen, J.; Toivonen, H. Principles of UV–gamma coincidence spectrometry. *Nuclear Inst. Methods Phys. Res. A* **2012**, *690*, 79–84.
 15. Lamadie, F.; Delmas, F.; Mahe, C.; Girones, P.; Le Goaller, C.; Costes, J.R. Remote alpha imaging in nuclear installations: New results and prospects. *IEEE Trans. Nuclear Sci.* **2005**, *52*, 3035–3039.
 16. Kume, N.; Takakura, K.; Nakayama, K.; Kuroda, H.; Izumi, M.; Mukai, N. Remote detector of alpha-ray using ultraviolet ray emitted by Nitrogen in air. In Proceedings of the Nuclear Science Symposium and Medical Imaging Conference (NSS/MIC), Seoul, Korea, 27 October–2 November **2013**; pp. 1–6.
 17. Sand, J., Hannuksela, V., Ihantola, S., Perajarvi, K., Toivonen, H., Toivonen, J. Remote Optical Detection of Alpha Radiation. In *IAEA International Nuclear Information System*; International Atomic Energy Agency (IAEA): Vienna, Austria, **2010**. Available online: http://www.iaea.org/inis/collection/NCLCollectionStore/_Public/42/081/42081464.pdf (accessed on 12 January 2018).

18. Sand, J., Nicholl, A., Hrneck, E., Toivonen, H., Toivonen, J., Perajarvi, K. Stand-Off Radioluminescence Mapping of Alpha Emitters Under Bright Lighting. *IEEE Trans. Nuclear Sci.* **2016**, *63*, 1777–1783.
19. Sackey S.S., Vowotor, M.K., Owusu, A., Mensah-Amoah, P., Tatchie, E.T., Sefa-Ntiri, B., Hood C.o., Atiemo, S.M. Spectroscopic Study of UV Transparency of Some Materials. *Environment and Pollution*; Vol. 4, No. 4; **2015**, published by *Canadian Center of Science and Education*.
20. Product Catalogue Best Sellers, optical components for uv/vis/nir spectroscopy, **2018**, HellmaAnalytics. Available online: https://www.hellma.com/en/hellma/downloads/?tx_rlhellma_downloadplugin%5Burl%5D=bHJ5YS9oY2UxS1BSZzJCVmFQWmsxeGhHVUJDVzNNQmhnXRYWdZvcUI0ZHFLSUxTVFOVDZnVUY3UTZrNnpYV3BPRWJhKzcxOGhMN2QvSmZjYndJYWE3S1IrT3RsLzhRR1FQa3ZGMjNyL1VpQVFZL1hXNIF5Wm10NkpuUnY0aitGZXhaNzgrNWVKVXpmU0l5S2ZjS2VVZlVWdk9EaXIRWdk5R3Q1V2hibGlvPQ%3D%3D&tx_rlhellma_downloadplugin%5Baction%5D=download&tx_rlhellma_downloadplugin%5Bcontroller%5D=Download&cHash=08f107fa8f93f5459065c8591d61ba5e (accessed 15th March 2019)
21. Metallic Mirror Coatings. Edmund optics. Available online: <https://www.edmundoptics.com/resources/application-notes/optics/metallic-mirror-coatings/> (accessed 19th June **2019**)
22. Precision Ultraviolet Mirrors. Edmund optics. Available online: <https://www.edmundoptics.com/f/Precision-Ultraviolet-Mirrors/13325/> (accessed 15th March **2019**)
23. International Atomic Energy Agency, Classification of Radioactive Waste, IAEA Safety Standards Series, No. GSG-1, IAEA, Vienna, **2009**.
24. Southern Scientific. Isotope Probe Look-Up Table. Available online: <https://www.southernscientific.co.uk/data/file/9/c/Isotope%20Probe%20Look-up%20Table.1438855315.pdf> (accessed on 11 January **2018**).
25. World Information Service on Energy. Uranium Radiation Properties; World Information Service on Energy: Amsterdam, The Netherlands, last updated May 2016. Available online: <http://www.wise-Uranium.org/rup.html> (accessed on 11 January **2018**).
26. Inrig, E., Koslowsky, V., Andrews, B., Dick, M., Forget, P., Ing, H., Hugron, R., Wong, L. Development and testing of an air fluorescence imaging system for the detection of radiological contamination. *AIP Conf. Proc.* **2011**, *1412*, 393–400.

27. Jenkins, A. (Characterisation, Inspection & Decontamination Group, Sellafield Ltd., Cumbria, UK). Personal Communication with Anita Crompton, **2015**.
28. Chichester, D., Watson, S. Multispectral UV-Visual Imaging as a Tool for Locating and Assessing Ionizing Radiation in Air. *IEEE Trans. Nuclear Sci.* **2011**, *58*, 2512–2518.
29. Waldenmaier, T., Blümer, J., Klages, H. Spectral resolved measurement of the Nitrogen fluorescence emissions in air induced by electrons. *Astropart. Phys.* **2008**, *29*, 205–222.
30. Hannuksela, V., Toivonen, J., Toivonen, H., Sand, J. Optical remote detection of alpha radiation. In *Proceedings of the Third European IRPA Congress, Helsinki, Finland*, 14–18 June **2010**; pp. 1750–1756.
31. Khan, A. Device physics: A bug-beating diode. *Nature* **2006**, *441*, 299.
32. Kerst, T.H.G., Sand, J.; Toivonen, J. Dynamic enhancement of radioluminescence in solar blind spectral region. In *Proceedings of the 2017 Conference on Lasers and Electro-Optics Europe & European Quantum Electronics Conference (CLEO/Europe-EQEC), Munich, Germany*, 25–29 June **2017**.
33. Crompton, A.J., Gamage, K.A.A., Bell, S.; Wilson, A.P., Jenkins, A., Trivedi, D. First Results of Using a UVTRON Flame Sensor to Detect Alpha-Induced Air Fluorescence in the UVC Wavelength Range. *Sensors* **2017**, *17*, 2756.
34. Sand, J., Ihantola, S., Peräjärvi, K., Toivonen, H., Toivonen, J. Radioluminescence yield of alpha particles in air. *New J. Phys.* **2014**, *16*, 13.
35. Thompson, B., Shenton-Taylor, C. Predicting the air fluorescence yield of radioactive sources. *Radiat. Meas.* **2016**, *88*, 48–54.
36. Shaw, G.A., Siegel, A.M., Model, J., Geboff, A., Soloviev, S., Vert, A., Sandvik, P. Deep UV photon-counting detectors and applications. *Advanced Photon Counting Techniques III*; Itzler, M.A., Campbell, J.C., Eds.; SPIE: Orlando, FL, USA, **2009**; Volume 7320.
37. Sayre, R.; Dowdy, J.; Poh-Fitzpatrick, M. Dermatological Risk of Indoor Ultraviolet Exposure from Contemporary Lighting Sources. *Photochem. Photobiol.* **2004**, *80*, 47–51.
38. Feener, J.; Charlton, W. Preliminary results of nuclear fluorescence imaging of alpha and beta emitting sources. In *Proceedings of the 3rd International Conference on Advancements in Nuclear Instrumentation Measurement Methods and Their Applications (ANIMMA), Marseille, France*, 23–27 June **2013**.

39. Morishita, Y.; Yamamoto, S.; Izaki, K.; Kaneko, J.H.; Toi, K.; Tsubota, Y. Development of a Si-PM based alpha camera for Plutonium detection in nuclear fuel facilities. *Nuclear Inst. Methods Phys. Res. A* **2014**, *747*, 81–86.
40. Canberra Industries Inc. Company Website Product Information. Available online: <http://www.canberra.com> (accessed on 12 January **2018**).
41. Giakos, G.C. Stand-off detection of mixed radiation fields. *Proc. SPIE Int. Soc. Opt. Eng.* **2008**, *6935*.
42. Ivanov, O.; Danilovich, A.; Stepanov, V.; Smirnov, S.; Volkovich, A. Visualization of Radioactive Sources without Gamma-Radiation with UV Imaging Systems. In *Proceedings of the ASME 2009 12th International Conference on Environmental Remediation and Radioactive Waste Management, Liverpool, UK, 11–15 October 2009*; Volume 2, pp. 321–325.
43. Ivanov, O.P.; Stepanov, V.E.; Smirnov, S.V.; Volkovich, A.G. Development of method for detection of alpha contamination with using UV-camera “DayCor” by OFIL. In *Proceedings of the Nuclear Science Symposium and Medical Imaging Conference (NSS/MIC), Valencia, Spain, 23–29 October 2011*; pp. 2192–2194.
44. Leybourne, A.E.; Creasey, S.; Dixon, J.; Lee, J.; Messer, G.; Neal, S.; Rayborn, G.H.; Speaks, D.; Stephens, J.; Strange, T.; et al. Long range detection of radiation induced air fluorescence. Abstract#709. In *Proceedings of the Institute of Nuclear Materials Management Annual Meeting, Baltimore, MD, USA, 11–15 July 2010*; pp. 1498–1509.
45. Pineau, J.-F.; Imbard, G. Remote Alpha Source Location Device and Method. *U.S. Patent 6,281,502 B1*, 28 August **2001**.
46. Haslip, D.S.; Cousins, T.; Koslowsky, V.; Ing, H.; Andrews, H.R.; Clifford, E.T.H.; Locklin, D. Standoff Radiation Imaging Detector. *U.S. Patent 7,317,191 B1*, 8 January **2008**.
47. Sprangle, P.; Hafizi, B.; Milchberg, H.; Nusinovich, G.; Zigler, A. Active remote detection of radioactivity based on electromagnetic signatures. *Phys. Plasmas* **2014**, *21*.
48. Yao, J.; Brenizer, J.; Hui, R.; Yin, S. Standoff alpha radiation detection via excited state absorption of air. *Appl. Phys. Lett.* **2013**, *102*.
49. Allander, K.S.; Bounds, J.A.; Caress, R.W.; Catlett, M.M.; Garner, S.E.; Johnson, J.P.; Johnson, J.D.; MacArthur, D.W.; Rutherford, D.A. Long-Range Alpha Detector (LRAD) Technology Applied to ER and D&D Problems; Los Alamos National Laboratory: Los Alamos, NM, USA, **1993**.

50. Morse, F.; Harteck, P.; Dondes, S. Excited species of gases produced in the nuclear reactor. *Radiat. Res.* **1966**, *29*, 317–328.
51. FV40. 3M. Available online: <https://gasdetection.3m.com/en/gas-detector-transmitter-fv40> (accessed 19th June **2019**)
52. Morley FSL 100 UV Flame Detector. Acorn Fire and Security. Available online: https://www.acornfiresecurity.com/morley-fsl100-uv-flame-detector?gclid=EAIaIQobChMI_6HoloH24gIVxLHtCh3dOQtmEAQYAyABEgI4NPD_BwE (accessed 19th June **2019**)
53. Hamamatsu. Flame Sensor UVTRON. 2010. Available online: http://www.hamamatsu.com/resources/pdf/etd/R9454_R9533_TPT1019E.pdf (accessed on 27 November **2017**).
54. Hamamatsu. Flame Sensor UVTRON R9454, R9533. Available online: https://www.hamamatsu.com/resources/pdf/etd/R9454_R9533_TPT1019E.pdf (accessed 6th March **2019**)
55. Hamamatsu. C10423, C10807 Instruction Manual. May **2010**.
56. Mahe, C. Characterization and Visualization Technologies in DD&R—Alpha Imaging. In *Practical Workshop on Characterization and Visualization Technologies in DD&R*; IAEA: Marcoule, France, **2011**.
57. Laboratoire National Henri Bequerel. Recommended Data Table for ²¹⁰Po. Available online: http://www.nucleide.org/DDEP_WG/Nuclides/Po-210_tables.pdf (accessed on 11 September **2017**).
58. UQG Optics, UV Fused Silica—Spectrosil—Data Sheet. Available online: <http://www.uqgoptics.com/pdf/Fused%20Silica%20-%20Spectrosil1.pdf> (accessed on 7 September **2017**).
59. Hurst, G.S.; Bortner, T.E.; Strickler, T.D. Proton Excitation of the Argon Atom. *Phys. Rev.* **1969**, *178*, 4–10.
60. Brett, J.; Koehler, K.E.; Bischak, M.; Famiano, M.; Jenkins, J.; Klankowski, L.; Niraula, P.; Pancella, P.; Lakis, R. Spectral measurements of alpha-induced radioluminescence in various gases. *Nuclear Instrum. Methods Phys. Res. A* **2017**, *184*, 88–93.
61. Hurst, G.S.; Bortner, T.E.; Strickler, T.D. Proton Excitation of the 1300-Å Continuum in Argon. *J. Chem. Phys.* **1968**, *49*, 2460–2461.

62. Strickler, T.D.; Arakawa, E.T. Optical Emissions from Argon Excited by Alpha Particles: Quenching Studies. *J. Chem. Phys.* **1964**, *41*, 1783–1789.
63. Saito, K.; Tawara, H.; Sanami, T.; Shibamura, E.; Sasaki, S. Absolute number of scintillation photons emitted by alpha particles in rare gases. *IEEE Trans. Nuclear Sci.* **2002**, *49*, 1674–1680.
64. Melton, C.E.; Hurst, G.S.; Bortner, T.E. Ionization Produced by 5-MeV Alpha Particles in Argon Mixtures. *Phys. Rev.* **1954**, *96*, 643–645.
65. Jesse, W.P.; Forstat, H.; Sadauskis, J. The ionization in Argon and air by the single alpha-particles as a function of their energy. *Phys. Rev.* **1950**, *77*, 782–786.
66. Jesse, W.P.; Sadauskis, J. Alpha-particle Ionization in Mixtures of the Noble Gases. *Phys. Rev.* **1952**, *88*, 417–418.
67. Morii, H.; Mizouchi, K.; Nomura, T.; Sasao, N.; Sumida, T.; Kobayashi, M.; Murayama, Y.; Takashima, R. Quenching effects in Nitrogen gas scintillation. *Nuclear Instrum. Methods Phys. Res. Sect. A Accel. Spectrom. Detect. Assoc. Equip.* **2004**, *526*, 399–408.
68. Saito, K.; Sasaki, S.; Tawara, H.; Sanami, T.; Shibamura, E. Simultaneous measurement of absolute numbers of electrons and scintillation photons produced by 5.49 MeV alpha particles in rare gases. *IEEE Trans. Nuclear Sci.* **2003**, *50*, 2452–2459.
69. Gray, L. The ionisation method of measuring neutron energy. *Math. Proc. Camb. Philos. Soc.* **1944**, *40*, 72–102.
70. Gibson, G.E.; Gardiner, E.W. The Ionisation and Stopping Power of Various Gases for Alpha-Particles from Polonium: I. *Phys. Rev.* **1927**, *30*, 543–552.
71. Hurtgen, C.; Jerome, S.; Woods, M. Revisiting Currie—How low can you go? *Appl. Radiat. Isot.* **2000**, *53*, 45–50.
72. Crompton, A.J.; Gamage, K.A.A.; Jenkins, A.W.; Taylor, C.J. Alpha Particle Detection Using Alpha-Induced Radioluminescence: A Review and Future Prospects for Preliminary Radiological Characterisation for Nuclear Facilities Decommissioning. *Sensors* **2018**, *18*, 1015.
73. Hamamatsu. Flame Sensors UVTRON. Available online: https://www.hamamatsu.com/eu/en/product/optical-sensors/uv_flame-sensor/flame-sensor_uv-tron/index.html (accessed on 16 October **2018**).

References

74. Crompton, A.J.; Gamage, K.A.A.; Bell, S.; Wilson, A.P.; Jenkins, A.W.; Trivedi, D. Gas Flow to Enhance the Detection of Alpha-Induced Air Radioluminescence Based on a UVTRON Flame Sensor. *Sensors* **2018**, *18*, 1842.
75. OSRAM. L 36 W/840 LUMILUX T8 Tubular fluorescent lamp 26 mm, with G13 bases. Available online: <https://www.watt24.com/media/Datasheet-Osram-T8-Fluorescent-Lamp-L-36W-840-4050300517872.pdf> (accessed on 11 December **2018**).
76. Hamamatsu. Flame Sensor UVTRON. Available online: https://www.hamamatsu.com/resources/pdf/etd/uvtron_TPT1034E.pdf (accessed on 20 November **2018**).
77. Delacroix, D.; Guerre, J.P.; Leblanc, P.; Hickman, C. Radionuclide and Radiation Protection Data Handbook 2002. *Radiat. Prot. Dosim.* **2002**, *98*, 1–168.
78. Crompton, A.J.; Gamage, K.A.A.; Trivedi, D.; Jenkins, A. The Effect of Gamma and Beta Radiation on a UVTRON Flame Sensor: Assessment of the Impact on Implementation in a Mixed Radiation Field. *Sensors* **2018**, *18*(12), 4394.
79. Wolfmet. Radiation Shielding. September **2015**. Available online: https://www.wolfmet.com/wp-content/uploads/2017/01/Wolfmet_Tungsten_Alloys_Technical_Information1.pdf (Accessed on 3 July 2019)
80. Photon Engineering. What is FRED. Available online: <https://photonengr.com/fred-software/> (Accessed on 3 July **2019**)
81. The Litvinenko Inquiry - Report into the death of Alexander Litvinenko. January **2016**. Available online at: https://assets.publishing.service.gov.uk/government/uploads/system/uploads/attachment_data/file/493860/The-Litvinenko-Inquiry-H-C-695-web.pdf (Accessed on 3 July 2019)